Contents

Chapter 1

Introduction

The relevance of exactly solvable models and their role for the understanding of complex systems in statistical physics is unquestioned. One of the most studied models in the literature is the one-dimensional XY quantum spin chain describing L interacting spin 1/2 particles on a one-dimensional lattice in the presence of an external longitudinal magnetic field h. The Hamiltonian is given by

$$\mathcal{H}_{XY} = \sum_{j=1}^{L} J \left[(1+\gamma)\sigma_j^x \sigma_{j+1}^x + (1-\gamma)\sigma_j^y \sigma_{j+1}^y\right] + h \sum_{j}^{L} \mu \sigma_j^z \tag{1.1}$$

where by σ_j^x, σ_j^y and σ_j^z we denote the Pauli matrices. Periodic boundary conditions are realized by identifying σ_{L+1}^μ with σ_1^μ where $\mu = x, y$, whereas setting $\sigma_{L+1}^\mu = 0$ implies free boundary conditions. The isotropic chain ($\gamma = 0$) is also referred to as XX-model.

One of the main reasons for the popularity of the model (1.1) is that it can be diagonalized in terms of free fermions [1], which provides relatively easy access not only to the spectra, but also to the wavefunctions. Despite its simplicity, the model embeds many interesting physical properties and after its introduction [2] it has often served as a testing ground for various techniques and physical concepts.

The Hamiltonian (1.1) appears in the study of reaction diffusion systems [3], in the domain wall theory of two-dimensional commensurate-incommensurate phase transitions [4], in Glauber's kinetic Ising model [5] and in the theory of Frenkel excitons [6, 7]. Furthermore, the isotropic chain appears as a special case of the XXZ spin 1/2 Heisenberg chain [8] which since the seminal paper of Belavin *et al* [9] served as a paradigm of a conformally invariant system with central charge $c = 1$.

Based on the large amount of theoretical results, experimental evidence for physical systems with XY interaction has been found in various measurements [10]-[16].

In this thesis we will study the XX-chain with general boundary terms. However, before defining the Hamiltonian under study, we will give a brief survey on the existing literature.

The model (1.1) has been introduced by Lieb *et al* [2] for the case $h = 0$. The authors considered periodic boundary conditions as well as free ends. They computed the ground-state energy, the elementary excitations and presented a method to calculate the time independent two–point functions of the spin operators. Various thermodynamic properties, such as the magnetization, the susceptibility and the specific heat, have been computed by Katsura [17] for the periodic boundary condition and in the presence of the magnetic field.

The investigation of the two-point correlation functions for the periodic chain has been the subject of many of the following publications. McCoy [18] computed the long range behaviour of the equal time correlation functions $\langle\sigma_0^\mu\sigma_R^\mu\rangle$ for the case $h=0$ where $\mu = x, y, z$. This work has been extended by Barouch and McCoy [19] to the case $h \neq 0$. Based on these results they have derived the phase diagram of the model.

The time-dependent longitudinal correlation function $\langle\sigma_0^z(t)\sigma_R^z(0)\rangle$ has been studied by Niemeijer [20] and Katsura *et al* [21] for arbitrary values of the temperature T, whereas the time-dependent transversal correlation functions $\langle\sigma_0^{x,y}(t)\sigma_R^{x,y}(0)\rangle$ have been investigated by McCoy *et al* [22] in the limit of large R and only at $T=0$. Exact expressions for the time-dependent ground-state correlation functions of σ_j^x and σ_j^y for all values of R and t have been computed by Vaidya and Tracy [23]. The off diagonal ground-state correlation functions $\langle\sigma_0^\mu(t)\sigma_R^\nu(0)\rangle$ where $\mu \neq \nu$ and $\mu, \nu = x, y, z$ have been studied by Johnson and McCoy [24].

The time dependent, longitudinal and transversal spin correlation functions at infinite temperature have been studied by Sur *et al* [25] for the case $\gamma = 0$ and $h = 0$. This work has been extended to general values of γ by Capel and Perk [26]. The case $\gamma, h \geq 0$ has been studied by Brandt and Jacoby [27]. Cruz and Gonçalves [28] investigated the time-dependent correlation functions at $T = 0$ and $T = \infty$ for the open XX-chain in view to boundary effects.

More recent there have been attempts to compute the dynamical correlation functions $\langle\sigma_0^+(t)\sigma_R^-(0)\rangle$ at arbitrary values of the temperature for the isotropic chain. In the thermodynamical limit these correlation functions have been represented as Fredholm determinants of linear integral operators by Colomo *et al* [29]. The asymptotic behaviour ($R, t \to \infty, R/t$ fixed) of these determinants has been analyzed by Its *et al* [30].

Relaxation processes have been studied by assuming the magnetic field h to be time-dependent. Non-ergodic behaviour of the longitudinal magnetization in response to a step-function change in the external field has been reported by several authors [31]-[35]. The same phenomenon has been observed for the correlation functions $\langle\sigma_0^\mu(t)\sigma_R^\mu(t)\rangle$ [36]. The chain has also been used to study finite-size scaling for quantum chains with an oscillatory energy gap [37]. An early renormalization group study applied to the XX-chain can be found in [38].

However, the effect of various modifications of the Hamiltonian (1.1) which conserve the possibility to diagonalize it in terms of free fermions has also been studied. The XY-chain with Dzyaloshinsky-Moriya interactions which is obtained by adding a term $\sum_j^L D\left(\sigma_j^x\sigma_{j+1}^y - \sigma_j^y\sigma_{j+1}^x\right)$ has been investigated in [39]-[41]. Furthermore, the effect of impurities located in the bulk [42] or at the boundary [43, 44] has been considered.

Certain types of disorder have been studied by assuming the exchange coupling J and the magnetic moment μ to be functions of the lattice site j. The effect of randomly distributed couplings J_j on the thermodynamic properties has been studied by Smith [45] and by Derzhko and Richter [46]. The case of randomly distributed magnetic moments μ_j has been considered by Barouch and Oppenheim [47] and Nishimori [48]. The low temperature dynamics of the chain with quasiperiodic exchange couplings J_j has been investigated by Luck and Nieuwenhuizen [49].

More recently, the open XY-chain has been studied in the presence of diagonal boundary terms. It has been shown, for certain choices of the parameters, that the Hamiltonian is invariant under a two parameter deformation of the $su(1|1)$ superalgebra [50] and the invariant, instantaneous ground-state correlation functions of σ_j^z have been computed in [51]. An interesting generalized duality transformation of the chain in the presence of diagonal boundary terms has been found in [52].

Much less is known about the chain with non-diagonal boundary terms. So far, only the semi-infinite XX chain in the presence of a transverse field at the boundary has been considered in [43, 53]. In [43] the model was used to study non-equilibrium properties of an impurity located at the boundary whereas in [53] it served as the discrete version of a model of a particle in a periodic potential interacting with an external environment. Using the free fermion approach, the author computed the mobility of the particle in the continuum limit.

In this thesis we are going to consider the XX–model with general (diagonal and non-diagonal), not necessarily hermitian boundaries

$$\mathcal{H} = \frac{1}{4}\sum_{j=1}^{L-1}\left[\sigma_j^x\sigma_{j+1}^x + \sigma_j^y\sigma_{j+1}^y\right] + \frac{1}{\sqrt{8}}\left[\alpha_-\sigma_1^- + \alpha_+\sigma_1^+ + \alpha_z\sigma_1^z + \beta_+\sigma_L^+ + \beta_-\sigma_L^- + \beta_z\sigma_L^z\right] \tag{1.2}$$

where the parameters $\alpha_\pm, \beta_\pm, \alpha_z$ and β_z are arbitrary complex numbers. Note that the $U(1)$ symmetry is broken by the non-diagonal boundary terms. Although this Hamiltonian is known to be integrable [54, 55], Bethe ansatz equations have not yet been obtained, because it is not known how to construct a reference state.

Note also that this Hamiltonian can not be diagonalized in terms of free fermions using the Jordan-Wigner transformation [1], since it is not quadratic in fermionic creation and annihilation operators. However, following [43] we will be able to diagonlize the Hamiltonian $\mathcal{H}$ by using an auxiliary Hamiltonian $\mathcal{H}_{\text{long}}$ which is obtained by adding a phantom site at each end of the chain and which can be diagonalized in terms of free fermions. The diagonalization of $\mathcal{H}_{\text{long}}$ has already been the subject of a previous thesis [56].

The present work is organized as follows: We start with the diagonalization of the Hamiltonian on the finite chain in chapter 2. This part is very technical by nature. We will briefly review the diagonalization of $\mathcal{H}_{\text{long}}$ in order to fix our notation. Afterwards we will show in detail how to obtain the spectra and eigenvectors of $\mathcal{H}$ using the results for the auxiliary Hamiltonian $\mathcal{H}_{\text{long}}$. This will be applied to the computation of the ground-state energies of $\mathcal{H}$ for certain boundary terms. As a by-product of our computations, we will obtain the one- and two-point functions of the σ_j^x operator in terms of pfaffians.

In chapter 3 we will consider the continuum limit of the spectra of $\mathcal{H}$ and $\mathcal{H}_{\text{long}}$. Among other things we will identify the partition functions of the free boson field compactified on a circle with Neumann-Neumann, Dirichlet-Neumann and Dirichlet-Dirichlet boundary conditions.

We will present the "topological" charge on the finite chain for two types of non-diagonal boundary terms in chapter 4. The "topological" charge represents the analogue of the $U(1)$-charge in the case of diagonal boundaries, i.e. the projection of the total spin onto the z-axis.

In chapter 5 we study the ground-state magnetization profiles for hermitian boundary conditions. As opposed to the periodic boundary condition, the behaviour of the profiles is non-trivial in the presence of boundary terms. Our results will be compared to the predictions of conformal field theory. Furthermore, we will discuss the appearance of boundary bound states by studying the profiles of certain excited states. The results of this chapter are based on exact as well as on numerical computations.

We will give a summary of our results in chapter 6. Further details on our results can be found in the conclusions presented at the end of each chapter. The details of our calculations are given in the appendix. The computation of the asymptotic behaviour of the fermion energies for large values of L yielding the results presented in chapter 3 is the subject of appendix A. In appendix B we discuss the computation of the magnetization profiles. The results of the present work have been published in [57, 58, 59, 60].

Chapter 2

Diagonalization of the finite chain

As already mentioned in the introduction, it is not possible to diagonalize the Hamiltonian (1.2) in terms of free fermions directly. As will be explained shortly, the spectra and the eigenvectors of $\mathcal{H}$ may be obtained by considering the auxiliary Hamiltonian

$$\begin{aligned}\mathcal{H}_{\text{long}} = & \frac{1}{2}\sum_{j=1}^{L-1}\left[\sigma_j^+\sigma_{j+1}^- + \sigma_j^-\sigma_{j+1}^+\right] \\ & + \frac{1}{\sqrt{8}}\left[\alpha_-\sigma_0^x\sigma_1^- + \alpha_+\sigma_0^x\sigma_1^+ + \alpha_z\sigma_1^z + \beta_+\sigma_L^+\sigma_{L+1}^x + \beta_-\sigma_L^-\sigma_{L+1}^x + \beta_z\sigma_L^z\right]\end{aligned} \quad (2.1)$$

which in turn may be diagonalized in terms of free fermions [1]. Notice that $\mathcal{H}_{\text{long}}$ is $Z(2)\times Z(2)$ symmetric since the matrices σ_0^x and σ_{L+1}^x commute with $\mathcal{H}_{\text{long}}$. Therefore the spectrum of $\mathcal{H}_{\text{long}}$ decomposes into four sectors $(+,+)$, $(-,-)$, $(+,-)$, $(-,+)$ corresponding to the eigenvalues ± 1 of σ_0^x and σ_{L+1}^x. The Hamiltonian $\mathcal{H}$ given by (1.2) corresponds to the $(+,+)$ sector. Actually the symmetry of $\mathcal{H}_{\text{long}}$ is larger than $Z(2)\times Z(2)$, it is the finite non-abelian group with the three generators $\sigma_0^x, \sigma_{L+1}^x$ and $U = \sigma_0^z\sigma_1^z\cdots\sigma_{L+1}^z$ (which also commutes with $\mathcal{H}_{\text{long}}$). Moreover using the obvious relations:

$$\{\sigma_0^x, U\} = \{\sigma_{L+1}^x, U\} = 0; \qquad U^2 = 1 \quad (2.2)$$

one can show that if $|\mu,\nu,E\rangle$ is an eigenvector of $\mathcal{H}_{\text{long}}$ in the (μ,ν) sector, corresponding to the eigenvalue E, then

$$U \mid \mu,\nu,E\rangle = \mid -\mu,-\nu,E\rangle \quad (2.3)$$

is also an eigenvector of $\mathcal{H}_{\text{long}}$, in the $(-\mu,-\nu)$ sector corresponding to the same eigenvalue E. As a result, the whole spectrum of $\mathcal{H}_{\text{long}}$ is doubly degenerate: the spectra in the sectors $(+,+)$ and $(-,-)$ (respectively $(+,-)$ and $(-,+)$) are identical. Since the degeneracy includes the ground-state, the symmetry is spontaneously broken. We will see that this degeneracy manifests itself as a zero mode in the fermionic language.

Since the diagonalization of $\mathcal{H}_{\text{long}}$ has already been the subject of another thesis [56], we will only briefly review the main results of this procedure in section 2.1. Afterwards we will show in detail how to project onto the $(+,+)$-sector in order to obtain the eigenvalues and eigenvectors of the original Hamiltonian $\mathcal{H}$ in section 2.2. For special cases our results will be applied to the computation of the ground-state energies of $\mathcal{H}$ in terms of the ground-state energies of $\mathcal{H}_{\text{long}}$ which have already been given in [56]. This chapter is based on [57].

2.1 Diagonalization of $\mathcal{H}_{\text{long}}$

In its diagonal form the Hamiltonian $\mathcal{H}_{\text{long}}$ is given by

$$\mathcal{H}_{\text{long}} = \sum_{k=0}^{L+1} 2\Lambda_k b_k a_k - \sum_{k=0}^{L+1} \Lambda_k \tag{2.4}$$

where the b_k and a_k satisfy the anticommutation relations of fermionic creation and annihilation operators, i.e.

$$\{b_n, a_m\} = \delta_{n,m} \qquad \{b_n, b_m\} = 0 \qquad \{a_n, a_m\} = 0. \tag{2.5}$$

Note that in general the a_n, b_n are not mutually adjoint, since $\mathcal{H}_{\text{long}}$ is non-hermitian without further constraints. The values of the Λ_k are determined by the eigenvalues of a skew-symmetric $(2L+4)\times(2L+4)$ matrix M, i.e.

$$\mathsf{M}(\phi_k^{\pm}) = \pm\Lambda_k(\phi_k^{\pm}) \tag{2.6}$$

The explicit form of M is given by

$$\mathsf{M} = \begin{pmatrix} 0 & \mathsf{G} & & & & \\ -\mathsf{G}^{\mathrm{t}} & 2\mathsf{I} & \mathsf{F} & & & \\ & -\mathsf{F}^{\mathrm{t}} & 0 & \mathsf{F} & & \\ & & \ddots & \ddots & \ddots & \\ & & & -\mathsf{F}^{\mathrm{t}} & 2\mathsf{J} & \mathsf{K} \\ & & & & -\mathsf{K}^{\mathrm{t}} & 0 \end{pmatrix} \tag{2.7}$$

where

$$\mathsf{G} = \frac{1}{2}\begin{pmatrix} \frac{1}{\sqrt{8}}(\alpha_- - \alpha_+) & \frac{\mathrm{i}}{\sqrt{8}}(\alpha_- + \alpha_+) \\ 0 & 0 \end{pmatrix} \qquad \mathsf{K} = \frac{1}{2}\begin{pmatrix} 0 & \frac{\mathrm{i}}{\sqrt{8}}(\beta_+ + \beta_-) \\ 0 & \frac{1}{\sqrt{8}}(\beta_+ - \beta_-) \end{pmatrix}$$
$$\mathsf{F} = \frac{1}{4}\begin{pmatrix} 0 & \mathrm{i} \\ -\mathrm{i} & 0 \end{pmatrix} \quad \mathsf{I} = \frac{1}{2}\begin{pmatrix} 0 & -\frac{\mathrm{i}}{\sqrt{8}}\alpha_z \\ \frac{\mathrm{i}}{\sqrt{8}}\alpha_z & 0 \end{pmatrix} \quad \mathsf{J} = \frac{1}{2}\begin{pmatrix} 0 & -\frac{\mathrm{i}}{\sqrt{8}}\beta_z \\ \frac{\mathrm{i}}{\sqrt{8}}\beta_z & 0 \end{pmatrix} \tag{2.8}$$

The eigenvectors $(\phi_k^{\pm})$ can be used to express the a_k, b_k operators in terms of the Clifford operators $\tau_j^{\pm}$, which are defined by

$$\tau_j^{+,-} = \left(\prod_{i=0}^{j-1} \sigma_i^z\right) \sigma_j^{x,y} \tag{2.9}$$

in the following way:

$$a_k = \frac{1}{2}\sum_{j=0}^{L+1}\sum_{\mu=\pm1} (\phi_k^+)_j^{\mu}\tau_j^{\mu} \qquad b_k = \frac{1}{2}\sum_{j=0}^{L+1}\sum_{\mu=\pm1} (\phi_k^-)_j^{\mu}\tau_j^{\mu} \tag{2.10}$$

where we used the notation $(\phi_k^\pm) = ((\phi_k^\pm)_0^-, (\phi_k^\pm)_0^+, (\phi_k^\pm)_1^-, (\phi_k^\pm)_1^+, \ldots, (\phi_k^\pm)_{L+1}^-, (\phi_k^\pm)_{L+1}^+)$. If M is diagonalizable (which is always the case if $\mathcal{H}$ is hermitian), one can show [57] that the $(\phi_k^\pm)$ fulfil the orthogonality relations

$$\sum_{j=0}^{L+1} \sum_{\gamma} (\phi_l^\mu)_j^\gamma (\phi_k^{-\nu})_j^\gamma = 2\delta_{lk}^{\mu\nu} \tag{2.11}$$

$$\sum_{k=0}^{L+1} \sum_{\mu} (\phi_k^\mu)_j^\gamma (\phi_k^{-\mu})_i^\nu = 2\delta_{ij}^{\gamma\nu}. \tag{2.12}$$

This ensures the validity of the anticommutation relations (2.5). It has also been shown in [57], that the eigenvalues Λ_k can be obtained by the zeros x_k of a polynomial $p(x^2)$, i.e.

$$\Lambda_k = \frac{1}{4}(x_k + 1/x_k) \tag{2.13}$$

where the polynomial is given by

$$\begin{aligned} p(z) = \Big[& z^{2L+4} + 1 - A(z^{2L+3} + z) + (B + E^2)(z^{2L+2} + z^2) \\ & + (D + 2E^2)(z^{2L+1} + z^3) + E^2(z^{2L} + z^4) - 2E(z^{L+4} + z^L) \\ & + \left((A - B - D - 1)/2 - (-1)^L C - 2E^2\right)(z^{L+3} + z^{L+1}) \\ & + \left(A - B - D - 1 + 2(-1)^L C + 4E - 4E^2\right) z^{L+2} \Big] \Big/ (z-1)^2 \end{aligned} \tag{2.14}$$

The coefficients appearing in (2.14) are functions of the boundary parameters:

$$\begin{aligned} & A = 2(\alpha_-\alpha_+ + \beta_-\beta_+ + \alpha_z^2 + \beta_z^2 - 1) \qquad C = (\alpha_-^2\beta_+^2 + \alpha_+^2\beta_-^2) \\ & B = (2\alpha_-\alpha_+ - 1)(2\beta_-\beta_+ - 1) + 4\beta_z^2(\alpha_-\alpha_+ - 1) + 4\alpha_z^2(\beta_+\beta_- - 1) \\ & D = \beta_z^2(4\alpha_-\alpha_+ - 2) + \alpha_z^2(4\beta_+\beta_- - 2) \qquad E = 2\alpha_z\beta_z. \end{aligned} \tag{2.15}$$

We have also shown in [57] how to compute the eigenvectors $(\phi_k^\pm)$ as a function of the x_k. This knowledge is essential for the computation of expectation values (as we will see in section 2.2.3). However, we are not going to repeat this procedure here (see [57] for details).

The zeros of the polynomial (2.14) are in general hard to find. However, we have found [57] several cases (see table 2.1) where the numerator of (2.14) factorizes into cyclotomic polynomials (see [56] for details). In these cases the zeros are quite easy to find, which allows for exact computations of the Λ_k and $(\phi_k^\pm)$ on the finite chain. As an application, the ground-state energies of $\mathcal{H}_{\rm long}$ for the factorizable cases have been given in [57].

Due to equation (2.6) the sign of the Λ_k is not fixed. From (2.10) we see that changing the sign of one of the Λ_k has just the effect of exchanging the corresponding creation and annihilation operators. Thus the diagonal form of $\mathcal{H}_{\rm long}$ given in equation (2.4) remains unchanged, but we want to remark that the vacuum state defined by

$$a_k|vac\rangle = 0 \quad \forall k \tag{2.16}$$

Table 2.1. Cases where the numerator $q(z) = p(z)(z-1)^2$ of the polynomial (2.14) factorizes into cyclotomic polynomials. The parameter s may be chosen to be an arbitrary complex number.

case	A	B	$(-1)^L C$	D	E	$q(z)$
1	1	0	0	0	0	$(1-z)(1-z^{2L+3})$
2	0	-1	0	0	0	$(1-z^2)(1-z^{2L+2})$
3	-1	0	0	0	0	$(1+z)(1-z^{L+1})(1-z^{L+2})$
4	1	-1	0	1	0	$(1+z)(1-z)^2(1+z^{2L+1})$
5	0	0	$\frac{1}{2}$	0	0	$(1-z^{L+1})(1-z^{L+3})$
6	0	0	$-\frac{1}{2}$	0	0	$(1-z^{L+2})^2$
7	1	0	1	0	0	$(1-z)(1-z^{L+1})(1+z^{L+2})$
8	1	0	-1	0	0	$(1-z)(1+z^{L+1})(1-z^{L+2})$
9	2	1	$s+1/s$	0	0	$(1-z)^2(1-sz^{L+1})(1-1/sz^{L+1})$
10	$s+1/s$	1	$\frac{1}{2}(2+s+1/s)$	0	0	$(1-sz)(1-1/sz)(1-z^{L+1})^2$
11	$1+s+1/s$	$1+s+1/s$	0	-1	0	$(1-sz)(1-1/sz)(1-z)(1-z^{2L+1})$
12	0	$-1-s-1/s$	$\frac{1}{2}(-2+s+1/s)$	-2	1	$(1-sz^2)(1-1/sz^2)(1-z^L)^2$
13	$s+1/s$	1	$-2-s-1/s$	$-2-s-1/s$	1	$(1-sz)(1-1/sz)(1+z^2)(1-z^L)^2$
14	$2+s+1/s$	$1+2s+2/s$	$4+2s+2/s$	$-4-s-1/s$	-1	$(1-sz)(1-1/sz)(1-z)^2(1+z^L)^2$
15	$2+s+1/s$	$1+2s+2/s$	$-4-2s-2/s$	$-4-s-1/s$	1	$(1-sz)(1-1/sz)(1-z)^2(1-z^L)^2$
16	$-2+s+1/s$	$1-2s-2/s$	0	$-2-s-1/s$	1	$(1-sz)(1-1/sz)(1+z)^2(1-z^L)^2$

changes. Thus the vacuum state may be not a ground-state of the chain (in fact, there may be more than one ground-state due to the possible existence of fermionic modes with an energy, which has vanishing real part). However, this does not affect the general formalism and sometimes it may be useful to consider the vacuum not to be a ground-state.

The spectrum of $\mathcal{H}_{\text{long}}$ always contains a zero mode. As can be seen readily from the form of M (cf. (2.7) and (2.8)), the associated eigenvectors ($\phi_0^{\pm}$) are given by

$$\phi_0^+ = (0, 1, 0, \cdots, 0, \mathrm{i}, 0) \qquad \phi_0^- = (0, 1, 0, \cdots, 0, -\mathrm{i}, 0). \tag{2.17}$$

As will become clear in the next section, this zero mode does not appear as fermionic excitation in the spectrum of $\mathcal{H}$ and therefore has been called spurious zero mode in [57].

2.2 Projection method and the 1-point functions of σ^x

Up to now we have dealt only with the Hamiltonian $\mathcal{H}_{\text{long}}$ given by (2.1) which was obtained from $\mathcal{H}$ (see (1.2)) by adding one lattice site at each end of the chain. In this section we will explain how the spectrum of $\mathcal{H}$ is related to the spectrum of $\mathcal{H}_{\text{long}}$.

Since, as already mentioned at the beginning of this chapter, σ_0^x and σ_{L+1}^x commute with $\mathcal{H}_{\text{long}}$ the spectrum decomposes into four sectors $(+,+)$, $(+,-)$, $(-,+)$, $(-,-)$ corresponding to the eigenvalues ± 1 of σ_0^x and σ_{L+1}^x. The eigenvalues and eigenvectors of $\mathcal{H}$ are related to the $(+,+)$-sector in the following way:

If $|E\rangle$ is an eigenvector of $\mathcal{H}$ corresponding to an eigenvalue E then $|E_{\text{long}}\rangle = |+\rangle \otimes |E\rangle \otimes |+\rangle$ is an eigenvector of $\mathcal{H}_{\text{long}}$ corresponding to the same eigenvalue E, where $\sigma_0^x|+\rangle = |+\rangle$ and $|E_{\text{long}}\rangle$ is element of the space $\mathbb{C}^2 \otimes \mathbb{C}^L \otimes \mathbb{C}^2$. Thus the whole spectrum of $\mathcal{H}$ is contained in the spectrum of $\mathcal{H}_{\text{long}}$ projected onto the $(+,+)$-sector. Since the dimension of the of $(+,+)$-sector is 2^L we conclude that the spectrum of $\mathcal{H}$ is identical to the spectrum of $\mathcal{H}_{\text{long}}$ projected onto the $(+,+)$-sector.

Before describing how we will proceed to project to the $(+,+)$-sector, we make some definitions which are needed later. First, we want to remind the reader that M defined by (2.7) always has a twofold degenerate eigenvalue 0 corresponding to eigenvectors (2.17) of M. Using the Clifford operators $\tau_j^{\pm}$ given by (2.9), we now define the corresponding ladder operators

$$b_0 = (\tau_0^+ - \mathrm{i}\tau_{L+1}^-)/2 \qquad a_0 = (\tau_0^+ + \mathrm{i}\tau_{L+1}^-)/2. \tag{2.18}$$

We also define the vacuum representation with the lowest weight vector $|vac\rangle$ by

$$a_k|vac\rangle = 0 \quad \forall k. \tag{2.19}$$

Because we are interested in eigenstates of σ_0^x and σ_{L+1}^x we define the vectors

$$|v^{\pm}\rangle = \frac{1}{\sqrt{2}}(|vac\rangle \pm |0\rangle) \tag{2.20}$$

where $|0\rangle = b_0|vac\rangle$. Observe that due to (2.18)

$$\sigma_0^x|v^{\pm}\rangle = \pm|v^{\pm}\rangle. \tag{2.21}$$

Now we will proceed in four steps. In the first step (section 2.2.1) we will show, using some algebraic considerations, that the vectors $|v^{\pm}\rangle$ are also eigenvectors of σ_{L+1}^x. It will turn out that the eigenvalues of σ_{L+1}^x corresponding to the eigenvectors $|v^+\rangle$ and $|v^-\rangle$ always have opposite signs, i.e.

$$\sigma_{L+1}^x|v^{\pm}\rangle = \pm\eta|v^{\pm}\rangle \tag{2.22}$$

with $\eta^2 = 1$.The value of η plays a crucial role in the following. We will also show that the $(+,+)$-sector consists either of the states

$$\prod_{j=1}^{r} b_{k_j}|v^+\rangle \quad \text{with } r \text{ even} \tag{2.23}$$

or

$$\prod_{j=1}^{r} b_{k_j}|v^-\rangle \quad \text{with } r \text{ odd} \tag{2.24}$$

where $0 < k_j \leq k_{j+1}$. Since $k_j \neq 0$, the creation operator of the spurious zero mode defined by (2.18) does not appear in (2.23) and (2.24). The ground state of $\mathcal{H}$ corresponds to $|v^+\rangle$ or to $b_k|v^-\rangle$, where b_k denotes the creation operator corresponding to the fermionic energy with smallest real part and $k \neq 0$.

Whether the $(+,+)$-sector consists of the states (2.23) or (2.24) will be shown to depend on the value of η (see (2.22)) which will be calculated by computing the expectation value $\langle v^+|\sigma_{L+1}^x|v^+\rangle$. Note that we define $\langle v^{\pm}|$ via

$$\langle v^{\pm}| = \frac{1}{\sqrt{2}}(\langle vac| \pm \langle vac|a_0) \tag{2.25}$$

where $\langle vac|$ denotes the left vacuum of $\mathcal{H}_{\text{long}}$, i.e.

$$\langle vac|b_k = 0. \tag{2.26}$$

Note that if $\mathcal{H}_{long}$ is not hermitian, $\langle vac|$ is not equal to $|vac\rangle^\dagger$ in general.

In the second step (section 2.2.2) we will derive some special properties of the eigenvectors $(\phi_k^{\pm})$, which will play a crucial role in step three and four. In the third step (section 2.2.3), we are going to show how to calculate the one–point function

$$f(j) = \langle v^+|\sigma_j^x|v^+\rangle \tag{2.27}$$

In the present context, this is done merely for technical reasons in order to calculate $f(L+1)$, however it will be essential in another context. Namely, the explicit calculation of $f(j)$ will be presented in chapter 5. We would already like to remark that the calculation of $f(j)$ is similar to the calculation of the two-point function

$$g(i,j) = \langle v^+|\sigma_i^x\sigma_j^x|v^+\rangle. \tag{2.28}$$

Note that due to (2.21) one already sees that $f(j) = g(0, j)$. We show in section 2.2.3 that the functions $f(j)$ and $g(i, j)$ are both given by Pfaffians of submatrices of the same matrix. We will furthermore generalize these considerations to states of the form (2.23) and (2.24). These results also apply to $\mathcal{H}$ although we started with the larger space of states of $\mathcal{H}_{\mathrm{long}}$.

Using the results of step two we will obtain determinant representations for $f(j)$ and $g(i, j)$ which can be treated analytically in the calculation of $f(L+1)$. This calculation can be found in section 2.2.4 and will be the fourth step.

2.2.1 Algebraic considerations

In this subsection, we will show that the $(+,+)$-sector consists either of the states given by (2.23) or (2.24) and clarify the role of η given in (2.22). Because

$$(\phi_k^{\pm})_0^{+} = (\phi_k^{\pm})_{L+1}^{-} = 0, \forall k \neq 0 \tag{2.29}$$

which can be seen directly from the matrix M, we obtain the commutation relations

$$[\sigma_{L+1}^x, b_k] = [\sigma_{L+1}^x, a_k] = \{\sigma_0^x, b_k\} = \{\sigma_0^x, a_k\} = 0 \quad , \forall k \neq 0 \tag{2.30}$$

from (2.10) and therefore

$$[\sigma_0^x, N_k] = [\sigma_{L+1}^x, N_k] = 0 \quad , \forall k \neq 0. \tag{2.31}$$

Due to (2.31) the vectors $|v^{\pm}\rangle$ have to be eigenvectors of σ_{L+1}^x, i.e.

$$\sigma_{L+1}^x |v^{\pm}\rangle = \eta^{\pm} |v^{\pm}\rangle. \tag{2.32}$$

Thus the sector containing $|v^+\rangle$ respectively $|v^-\rangle$ is well defined and given by the value of η^+ and η^- respectively. Note that (2.32) is not as precise as (2.22) because (2.22) implies $\eta^+ = -\eta^-$.

Due to (2.30) we can make the following statement concerning the vectors of a given sector: If an arbitrary vector $|v\rangle$ is element of the $(\pm, \epsilon)$-sector where $\epsilon \in \{+, -\}$ then $b_k|v\rangle$ with $k \neq 0$ is element of the $(\mp, \epsilon)$-sector. Now one has to distinguish two cases:

First, if $|v^+\rangle$ is an element of the $(+,+)$-sector, i.e. $\eta^+ = +1$, then all the states given by (2.23) are also elements of the $(+,+)$-sector. The vector $|v^-\rangle$ then has to be an element of the $(-,-)$-sector because otherwise the $(-,-)$-sector would be missing in the space of states which is not the case. Thus we have $\eta^- = -1$.

Second, if $|v^+\rangle$ is an element of the $(+,-)$-sector, i.e. $\eta^+ = -1$, then $|v^-\rangle$ has to be an element of the $(-,+)$-sector. Otherwise $|v^-\rangle$ would be an element of the $(-,-)$-sector and there would be no $(+,+)$-sector. As a consequence we have that $\eta^- = +1$ and all the states given by (2.24) are elements of the $(+,+)$-sector.

In both cases, the subspace spanned by the vectors (2.23) respectively (2.24) has dimension 2^L and thus they form a basis of the $(+,+)$-sector. Because the values of η^+ and η^- always have opposite signs, we will use the variable η defined by (2.22) in the following.

2.2.2 Special properties of the eigenvectors of M

In this section we will show that in some cases there exist further relations between the eigenvectors $(\phi_k^{\pm})$ on top of the orthogonality relations (2.11) and (2.12). They will be used in the calculation of correlation functions and are also necessary for the computation of η. First notice that if $\alpha_z = \beta_z = 0$, the matrices M and M^2 respectively take the form

$$\mathsf{M} = \begin{pmatrix} 0 & * & 0 & * & \cdots \\ * & 0 & * & 0 & \\ 0 & * & 0 & * & \\ * & 0 & * & 0 & \\ \vdots & & & & \ddots \end{pmatrix} \qquad \mathsf{M}^2 = \begin{pmatrix} * & 0 & * & 0 & \cdots \\ 0 & * & 0 & * & \\ * & 0 & * & 0 & \\ 0 & * & 0 & * & \\ \vdots & & & & \ddots \end{pmatrix} \tag{2.33}$$

where $*$ and 0 both denote 2×2 matrices. Note that $*$ is the notation for an arbitrary 2×2 matrix and is not necessarily different from zero. Looking at (2.33) we see that we can choose an eigenvector $\tilde{\psi}_k^+$ of M^2 with eigenvalue Λ_k^2, i.e.

$$\mathsf{M}^2\tilde{\psi}_k^+ = \Lambda_k^2\tilde{\psi}_k^+ \tag{2.34}$$

which satisfies

$$(\tilde{\psi}_k^+)_i^{\pm} = 0 \quad \text{for } i \text{ odd.} \tag{2.35}$$

Now we define $\tilde{\psi}_k^-$ by

$$\mathsf{M}\tilde{\psi}_k^+ = -\mathrm{i}\Lambda_k\tilde{\psi}_k^- \tag{2.36}$$

which is also an eigenvector of M^2 with eigenvalue Λ_k^2. Note that this definition does not work if $\Lambda_k = 0$ and thus we have to exclude in the following $k = 0$ which labels the eigenvectors corresponding to the spurious zero mode. Using (2.33) and (2.35) we obtain

$$(\tilde{\psi}_k^-)_i^{\pm} = 0 \quad \text{for } i \text{ even.} \tag{2.37}$$

Due to (2.34) and (2.36) $\tilde{\psi}_k^+$ and $\tilde{\psi}_k^-$ also satisfy the relation

$$\mathsf{M}\tilde{\psi}_k^- = \mathrm{i}\Lambda_k\tilde{\psi}_k^+ \tag{2.38}$$

and thus we obtain eigenvectors $\tilde{\phi}_k^{\pm} = \tilde{\psi}_k^+ \mp \mathrm{i}\tilde{\psi}_k^-$ of M with

$$(\tilde{\phi}_k^+)_j^{\mu} = (-1)^j(\tilde{\phi}_k^-)_j^{\mu}. \tag{2.39}$$

Therefore for each pair of vectors ϕ_k^+, ϕ_k^- satisfying (2.11), there exists a constant $c \in \mathbb{C}$ such that

$$(\phi_k^+)_j^{\mu} = c(-1)^j(\phi_k^-)_j^{\mu}. \tag{2.40}$$

Now (2.12) can be rewritten as

$$(1 + (-1)^{i+j})\sum_{k=0}^{L+1}(\phi_k^+)_j^{\gamma}(\phi_k^-)_i^{\nu} = 2\delta_{ij}^{\gamma\nu} \tag{2.41}$$

and we end up with

$$\sum_{k=0}^{L+1}(\phi_k^+)_j^\gamma(\phi_k^-)_i^\nu = \delta_{ij}^{\gamma\nu} \qquad \text{for} \quad i+j \quad \text{even}. \tag{2.42}$$

Since (2.40) is not valid for $k=0$ and odd L (see (2.17)) we exclude $i=0, \nu=+, j=L+1, \gamma=-$ and $j=0, \gamma=+, i=L+1, \nu=-$ in (2.41) and (2.42).

If diagonal boundary terms are included, and if $\alpha_- = \alpha_+$ and $\beta_- = \beta_+$, the eigenvectors again have a special property. In this case M and M^2 have also the form of equation (2.33), but now $*$ and 0 just denote complex numbers and, in place of (2.40), we obtain

$$(\phi_k^+)_j^\pm = \pm c'(\phi_k^-)_j^\pm \tag{2.43}$$

which gives

$$\sum_{k=0}^{L+1}(\phi_k^-)_i^\mu(\phi_k^+)_j^\mu = \delta_{ij}. \tag{2.44}$$

Both of the equations (2.42) and (2.44) will appear to play a crucial role in section 2.2.3 and section 2.2.4.

Note that the proof of (2.42) and (2.44) shown above is not valid if there are degeneracies or zero modes on top of the spurious zero mode in the spectrum of M. However, one can show that it is always possible to build appropriate linear combinations of the eigenvectors corresponding to the same eigenvalue such that (2.42) and (2.44) remain valid in addition to (2.11) and (2.12). This is not automatically true and therefore in explicit calculations one should take care in choosing the right linear combination of eigenvectors corresponding to the degenerate eigenvalues.

If both conditions $\alpha_- = \alpha_+, \beta_- = \beta_+$ and $\alpha_z = \beta_z = 0$ are satisfied at the same time, then both of the equations (2.42) and (2.44) can be satisfied simultaneously. By comparing (2.40) and (2.43) we obtain the following relation

$$(\phi_k^-)_j^\pm = \begin{cases} \pm\frac{c'}{c}(\phi_k^-)_j^\pm & \text{for } j \text{ even} \\ \mp\frac{c'}{c}(\phi_k^-)_j^\pm & \text{for } j \text{ odd} \end{cases}. \tag{2.45}$$

Thus $\frac{c'}{c}$ is either 1 or -1 because otherwise the vectors $\phi_k^\pm$ would vanish.

We will now turn to the computation of the 1– and 2–point functions, where we will make use of the equations (2.42) for $\alpha_z = \beta_z = 0$ respectively (2.44) for $\alpha_- = \alpha_+, \beta_- = \beta_+$.

2.2.3 1- and 2- point functions of σ^x

In this section we are going to show how to compute the 1- and 2-point functions for the σ_j^x operator with respect to the states $|v^\pm\rangle$ defined by (2.20) and $\langle v^\pm|$ defined by (2.25) following the way of Lieb, Schultz and Mattis (LSM) [2]. The computation of the correlators of the operators σ_j^y can be done similarly. However, in this chapter we are only interested in the value of $\langle v^+|\sigma^x_j|v^+\rangle$ at the particular point $j = L+1$ which is calculated in section 2.2.4 using the results of this section. Due to (2.22) we thereby obtain the value of η which is needed for the projection from $\mathcal{H}_{\mathrm{long}}$ to $\mathcal{H}$ as described in the section 2.2. The calculation for general values of j will be the subject of section 5.

The main difference in comparison to the problem of LSM [2] is that in our case the 1-point functions do not vanish because of the non-diagonal boundary terms we are considering. They can be calculated in the same way as the 2-point correlators. At the end of this section, we will briefly remark how to compute the 1- and 2-point functions for excited states of $\mathcal{H}_{\mathrm{long}}$ of the form (2.23) and (2.24). This is not necessary for the calculation of η defined in (2.22), but it is needed for the calculation of the 1– and 2–point functions for the eigenstates of $\mathcal{H}$. Note that if $\eta = -1$ the ground state of $\mathcal{H}$ corresponds to an excited state of $\mathcal{H}_{\mathrm{long}}$.

We now proceed to the calculation of the 1– and 2–point functions. Writing σ^x_j in terms of the $\tau^\pm_i$ defined in (2.9) we obtain

$$\langle v^\pm \mid \sigma^x_j \mid v^\pm\rangle = \pm(-\mathrm{i})^j \langle v^\pm \mid \tau^-_0 \prod_{0<k<j} \tau^+_k \tau^-_k \tau^+_j \mid v^\pm\rangle \tag{2.46}$$

which is up to the sign exactly the 2–point function $\langle v^\pm \mid \sigma^x_0 \sigma^x_j \mid v^\pm\rangle$. In general

$$\langle v^\pm \mid \sigma^x_i \sigma^x_j \mid v^\pm\rangle = (-\mathrm{i})^{j-i} \langle v^\pm \mid \tau^-_i \prod_{i<k<j} \tau^+_k \tau^-_k \tau^+_j \mid v^\pm\rangle. \tag{2.47}$$

Of course i denotes $\sqrt{-1}$. Using (2.12) and (2.10) the $\tau^\pm_j$ can be expressed in terms of the creation and annihilation operators a_k and b_k, i.e.

$$\tau^\mu_j = \sum_{k=0}^{L+1} (\phi^-_k)^\mu_j a_k + (\phi^+_k)^\mu_j b_k. \tag{2.48}$$

Because $(\phi^\pm_0)^\mu_j$ is only different from zero if either $j = 0$ and $\mu = +$ or $j = L+1$ and $\mu = -$ (see (2.17)) we have

$$\langle v^\pm \mid \tau^-_i \prod_{i<k<j} \tau^+_k \tau^-_k \tau^+_j \mid v^\pm\rangle = \langle vac \mid \tau^-_i \prod_{i<k<j} \tau^+_k \tau^-_k \tau^+_j \mid vac\rangle. \tag{2.49}$$

For simplicity, we will denote $\langle vac|\hat{O}|vac\rangle$ by $\langle\hat{O}\rangle$ in the following where $\hat{O}$ denotes an arbitrary operator. Using Wick's theorem we are left with the calculation of the Pfaffian of the antisymmetric Matrix A, i.e.

$$\langle \tau^-_i \prod_{i<k<j} \tau^+_k \tau^-_k \tau^+_j \rangle = \mathrm{Pf}\mathsf{A} \tag{2.50}$$

where

$$\mathsf{A} = \begin{pmatrix} 0 & \langle\tau^-_i\tau^+_{i+1}\rangle & \langle\tau^-_i\tau^-_{i+1}\rangle & \langle\tau^-_i\tau^+_{i+2}\rangle & \cdots & \langle\tau^-_i\tau^+_j\rangle \\ \langle\tau^+_{i+1}\tau^-_i\rangle & 0 & \langle\tau^+_{i+1}\tau^-_{i+1}\rangle & \langle\tau^+_{i+1}\tau^+_{i+2}\rangle & \cdots & \langle\tau^+_{i+1}\tau^+_j\rangle \\ \langle\tau^-_{i+1}\tau^-_i\rangle & \langle\tau^-_{i+1}\tau^+_{i+1}\rangle & 0 & \langle\tau^-_{i+1}\tau^+_{i+2}\rangle & \cdots & \langle\tau^-_{i+1}\tau^+_j\rangle \\ \langle\tau^+_{i+2}\tau^-_i\rangle & \langle\tau^+_{i+2}\tau^+_{i+1}\rangle & \langle\tau^+_{i+2}\tau^-_{i+1}\rangle & 0 & \cdots & \langle\tau^+_{i+2}\tau^+_j\rangle \\ \vdots & \vdots & \vdots & \vdots & \ddots & \vdots \\ \langle\tau^+_j\tau^-_i\rangle & \langle\tau^+_j\tau^+_{i+1}\rangle & \langle\tau^+_j\tau^-_{i+1}\rangle & \langle\tau^+_j\tau^+_{i+2}\rangle & \cdots & 0 \end{pmatrix}. \tag{2.51}$$

We want to remind the reader that the Pfaffian of a $2n \times 2n$ antisymmetric matrix A with matrix elements a_{ij} is defined by

$$\mathrm{Pf}\mathsf{A} = \frac{1}{n!2^n} \sum_{\sigma \in S_{2n}} \mathrm{sgn}(\sigma) a_{\sigma(1)\sigma(2)} a_{\sigma(3)\sigma(4)} \cdots a_{\sigma(2n-1)\sigma(2n)} \tag{2.52}$$

where S_{2n} denotes the symmetric group of degree $2n$.

The expectation values of the basic contractions of pairs which form the entries of A are evaluated using (2.48). Due to the property of $\langle vac|$ (cf. (2.26)) we obtain

$$\langle \tau_i^\mu \tau_j^\nu \rangle = \sum_{k=0}^{L+1} (\phi_k^-)_i^\mu (\phi_k^+)_j^\nu. \tag{2.53}$$

In general, no further simplification is possible.

Nevertheless there exist two special cases where the calculation of the Pfaffian can be reduced to the calculation of a determinant. Namely, this is possible if no diagonal boundary terms are present or if $\alpha_- = \alpha_+$ and $\beta_- = \beta_+$. This reduction uses the additional relations for the eigenvectors given by (2.42) or (2.44) respectively. Note that the general relation $(\mathrm{Pf}\mathsf{A})^2 = \det \mathsf{A}$ is of no use because we are exactly interested in the sign of η.

In the absence of diagonal boundaries we can use (2.42) to simplify (2.53). Using similar arguments as LSM we also obtain a determinant representation for the correlation functions, however, the contributing contractions are different from theirs. In fact, using (2.42) results in

$$\langle \tau_i^\mu \tau_j^\nu \rangle = 0 \quad \text{for } i+j \text{ even} \tag{2.54}$$

and thus the correlation functions are given by subdeterminants of the $(L+1) \times (L+1)$ matrix

$$\mathsf{D} = \begin{pmatrix} \langle \tau_0^- \tau_1^+ \rangle & \langle \tau_0^- \tau_1^- \rangle & \langle \tau_0^- \tau_3^+ \rangle & \cdots \\ \langle \tau_2^+ \tau_1^+ \rangle & \langle \tau_2^+ \tau_1^- \rangle & \langle \tau_2^+ \tau_3^+ \rangle & \cdots \\ \langle \tau_2^- \tau_1^+ \rangle & \langle \tau_2^- \tau_1^- \rangle & \langle \tau_2^- \tau_3^+ \rangle & \cdots \\ \vdots & \vdots & \vdots & \ddots \end{pmatrix}. \tag{2.55}$$

Denoting by D_j^i the matrix D after elimination of the first i rows and columns and the last $L+1-j$ rows and columns we can write

$$\mathrm{Pf}\mathsf{A} = \mathrm{i}^{j-i} f_{ij} \det \mathsf{D}_j^i \tag{2.56}$$

where

$$f_{ij} = \begin{cases} -\mathrm{i} & \text{if } i \text{ even and } j \text{ odd} \\ \mathrm{i} & \text{if } i \text{ odd and } j \text{ even} \\ 1 & \text{otherwise} \end{cases}. \tag{2.57}$$

The calculation of $\mathrm{Pf}\mathsf{A}$ also simplifies if $\alpha_+ = \alpha_-$ and $\beta_+ = \beta_-$. In this case we can utilize (2.44) to obtain

$$\langle \tau_i^\mu \tau_j^\mu \rangle = 0. \tag{2.58}$$

This again results in a determinant representation of PfA, i.e.

$$\mathsf{PfA} = \begin{vmatrix} \langle\tau_i^-\tau_{i+1}^+\rangle & \langle\tau_i^-\tau_{i+2}^+\rangle & \cdots & \langle\tau_i^-\tau_j^+\rangle \\ \langle\tau_{i+1}^-\tau_{i+1}^+\rangle & \langle\tau_{i+1}^-\tau_{i+2}^+\rangle & \cdots & \langle\tau_{i+1}^-\tau_j^+\rangle \\ \vdots & \vdots & & \vdots \\ \langle\tau_{j-1}^-\tau_{i+1}^+\rangle & \langle\tau_{j-1}^-\tau_{i+2}^+\rangle & \cdots & \langle\tau_{j-1}^-\tau_j^+\rangle \end{vmatrix}. \tag{2.59}$$

Thus in (2.50) we are left with the calculation of the subdeterminants of a $(L{+}1)\times(L{+}1)$ matrix G with elements

$$\mathsf{G}_{kl} = \langle\tau_{k-1}^-\tau_l^+\rangle \tag{2.60}$$

where $1 \le k \le L+1$ and $1 \le l \le L+1$.

By simple modifications one can generalize the results of this section to excited states of the form (2.23) or (2.24). The argument runs as follows: Any state given by elementary excitations can be regarded as the vacuum state $|vac'\rangle$ of a new set of ladder operators, where the a_k and b_k of the excited fermions are interchanged. This corresponds to an interchange of the eigenvectors ϕ_k^- and ϕ_k^+ (see (2.10)). Thus the calculation of correlation functions for the states in (2.23) and (2.24) is equivalent to the calculation of the correlation functions for the states $|v^{+\prime}\rangle$ defined in the same way as $|v^+\rangle$ in (2.20) but now using

$$|vac'\rangle = \prod_{j=1}^{r} b_{k_j}|vac\rangle \tag{2.61}$$

as vacuum state where r is even or odd respectively and $k \neq 0$. The left vacuum defined by (2.26) has to be modified analogously. As consequence, we only have to replace (2.53) by

$$\langle\tau_i^\mu\tau_j^\nu\rangle = \sum_{k \text{ unexc.}} (\phi_k^-)_i^\mu(\phi_k^+)_j^\nu + \sum_{k \text{ exc.}} (\phi_k^+)_i^\mu(\phi_k^-)_j^\nu. \tag{2.62}$$

2.2.4 Calculation of $\langle\sigma_{L+1}^x\rangle$

If the diagonal boundary terms are absent or if $\alpha_+ = \alpha_-$ and $\beta_+ = \beta_-$, we can make use of (2.56) or (2.59) respectively in order to calculate

$$\eta = \langle v^+|\sigma_{L+1}^x|v^+\rangle. \tag{2.63}$$

Recall that we need the value of η to decide whether the $(+,+)$-sector of the space of states of $\mathcal{H}_{\text{long}}$ is given by the states of the form (2.23) or (2.24).

Thus if no diagonal boundary terms are present, we have to calculate $\det\mathsf{D}$ where D is defined by (2.55). This determinant can be written as the product of two determinants

$$(-1)^L \det\mathsf{D} = \det\mathsf{A}_\mathrm{g}\det\mathsf{A}_\mathrm{u} \tag{2.64}$$

where

$$\mathsf{A}_{\rm g} = \begin{pmatrix} (\phi_1^-)_0^- & (\phi_2^-)_0^- & (\phi_3^-)_0^- & \cdots \\ (\phi_1^-)_2^- & (\phi_2^-)_2^- & (\phi_3^-)_2^- & \cdots \\ (\phi_1^-)_2^+ & (\phi_2^-)_2^+ & (\phi_3^-)_2^+ & \cdots \\ \vdots & \vdots & \vdots & \ddots \end{pmatrix} \mathsf{A}_{\rm u} = \begin{pmatrix} (\phi_1^+)_1^- & (\phi_1^+)_1^+ & (\phi_1^+)_3^- & \cdots \\ (\phi_2^+)_1^- & (\phi_2^+)_1^+ & (\phi_2^+)_3^- & \cdots \\ (\phi_3^+)_1^- & (\phi_3^+)_1^+ & (\phi_3^+)_3^- & \cdots \\ \vdots & \vdots & \vdots & \ddots \end{pmatrix}. \tag{2.65}$$

The factor $(-1)^L$ is due to permutations of rows and columns which can be seen by comparing the product $\mathsf{A}_{\rm g}\mathsf{A}_{\rm u}$ with D. Without loss of generality we may assume that the eigenvectors are normalized in such a way that they satisfy (2.40) with $c = 1$. Using (2.42) we then find

$$\mathsf{A}_{\rm g}\mathsf{A}_{\rm g}^{\rm t} = \mathbf{1} \qquad \mathsf{A}_{\rm u}\mathsf{A}_{\rm u}^{\rm t} = -\mathbf{1}. \tag{2.66}$$

Due to the special form of the matrix M (see (2.33)) and to (2.40) the two matrices $\mathsf{A}_{\rm g}$ and $\mathsf{A}_{\rm u}$ are related by a matrix $\mathsf{M}_{\rm g\to u}$ via

$$\mathbf{\Lambda}^{-1}\mathsf{M}_{\rm g\to u}\mathsf{A}_{\rm g} = \mathsf{A}_{\rm u}^{\rm t} \tag{2.67}$$

where $\mathbf{\Lambda}_{kk'} = \Lambda_k\delta_{kk'}$ with $k > 0$. The matrix $\mathsf{M}_{\rm g\to u}$ is given by

$$\mathsf{M}_{\rm g\to u} = \begin{pmatrix} -\mathsf{G}'^{\rm t} & \mathsf{L} & 0 & 0 & 0 \\ 0 & -\mathsf{L}^{\rm t} & \ddots & 0 & 0 \\ 0 & 0 & \ddots & \mathsf{L} & 0 \\ 0 & 0 & 0 & -\mathsf{L}^{\rm t} & \mathsf{K}' \end{pmatrix} \tag{2.68}$$

for L odd or

$$\mathsf{M}_{\rm g\to u} = \begin{pmatrix} -\mathsf{G}'^{\rm t} & \mathsf{L} & 0 & 0 & 0 \\ 0 & -\mathsf{L}^{\rm t} & \ddots & 0 & 0 \\ 0 & 0 & \ddots & \mathsf{L} & 0 \\ 0 & 0 & 0 & -\mathsf{L}^{\rm t} & \mathsf{L} \\ 0 & 0 & 0 & 0 & -\mathsf{K}'^{\rm t} \end{pmatrix} \tag{2.69}$$

for L even, where we denoted by G' the matrix G of (2.8) with the second row eliminated and by K' the matrix K of (2.8) with the first column eliminated. Note that the eliminated rows and columns contain only entries which are equal to zero.

Using the (2.67) and (2.66) in (2.64), we obtain

$$\det\mathsf{D} = (-1)^L \det\mathbf{\Lambda}^{-1}\det\mathsf{M}_{\rm g\to u}. \tag{2.70}$$

The value of $\det\mathsf{M}_{\rm g\to u}$ can be computed in an elementary way

$$\det\mathsf{M}_{\rm g\to u} = \begin{cases} -(\alpha_-\beta_+ + \alpha_+\beta_-)/4^{L+1} & \text{for L odd} \\ -{\rm i}(\alpha_-\beta_+ + \alpha_+\beta_-)/4^{L+1} & \text{for L even} \end{cases} \tag{2.71}$$

Plugging this into (2.56), we end up with

$${\rm Pf}\mathsf{A} = (-{\rm i})^{L+1}\frac{\alpha_-\beta_+ + \alpha_+\beta_-}{4^{L+1}\prod_{k\neq 0}\Lambda_k}. \tag{2.72}$$

If $\alpha_- = \alpha_+$ and $\beta_- = \beta_+$, we obtain the same result by using equation (2.59) and performing a similar calculation. Combining the equations (2.46),(2.49) and (2.50) with (2.72) we are left in both cases with

$$\eta = \langle v^+ | \sigma^x_{L+1} | v^+ \rangle = (-1)^{L+1} \frac{\alpha_- \beta_+ + \alpha_+ \beta_-}{4^{L+1} \prod_{k \neq 0} \Lambda_k}. \tag{2.73}$$

Notice that in these cases the expression of η does not depend on α_z and β_z. It is not possible to calculate the product of all eigenvalues in (2.73) in general, but the squared product of eigenvalues can be calculated from $\det \mathsf{M}'$ where M' denotes the matrix M with the second and the last but one row and column eliminated. In both cases this yields

$$\det \mathbf{\Lambda}^2 = (-1)^{L+1} \det \mathsf{M}' = (\alpha_- \beta_+ + \alpha_+ \beta_-)^2 / 4^{2L+2} \quad . \tag{2.74}$$

If the Hamiltonian is hermitian, the product of eigenvalues is simply given by $\prod_{k \neq 0} \Lambda_k = |\alpha_- \beta_+ + \alpha_+ \beta_-| / 4^{L+1}$. This also holds for Hamiltonians with only real entries because in these cases the product is real and positive. Thus, we can apply equation (2.73) directly. Otherwise one would have to know all the eigenvalues explicitly.

Note that the value of η can only change by variation of the boundaries if one crosses a point in the parameter space at which an additional mode with $\mathrm{Re}\Lambda_k = 0$ and $k \neq 0$ exists. This is due to the fact that the eigenvalues of $\mathcal{H}$ and $\mathcal{H}_{\mathrm{long}}$ are continuous functions of the boundary parameters. But at a point satisfying the above condition the value of η is not well defined because the corresponding ladder operators a_k and b_k are not well defined and therefore one can aquire a change of sign in η by passing through such a point.

If $\mathcal{H}$ is hermitian the condition to have a mode with $\mathrm{Re}\Lambda_k = 0$ and $k \neq 0$ is equivalent to the existence of an additional zero mode. The presence of such a zero mode corresponds to the root $z = -1$ in the polynomial given by (2.14). This implies the condition $\alpha_- \beta_+ + \alpha_+ \beta_- = 0$. Thus if $\mathcal{H}$ is hermitian, i.e. $\alpha_+ = \alpha_-^*, \beta_+ = \beta_-^*$, we have to only distinguish the two regions $\mathrm{Re}(\alpha_- \beta_+) > 0$ and $\mathrm{Re}(\alpha_- \beta_+) < 0$. Thus, we conclude that if $\mathcal{H}$ is hermitian we obtain the following expression for η

$$\eta = (-1)^{L+1} \mathrm{sign}(\mathrm{Re}(\alpha_- \beta_+)). \tag{2.75}$$

The results of this section, namely the equations (2.73) and (2.75), allow us to calculate the ground state energy of $\mathcal{H}$ for the exactly solvable cases of table 2.1. This will be the subject of the next section.

2.3 Ground state energies for the Hamiltonian $\mathcal{H}$ in the exactly solvable cases

In section 2.2 we seen that the ground-state of $\mathcal{H}$ corresponds either to the state $|v^+\rangle$ or to $b_{\min} |v^-\rangle$ (see (2.20)), where by $b_{\min}$ we denote the creation operator associated to the fermion energy $2\Lambda_{\min}$ with the smallest real part, but which does not correspond to the spurious zero mode. Which of these two states corresponds to the ground state depends on the eigenvalue η of $|v^+\rangle$ with respect to the operation of σ^x_{L+1}. If $\eta = 1$, then the ground state corresponds to $|v^+\rangle$ and the ground state energy of $\mathcal{H}$ is equal to the ground state energy of $\mathcal{H}_{\text{long}}$. If $\eta = -1$, then the ground state corresponds to $b_{\text{min}}|v^-\rangle$ and the ground state energy of $\mathcal{H}$ is given by $E_0(\mathcal{H}_{\text{long}}) + 2\Lambda_{\text{min}}$. For the exactly solvable cases, the ground state energies for $\mathcal{H}_{\text{long}}$ are already given in [56].

However, as we have seen in the previous section η may be computed using (2.73) only if one of the following conditions is satisfied:

a. $\mathcal{H}_{\text{long}}$ is hermitian
b. $\mathcal{H}_{\text{long}}$ has no σ^z boundary terms ($\alpha_z = \beta_z = 0$)
c. $\alpha_- = \alpha_+$ and $\beta_+ = \beta_-$.

For case a. we may alternatively use (2.75) in order to obtain η.

Furthermore, note at this point that η may not be computed in terms of the parameters A, B, C, D, E given in (2.15). So for all the cases listed in table 2.1, we solved (2.15) for $\alpha_-, \alpha_+, \beta_-, \beta_+, \alpha_z, \beta_z$ and allowed only solutions which additionally satisfy one of the conditions a.-c. above. These solutions (which are obviously not unique) are listed in table 2.3. The choices of boundary parameters obtained from the ones given in table 2.3 by application of an obvious similarity transformation to the Hamiltonian $\mathcal{H}$ such as reflecting the Hamiltonian in the middle of the chain or performing a rotation around the z-axis are not explicitely listed.

In table 2.3 we have also given the value of Λ_{min}, which may depend on the value of the free parameter s and the lattice length (see e.g. case 14 L even or case 15 L odd). For some cases from table 2.1 which depend on a free parameter s, the conditions a.-c. restrict the possible values of s. This is indicated in the last but not least column of the table.

In the generic case the value of η is determined by the values of $\alpha_-, \alpha_+, \beta_-, \beta_+$ given in the fifth column. Using (2.73) (the values of the Λ_k can be obtained from the zeros of the polynomials $q(z)$ given in table 2.1) this yields $\eta = (-1)^{L+1}$ if $\text{Re}(\alpha_+\beta_- + \alpha_-\beta_+) > 0$ and $\eta = (-1)^L$ if $\text{Re}(\alpha_+\beta_- + \alpha_-\beta_+) < 0$. The values of η are not given in table 2.3, since there is still a freedom in the choice of the $\alpha_-, \alpha_+, \beta_-, \beta_+$.

In the case $\text{Re}(\alpha_+\beta_- + \alpha_-\beta_+) = 0$ one has to take some care. This may happen for the cases which depend on a free parameter s. For all these cases the value of $\alpha_+\beta_- + \alpha_-\beta_+$ is proportional to $\sqrt{s} + 1/\sqrt{s}$. Before one can give the value of η one has to fix which square root has to be taken in this expression and in the respective expressions for the fermion energies (see table 2.3). We omit any further discussion on this special case.

Note that (2.73) is of no use if there exists an additional zero mode on top of the spurious mode (which implies $\alpha_+\beta_- + \alpha_-\beta_+ = 0$). However, in this case the energies of the states $|v^+\rangle$ and $b_{\text{min}}|v^-\rangle$ are identical and hence the ground-state energy of $\mathcal{H}$ equals the ground-state energy of $\mathcal{H}_{\text{long}}$ independently of the value of η.

Table 2.2. The values of the boundary parameters for the factorizable cases in table 2.1 where the projection mechanism can be applied. The value of $2\Lambda_{\min}$ has to be added to the ground-state energy of $\mathcal{H}_{\text{long}}$ in order to obtain the ground-state energy of $\mathcal{H}$ if $\eta = (-1)$ (see (2.73)). Otherwise the ground-state energy of $\mathcal{H}$ equals the ground-state energy of $\mathcal{H}_{\text{long}}$. By $\min(a, b)$ we denote the value of either a or b, depending on which has the smaller real part.

Case	L	α_z	β_z	α_- α_+ β_+ β_-	s	$2\Lambda_{\min}$
1	arb.	0	0	$\alpha_-\alpha_+ = 1 \quad \beta_+\beta_- = \frac{1}{2} \quad \alpha_+\beta_- = \pm\frac{(1+\mathrm{i})}{2}$		$\sin\frac{\pi}{4L+6}$
2	arb.	0	0	$\alpha_-\alpha_+ = 1 \quad \beta_+ = \beta_- = 0$		0
	arb.	0	$\frac{1}{\sqrt{2}}$	$\alpha_- = \alpha_+ = \frac{1}{\sqrt{2}} \quad \beta_+ = \beta_- = 0$		0
3	arb.	0	0	$\alpha_-\alpha_+ = \frac{1}{2} \quad \beta_+ = \beta_- = 0$		0
4	arb.	0	$\frac{1}{\sqrt{2}}$	$\alpha_- = \alpha_+ = 1 \quad \beta_+ = \beta_- = 0$		0
	arb.	0	$\frac{\mathrm{i}}{\sqrt{2}}$	$\alpha_- = \alpha_+ = 0 \quad \beta_+ = \beta_- = \sqrt{2}$		0
5	even	0	0	$\alpha_-\alpha_+ = \frac{1}{2} \quad \beta_+\beta_- = \frac{1}{2} \quad \alpha_+\beta_- = \pm\frac{1}{2}$		$\sin\frac{\pi}{2L+6}$
	odd	0	0	$\alpha_-\alpha_+ = \frac{1}{2} \quad \beta_+\beta_- = \frac{1}{2} \quad \alpha_+\beta_- = \pm\frac{\mathrm{i}}{2}$		0
6	even	0	0	$\alpha_-\alpha_+ = \frac{1}{2} \quad \beta_+\beta_- = \frac{1}{2} \quad \alpha_+\beta_- = \pm\frac{\mathrm{i}}{2}$		0
	odd	0	0	$\alpha_-\alpha_+ = \frac{1}{2} \quad \beta_+\beta_- = \frac{1}{2} \quad \alpha_+\beta_- = \pm\frac{1}{2}$		$\sin\frac{\pi}{2L+4}$
7	even	0	0	$\alpha_-\alpha_+ = \frac{1}{2} \quad \beta_+\beta_- = 1 \quad \alpha_+\beta_- = \pm\frac{1}{\sqrt{2}}$		$\sin\frac{\pi}{2L+4}$
	odd	0	0	$\alpha_-\alpha_+ = \frac{1}{2} \quad \beta_+\beta_- = 1 \quad \alpha_+\beta_- = \pm\frac{\mathrm{i}}{\sqrt{2}}$		0
8	even	0	0	$\alpha_-\alpha_+ = \frac{1}{2} \quad \beta_+\beta_- = 1 \quad \alpha_+\beta_- = \pm\frac{\mathrm{i}}{\sqrt{2}}$		0
	odd	0	0	$\alpha_-\alpha_+ = \frac{1}{2} \quad \beta_+\beta_- = 1 \quad \alpha_+\beta_- = \pm\frac{1}{\sqrt{2}}$		$\sin\frac{\pi}{2L+4}$
9	even	0	0	$\alpha_-\alpha_+ = 1 \quad \beta_+\beta_- = 1 \quad \alpha_+\beta_- = \pm\sqrt{s}$		$\min(\sin(\frac{\pi}{2L+2} \pm \frac{\mathrm{i}\ln s}{2L+2}))$
	even	0	$\frac{\mathrm{i}}{\sqrt{2}}$	$\alpha_- = \alpha_+ = \pm\frac{1}{\sqrt{2}} \quad \beta_+ = \beta_- = \pm\sqrt{2}$ $\alpha_+\beta_- = \pm 1$	1	$\sin\frac{\pi}{2L+2}$
	odd	0	0	$\alpha_-\alpha_+ = 1 \quad \beta_+\beta_- = 1 \quad \alpha_+\beta_- = \pm\mathrm{i}\sqrt{s}$		$\min(\sin(\frac{\pi}{L+1} \pm \frac{\mathrm{i}\ln s}{2L+2}))$
	odd	0	$\frac{\mathrm{i}}{\sqrt{2}}$	$\alpha_- = \alpha_+ = \pm\frac{1}{\sqrt{2}} \quad \beta_+ = \beta_- = \pm\sqrt{2}$ $\alpha_+\beta_- = \pm 1$	-1	$\sin\frac{\pi}{2L+2}$
10	even	0	0	$\alpha_-\alpha_+ = \frac{s+1}{2} \quad \beta_+\beta_- = \frac{s+1}{2s}$ $\alpha_+\beta_- = \pm\frac{(\sqrt{s}+1/\sqrt{s})}{2}$		$\min(\sin\frac{\pi}{2L+2}, \frac{1}{2}(\sqrt{s}+1/\sqrt{s}))$
	even	0	$\frac{\mathrm{i}}{\sqrt{2}}$	$\alpha_- = \alpha_+ = \frac{1}{\sqrt{2}} \quad \beta_+ = \beta_- = \sqrt{\frac{2+s+1/s}{2}}$		$\min(\sin\frac{\pi}{2L+2}, \frac{1}{2}(\sqrt{s}+1/\sqrt{s}))$
	odd	0	0	$\alpha_-\alpha_+ = \frac{s+1}{2} \quad \beta_+\beta_- = \frac{s+1}{2s}$ $\alpha_+\beta_- = \pm\mathrm{i}\frac{(\sqrt{s}+1/\sqrt{s})}{2})$		0
	odd	0	$\frac{\mathrm{i}}{\sqrt{2}}$	$\alpha_- = \alpha_+ = \pm\frac{1}{\sqrt{2}} \quad \beta_+ = \beta_- = 0$	-1	0
11	arb.	0	$\frac{1}{\sqrt{2}}$	$\alpha_- = \alpha_+ = \beta_+ = \beta_- = 0$	-1	0
12	arb.	$\frac{1}{\sqrt{2}}$	$\frac{1}{\sqrt{2}}$	$\alpha_- = \alpha_+ = \beta_+ = \beta_- = 0$	1	0
	arb.	$\frac{\mathrm{i}}{\sqrt{2}}$	$\frac{-\mathrm{i}}{\sqrt{2}}$	$\alpha_- = \alpha_+ = 0 \quad \beta_+ = \beta_- = \sqrt{2}$	1	0
13	arb.	$\frac{\mathrm{i}}{\sqrt{2}}$	$\frac{-\mathrm{i}}{\sqrt{2}}$	$\alpha_- = \alpha_+ = 0 \quad \beta_+ = \beta_- = 1$	-1	0
14	even	$\frac{\mathrm{i}}{\sqrt{2s}}$	$\mathrm{i}\sqrt{\frac{s}{2}}$	$\alpha_- = \alpha_+ = \sqrt{\frac{1+s}{s}} \quad \beta_+ = \beta_- = \sqrt{1+s}$		$\min(\sin\frac{\pi}{2L}, \frac{1}{2}(\sqrt{s}+1/\sqrt{s}))$
	odd	$\frac{1}{\sqrt{2}}$	$\frac{-1}{\sqrt{2}}$	$\alpha_- = \alpha_+ = \beta_+ = \beta_- = 0$	-1	0
15	even	$\frac{1}{\sqrt{2}}$	$\frac{1}{\sqrt{2}}$	$\alpha_- = \alpha_+ = \beta_+ = \beta_- = 0$	-1	0
	odd	$\frac{\mathrm{i}}{\sqrt{2s}}$	$-\mathrm{i}\sqrt{\frac{s}{2}}$	$\alpha_- = \alpha_+ = \sqrt{\frac{1+s}{s}} \quad \beta_+ = \beta_- = \sqrt{1+s}$		$\min(\sin\frac{\pi}{2L}, \frac{1}{2}(\sqrt{s}+1/\sqrt{s}))$
16	arb.	$\frac{1}{\sqrt{2s}}$	$\sqrt{\frac{s}{2}}$	$\alpha_- = \alpha_+ = \beta_+ = \beta_- = 0$		0
	arb.	$\frac{\mathrm{i}}{\sqrt{2}}$	$\frac{-\mathrm{i}}{\sqrt{2}}$	$\alpha_- = \alpha_+ = 0 \quad \beta_+ = \beta_- = \sqrt{\frac{s}{2} + \frac{1}{\sqrt{2s}}}$		0

2.4 Conclusions

In this chapter we have shown how to obtain the eigenvalues and eigenvectors of the Hamiltonian $\mathcal{H}$ given by (1.2) using the respective results for the Hamiltonian $\mathcal{H}_{\text{long}}$ which can be diagonalized in terms of free fermions (see section 2.1).

We have seen in section 2.2 that the eigenvalues and eigenvectors of $\mathcal{H}$ are obtained from the spectrum of $\mathcal{H}_{\text{long}}$ by excluding the spurious zero mode (which is always present in the spectrum of $\mathcal{H}_{\text{long}}$) from the set of fermion energies and then taking the sector with an even or with an odd number of fermions being excited with respect to the state $|v^+\rangle$ respectively $|v^-\rangle$ (see (2.23) respectively (2.24)). The states $|v^\pm\rangle$ are defined in (2.20).

Whether one has to pick up the even or the odd sector has been shown to depend on the value of a parameter η defined by (2.22). The value of η is either $+1$ or -1. If $\eta = 1$ one has to take the even sector and if $\eta = -1$ one has to take the sector with an odd number of excitations.

The value of η has been calculated in section 2.2.4 by computing the expectation value $\langle v^+|\sigma^x_{L+1}|v^+\rangle$. If $\mathcal{H}$ is hermitian the value of η is given by (2.75) in terms of the boundary parameters α_- and β_+. If the Hamiltonian is non-hermitian our result is restricted to the cases where $\alpha_z = \beta_z = 0$ or $\alpha_+ = \alpha_-, \beta_+ = \beta_-$. For these cases the value of η is given by the expression (2.73) in terms of the parameters $\alpha_\pm, \beta_\pm$ and the fermion energies Λ_k. Both expressions ((2.75) and (2.73)) are not valid if there exists a zero mode on top of the spurious mode. However, in this case the spectra of the even and of the odd sector are identical.

In section 2.3 we applied our results to the computation of the ground-state energies of $\mathcal{H}$ for the exactly solvable cases (given in table 2.1) in terms of the ground-state energies of $\mathcal{H}_{\text{long}}$ which have already been given in [56].

As a by-product of our computations we have found a representation of the σ^x one– and two–point functions in terms of pfaffians in section 2.2.3 (see (2.46)-(2.51)). The calculation of the pfaffians may be reduced to the calculation of determinants if $\alpha_z = \beta_z = 0$ or $\alpha_+ = \alpha_-, \beta_+ = \beta_-$ (see (2.56) and (2.59)). We will make use of these results in chapter 5.

Chapter 3

Finite size scaling and partition functions

In the previous chapter we have shown how to diagonalize the Hamiltonian (1.2) by introducing the auxiliary Hamiltonian (2.1), which in turn may be diagonalized in terms of free fermions.

While in chapter 2 our focus was on the diagonalization of the finite chain, here we are going to examine the asymptotic behaviour of the energy levels for large values of L. In the case of conformal invariance this information is usually encoded in the partition function, which we define by

$$\mathcal{Z} = \lim_{L\to\infty} \operatorname{tr} z^{\frac{L}{\xi}(\mathcal{H} - e_\infty L - f_\infty)} \tag{3.1}$$

where $z < 1$ and e_∞ and f_∞ denote the free bulk and the free surface energy respectively. ξ may be considered as a normalization constant here.

In the case of hermitian boundary terms we will obtain the partition functions of the free compactified boson field on a cylinder with Neumann-Neumann, Dirichlet-Neumann or Dirichlet-Dirichlet boundary conditions. This applies also for certain non-hermitian boundaries. For the factorizable cases given in table 2.1 we will also compute the free surface energy. For certain non-hermitian boundary terms we will obtain logarithmic corrections to the free surface energy. We will also discuss the asymmetric version of the XX–model with boundaries (this includes the Dzyaloshinsky-Moriya interaction). We will also consider the partition functions for $\mathcal{H}_{\mathrm{long}}$. This chapter is based on [58].

3.1 Introduction

In the case of periodic boundary conditions the continuum limit of the XXZ–chain can be described by a free boson field Φ (see e.g. [61]), with action

$$S = \frac{1}{2}\int dx_1 dx_2 \left[(\partial_1\Phi)^2 + (\partial_2\Phi)^2\right] \tag{3.2}$$

being compactified on a circle of radius r, i.e. we identify Φ with $\Phi + 2\pi r$ (we follow the notation of [62]). The radius of compactification r is related to the value of the anisotropy in the XXZ–model. At the free fermion-point the anisotropy is zero and we have $r = 1/\sqrt{4\pi}$.

Consider the boson field on a cylinder of length L and circumference N imposing periodic boundary conditions in the direction of the cylinders length. Quantizing the field with time in N-direction yields the partition function [62]

$$\mathcal{Z}_{\text{periodic}} = \frac{1}{\eta(q)^2} \sum_{m,n\in\mathbb{Z}} q^{\frac{1}{2}\left(\frac{m^2}{2\pi r^2}+2\pi r^2 n^2\right)} \tag{3.3}$$

where $q = \mathrm{e}^{-2\pi N/L}$ and

$$\eta(q) = q^{\frac{1}{24}} \prod_{n=1}^{\infty}(1-q^n). \tag{3.4}$$

This expression coincides with the partition function for the periodic XXZ-chain, which has been studied extensively in [63, 64, 65]. The partition function for $\mathcal{H}_{\text{long}}$ in the periodic case is just $4\mathcal{Z}_{\text{periodic}}$.

Suppose now the case of open boundaries at both ends of the cylinder. There are two different boundary conditions preserving conformal invariance, i.e. the Dirichlet and the von Neumann (see e.g. [62, 66]). This yields three different partition functions corresponding to the various possible combinations of the two boundary conditions. The respective partition functions can be found in [62, 66]. Imposing Dirichlet boundary conditions at both ends of the cylinder results in

$$\mathcal{Z}_{\text{DD}}(\Delta) = \frac{1}{\eta(q)} \sum_{n\in\mathbb{Z}} q^{\frac{1}{2}(2\sqrt{\pi}rn+\Delta)^2} \tag{3.5}$$

where $q = \mathrm{e}^{-\pi N/L}$ and $\Delta = (\Phi_0 - \Phi_L)/\sqrt{\pi}$. By Φ_0 and Φ_L we denote the values of the boson field at the boundaries. This type of partition function has also been obtained for the open XXZ-chain with diagonal, hermitian boundary fields [67].

The Neumann-Neumann partition function is given by

$$\mathcal{Z}_{\text{NN}}(\Delta) = \frac{1}{\eta(q)} \sum_{m\in\mathbb{Z}} q^{2(m/(2\sqrt{\pi}r)+\Delta/2)^2} \tag{3.6}$$

where $\Delta = (\tilde{\Phi}_0 - \tilde{\Phi}_L)/\sqrt{\pi}$ and $\tilde{\Phi}_0, \tilde{\Phi}_L$ denote the values of the dual field $\tilde{\Phi}$ at the boundaries [62, 66]. The Dirichlet-Neumann boundary condition yields [62, 66]

$$\mathcal{Z}_{\text{DN}} = \frac{1}{2\eta(q)} \sum_{k\in\mathbb{Z}} q^{\frac{1}{4}(k-1/2)^2}. \tag{3.7}$$

In this case no free parameter appears.

Which boundary conditions of the Hamiltonian $\mathcal{H}$ lead to the partition functions (3.6) and (3.7) is yet not known. We will close this gap. We are going to see that, as long as the Hamiltonian $\mathcal{H}$ is hermitian, the partition function of the chain corresponds to one of the three boson partition functions for open boundaries. However, this may also be the case for certain non-hermitian boundary terms. See section 3.2 for a survey over the boundary conditions which we will consider.

In [90] it has been argued that non-diagonal boundary terms correspond to von Neumann boundary conditions for the boson field. Our results will show that this assumption is correct in the hermitian case, but not necessarily for non-hermitian boundaries.

In this chapter we also study the asymmetric XX–chain with boundaries (see equation (3.23)). This includes the quantum chain with Dzyaloshinsky-Moriya interactions, which was already studied in [68] for periodic boundary conditions. The partition function for real values of p and q in (3.23) and periodic boundary conditions was obtained in [71]. The special case $p = 1$ and $q = 0$ with boundaries has already been studied in [69].

The remaining part of this chapter is organized as follows: We will start with a summary of our results for the symmetric chain with hermitian and non-hermitian boundaries in section 3.2. The asymmetric XX-chain will be discussed in section 3.3. We will give our conclusions in section 3.4. The computation of the asymptotic behaviour of the fermion energies for $L \gg 1$, which yields the partition functions (see (3.1)), has been postponed to appendix A.

3.2 Summary of results

The structure of our results is most simply encoded in terms of new parameters F, C, G, K, J, where

$$\begin{aligned}
F &= 4\alpha_-\alpha_+\beta_+\beta_- \\
C &= \alpha_-^2\beta_+^2 + \alpha_+^2\beta_-^2 \\
G &= 2\alpha_-\alpha_+(1+2\beta_z^2) + 2\beta_-\beta_+(1+2\alpha_z^2) \\
K &= 2(\alpha_-\alpha_+ + \beta_-\beta_+) + (1+2\alpha_z^2)(1+2\beta_z^2) \\
J &= 8\alpha_z\beta_z - 4\alpha_z^2\beta_z^2 + 2(\alpha_-\alpha_+ + \beta_-\beta_+) + 2\alpha_z^2 + 2\beta_z^2 - 1.
\end{aligned} \tag{3.8}$$

The six different situations we considered are given in table 3.1. This table also indicates which kind of partition function we obtained for $\mathcal{H}$. For hermitian boundaries the cases in this table cover the whole parameter space. This is not the case for non-hermitian boundary terms.

For the cases in table 3.1 we computed analytically the energy gaps in the leading order as shown in appendix A. The exact ground-state energies of $\mathcal{H}_{\rm long}$ for certain cases, being listed in table 3.2, have already been obtained in [57].

However, the information of the energy gaps is already sufficient to obtain the partition functions for $\mathcal{H}_{\rm long}$ upto a factor $z^{-\frac{1}{24}+h_{\rm min}}$, where $h_{\rm min}$ denotes the lowest highest weight appearing in the representation of the Virasoro algebra. This information has to be extracted from the ground-state energies [70]

$$E_0 = e_\infty L + f_\infty - \frac{\pi}{L}\left(\frac{1}{24} - h_{\rm min}\right) + \ldots \tag{3.9}$$

Table 3.1. Conditions on the parameters F, C, G, K, J being considered in this chapter. An asterisk indicates that the corresponding value may be arbitrary. The partition functions $\mathcal{Z}_{DD}, \mathcal{Z}_{NN}$ and $\mathcal{Z}_{DN}$ are defined in (3.5),(3.6) and (3.7). For the last two cases we obtained anomalous behaviour of the energies (see section 2.5). We use h. and n-h. as a shortcut for hermitian and non-hermitian.

F	C	G	K	J		
$\neq 0$	*	*	*	*	$\mathcal{Z}_{NN}$	h. and n-h.
0	0	$\neq 0$	*	*	$\mathcal{Z}_{DN}$	h. and n-h.
0	0	0	$\neq 0$	*	$\mathcal{Z}_{DD}$	h. and n-h.
0	0	0	0	0	$2 \times \mathcal{Z}_{DD}$	n-h.
0	$\neq 0$	$\neq 0$	*	*	anom.	n-h.
0	0	0	0	$\neq 0$	anom.	n-h.

The value of the free bulk-energy is already known from the periodic chain, i.e. $e_\infty = -\frac{1}{\pi}$ [2]. The values of the free surface energies f_∞ and of h_{min} have been obtained for the cases given in table 3.2 expanding the exact expressions for the finite chain given in [57].

The results confirm the partition functions we will give for $\mathcal{H}_{\text{long}}$ in the following. For the cases not being listed in table 3.2 we checked our expressions numerically. The partition functions for $\mathcal{H}$ have been obtained afterwards by projecting onto the $(+,+)$-sector (see section 2.2 for details on the projection mechanism). We are now going to discuss the cases given in table 3.1 in detail.

3.2.1 Neumann-Neumann boundary conditions

The condition $F \neq 0$ simply implies that all non-diagonal boundary terms are present. The diagonal terms may be arbitrary. It is quite instructive to introduce a new parametrisation of the boundary parameters $\alpha_\pm$ and $\beta_\pm$ as follows:

$$\alpha_+ = R_\alpha \mathrm{e}^{\mathrm{i}\pi\varphi} \quad \alpha_- = R_\alpha \mathrm{e}^{-\mathrm{i}\pi\varphi} \quad \beta_+ = R_\beta \mathrm{e}^{\mathrm{i}\pi(\chi+\varphi)} \quad \beta_- = R_\beta \mathrm{e}^{-\mathrm{i}\pi(\chi+\varphi)} \tag{3.10}$$

where $R_\alpha, R_\beta \in \mathbb{R}^+, \chi, \varphi \in \mathbb{R}, -1 < \chi \leq 1$. The value of Δ which enters the partition function (3.6) is then given by

$$\Delta = \begin{cases} \chi & \text{for } L \text{ odd} \\ \chi + 1 & \text{for } L \text{ even} \end{cases} . \tag{3.11}$$

The partition function for $\mathcal{H}_{\text{long}}$ is given by

$$\mathcal{Z}_{\text{long}} = 2\mathcal{Z}_{NN}(\chi) + 2\mathcal{Z}_{NN}(\chi + 1) \tag{3.12}$$

for even and odd values of L. Note that the parametrization (3.10) does not work for non-hermitian boundaries. In this case we may define the parameter χ via

$$\chi = \frac{\mathrm{i}}{2\pi} \ln \left(\frac{\alpha_- \beta_+}{\alpha_+ \beta_-} \right) \tag{3.13}$$

Table 3.2. The values of the parameters F, C, G, K, J for the cases where the ground-state energy of $\mathcal{H}_{\mathrm{long}}$ has been obtained in [57]. The table shows the free surface energy f_∞ and the lowest highest weight $h_{\min}$ (cf. (3.9)). The expressions for f_∞ are also valid for $\mathcal{H}$. ζ denotes a free parameter, which has to be chosen such that $0 \le \mathrm{Re}\zeta \le 2\pi$ for case 12 and $-\pi < \mathrm{Re}\zeta < \pi$ otherwise. The parameter ζ is related to the parameter s in table 2.1 and table 2.3 by $s + 1/s = 2\cos\zeta$.

							$h_{\min}$	
case	F	$(-1)^L C$	G	H	J	f_∞	L even	L odd
1	2	0	5	4	2	$1/4 - 3/(2\pi)$	1/32	
2	0	0	2	3	1	$1/4 - 4/\pi$	1/16	
3	0	0	1	2	0	$1/2 - 3/2\pi$	1/16	
4	0	0	4	4	2	$-1/(2\pi)$	1/16	
5	1	$\frac{1}{2}$	3	3	1	$1/2 - 2/\pi$	0	1/8
6	1	$-\frac{1}{2}$	3	3	1	$1/2 - 2/\pi$	1/8	0
7	2	1	5	4	2	$1/4 - 3/(2\pi)$	0	1/8
8	2	-1	5	4	2	$1/4 - 3/(2\pi)$	1/8	0
9	4	$(-1)^L 2\cos\zeta$	8	5	3	$-1/\pi$	$\zeta^2/(8\pi^2)$	
10	$2+2\cos\zeta$	$1+\cos\zeta$	$4+4\cos\zeta$	$3+2\cos\zeta$	$1+\cos\zeta$	$1/2 - 1/\pi - \cos(\zeta/2)/2$	0	1/8
11	$4+4\cos\zeta$	0	$6+6\cos\zeta$	$4+2\cos\zeta$	$2+2\cos\zeta$	$1/4 - 1/(2\pi) - \cos(\zeta/2)/2$	1/32	
12	$2-2\cos\zeta$	$\cos\zeta - 1$	$2-2\cos\zeta$	4	4	$1/2 - (\cos(\zeta/4) + \sin(\zeta/4))/2$	1/8	0
13	$4+4\cos\zeta$	$-2-2\cos\zeta$	$4+4\cos\zeta$	$4+2\cos\zeta$	$4+2\cos\zeta$	$1/2 - 1/(2\sqrt{2}) - \cos(\zeta/2)/2$	1/8	0
14	$8+8\cos\zeta$	$-2-2\cos\zeta$	$8+8\cos\zeta$	$6+2\cos\zeta$	$2\cos\zeta - 2$	$-\cos(\zeta/2)/2$	0	1/8
15	$8+8\cos\zeta$	$-4-4\cos\zeta$	$6+6\cos\zeta$	$6+2\cos\zeta$	$6+2\cos\zeta$	$-\cos(\zeta/2)/2$	1/8	0
16	0	0	0	$2+2\cos\zeta$	$2+2\cos\zeta$	$1/2 - \cos(\zeta/2)/2$	1/8	0

where the logarithm is taken in a way such that $0 \leq |\mathrm{Re}(\chi)| \leq \frac{1}{2}$ for $\mathrm{Re}(\alpha_+\beta_- + \alpha_-\beta_+) > 0$ and $1 \geq |\mathrm{Re}(\chi)| \geq \frac{1}{2}$ for $\mathrm{Re}(\alpha_+\beta_- + \alpha_-\beta_+) < 0$. This rule is consistent with the parametrisation (3.10), which implies $\mathrm{Re}(\alpha_+\beta_- + \alpha_-\beta_+) = 2R_\alpha R_\beta \cos(\chi\pi)$. However, we cannot perform the projection onto the $(+,+)$-sector in general if the boundaries are non-hermitian. In this case our result for the partition function of $\mathcal{H}$ is restricted to the cases listed in table 3.2 which satisfy the conditions $\alpha_z = \beta_z = 0$ or $\alpha_+ = \alpha_-, \beta_+ = \beta_-$ (see section 2.2). The result for $\mathcal{H}_{\mathrm{long}}$ is valid in general.

3.2.2 Dirichlet-Neumann boundary conditions

The conditions for the Dirichlet-Neumann case yield

$$\beta_\pm = 0 \quad \alpha_\pm \neq 0 \quad \beta_z \neq \pm\frac{\mathrm{i}}{\sqrt{2}} \quad \text{or} \quad \beta_\pm \neq 0 \quad \alpha_\pm = 0 \quad \alpha_z \neq \pm\frac{\mathrm{i}}{\sqrt{2}}. \tag{3.14}$$

The value of α_z respectively of β_z may be arbitrary. The partition function for $\mathcal{H}_{\mathrm{long}}$ is just $\mathcal{Z}_{\mathrm{long}} = 4\mathcal{Z}_{DN}$ for L even and odd. The case of one non-diagonal boundary at the end of a semi-infinite XX–chain has already been considered in [53]. The author has shown, that the model can be decoupled into two Ising models with different boundary conditions. One of them being subject to a free boundary condition at the end, the other one being subject to the fixed boundary condition. The partition functions for the Ising model with free and mixed boundary conditions are well known [70, 72]. Taking the product of them also results in (3.7).

3.2.3 Dirichlet-Dirichlet boundary conditions

The Dirichlet-Dirichlet partition function is obtained for two different types of boundary terms. The first type is given by

$$\beta_z \neq \pm\frac{\mathrm{i}}{\sqrt{2}} \quad \alpha_z \neq \pm\frac{\mathrm{i}}{\sqrt{2}} \quad \beta_- = \alpha_- = 0. \tag{3.15}$$

where instead of the last equation we might have also chosen $\beta_+ = \alpha_+ = 0$. However, for this type of boundaries the non-diagonal boundary terms have no influence on the energies even on the finite chain which can be seen from (2.14). The second type is given by

$$\beta_\pm = 0 \quad \alpha_\pm \neq 0 \quad \beta_z = \pm\frac{\mathrm{i}}{\sqrt{2}} \quad \text{or} \quad \beta_\pm \neq 0 \quad \alpha_\pm = 0 \quad \alpha_z = \pm\frac{\mathrm{i}}{\sqrt{2}} \tag{3.16}$$

where the values of α_z respectively β_z may be chosen arbitrarily. Note that for this second type the boundary terms are non-hermitian. For both types of boundaries the value of Δ which enters (3.5) is given by

$$\Delta = \frac{1}{2\pi}\arccos\left((-1)^{L+1}\frac{J}{K}\right). \tag{3.17}$$

The partition function for $\mathcal{H}_{\mathrm{long}}$ is $\mathcal{Z}_{\mathrm{long}} = 4\mathcal{Z}_{DD}(\Delta)$ for even and odd L.

3.2.4 $F = C = G = K = J = 0$

For the case $F = C = G = K = J = 0$ the boundary parameters are nearly fixed, i.e.

$$\alpha_z = \pm\frac{\mathrm{i}}{\sqrt{2}} \quad \beta_z = \mp\frac{\mathrm{i}}{\sqrt{2}} \tag{3.18}$$

and $\alpha_+ = \beta_+ = 0$ or $\alpha_- = \beta_- = 0$. This case is special. The partition function we obtained does not fit into the picture suggested by the analogy to the free boson. Here an additional zero mode appears. The partition for $\mathcal{H}$ is given by $\mathcal{Z} = 4\mathcal{Z}_{DD}(\Delta)$, where the value of Δ is given by $\Delta = 0$ for odd L and by $\Delta = 1/2$ for even L. The partition function for $\mathcal{H}_{\text{long}}$ is given by $\mathcal{Z}_{\text{long}} = 8\mathcal{Z}_{DD}(\Delta)$.

3.2.5 Anomalous behaviour

For the last two cases in table 3.1 we obtained logarithmic corrections to the free surface energy. Note that there is no case in table 3.2 which corresponds to the boundaries in question. However, we computed the ground-state energy E_0 of $\mathcal{H}_{\text{long}}$ numerically for one example of boundaries which lead to the anomalous behaviour. Our computations suggest

$$E_0 \sim -\frac{L}{\pi} + f_\infty + \frac{1}{L}\left(\rho_1 \ln L + \rho_2\right) \tag{3.19}$$

where ρ_1, ρ_2 are complex numbers. Figure 3.1 and figure 3.2 show the real respectively the imaginary part of the Casimir amplitude. The computation has been done for $\alpha_z = 1/\sqrt{2}, \beta_z = \mathrm{i}/\sqrt{2}, \alpha_\pm = \beta_\pm = 0$ which corresponds to the last case in table 3.1. In both cases the fermionic energies scale as

$$2\Lambda \sim \frac{1}{L}\left[k\pi \pm \frac{1}{2}\left(\arg\Delta - \mathrm{i}\ln L\right)\right] \qquad k = 0, 1, 2, ... \tag{3.20}$$

where the value of Δ is given by

$$\Delta = -\frac{4C}{G} \tag{3.21}$$

for $F = 0, C, G \neq 0$ respectively by

$$\Delta = (-1)^L \frac{2J}{1 - 4\alpha_z^2\beta_z^2} \tag{3.22}$$

for $F = C = G = K = 0, J \neq 0$. Our result for the last case makes only sense for $(\alpha_z\beta_z)^2 \neq 1/4$. The factor 2 in (3.20) is just a remnant from our notation in section 2.1. Note the integer spacing of the energy gaps (3.20).

3.3 The asymmetric XX-chain

We also considered the asymmetric XX-chain which is defined by the Hamiltonian

$$\begin{aligned}\mathcal{H}_{\mathrm{a}} = &\sum_{j=1}^{L-1}\left[p\sigma_j^+\sigma_{j+1}^- + q\sigma_j^-\sigma_{j+1}^+\right] \\ &+ \frac{1}{\sqrt{8}}\left[\alpha'_-\sigma_1^- + \alpha'_+\sigma_1^+ + \alpha_z\sigma_1^z + \beta'_-\sigma_L^- + \beta'_+\sigma_L^+ + \beta_z\sigma_L^z\right].\end{aligned} \tag{3.23}$$

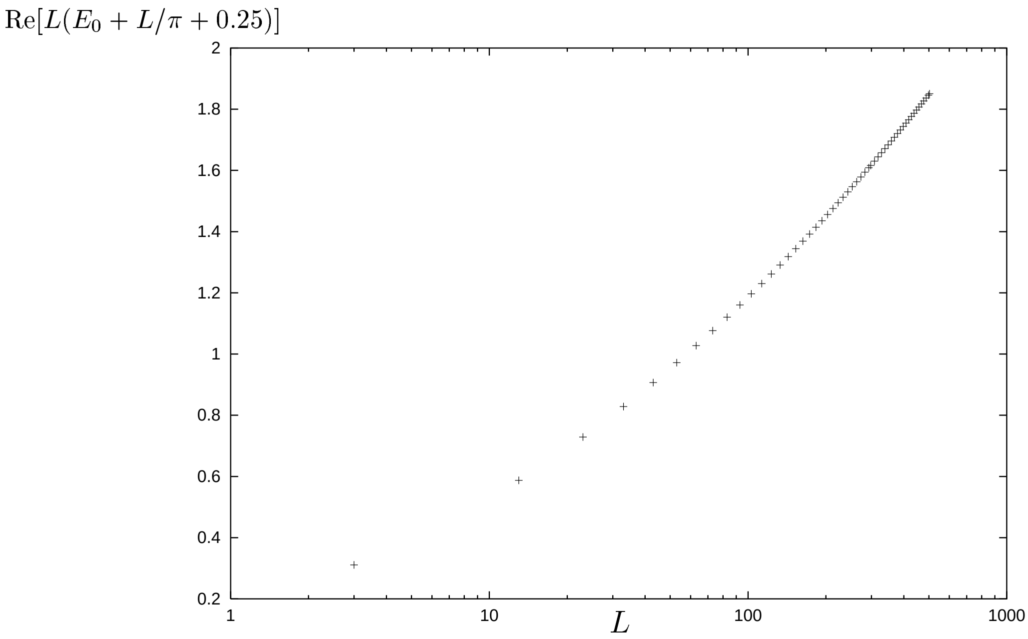

Figure 3.1. Real part of the Casimir amplitude ($\alpha_z = 1/\sqrt{2}, \beta_z = \mathrm{i}/\sqrt{2}, \alpha_\pm = \beta_\pm = 0$).

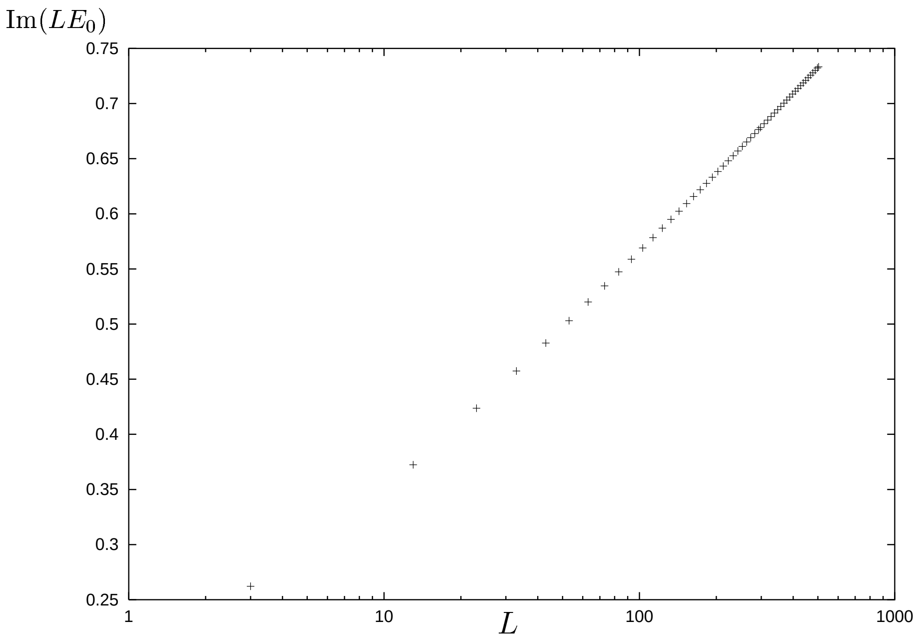

Figure 3.2. Imaginary part of the Casimir amplitude ($\alpha_z = 1/\sqrt{2}, \beta_z = \mathrm{i}/\sqrt{2}, \alpha_\pm = \beta_\pm = 0$).

Without loss of generality we restrict ourselves to $\sqrt{pq} = \frac{1}{2}$. Under this condition $\mathcal{H}_{\mathrm{a}}$ can be mapped on the symmetric chain (1.2) with boundary parameters

$$\alpha_- = Q^{\frac{1-L}{2}}\alpha'_- \quad \alpha_+ = Q^{\frac{L-1}{2}}\alpha'_+ \quad \beta_- = Q^{\frac{L-1}{2}}\beta'_- \quad \beta_+ = Q^{\frac{1-L}{2}}\beta'_+ \tag{3.24}$$

by a similarity transformation, where $Q = \sqrt{\frac{q}{p}}$. The diagonal terms remain unchanged. We will separate two cases in the following. First we will consider hermitian bulk terms, i.e.

$$p = \mathrm{e}^{\mathrm{i}\pi\kappa}/2, q = \mathrm{e}^{-\mathrm{i}\pi\kappa}/2. \tag{3.25}$$

This corresponds to Dzyaloshinsky-Moriya type interactions in the bulk. Thereafter we will turn to non-hermitian bulk terms with p, q in $\mathbb{R}$.

3.3.1 Dzyaloshinsky-Moriya interactions

We restricted ourselves to hermitian boundaries. In this case the value of κ has only an effect onto the spectra if non-diagonal boundary terms are present at both ends of the chain. We introduce the parametrization

$$\alpha'_+ = R'_\alpha \mathrm{e}^{\mathrm{i}\pi\varphi'} \quad \alpha'_- = R'_\alpha \mathrm{e}^{-\mathrm{i}\pi\varphi'} \quad \beta'_+ = R'_\beta \mathrm{e}^{\mathrm{i}\pi(\chi'+\varphi')} \quad \beta'_- = R'_\beta \mathrm{e}^{-\mathrm{i}\pi(\chi'+\varphi')}. \tag{3.26}$$

According to (3.24) and (3.10) the mapping onto symmetric bulk terms yields

$$R'_\alpha = R_\alpha \quad R'_\beta = R_\beta \quad \varphi = \varphi' + \kappa\frac{1-L}{2} \quad \chi = \chi' + \kappa(L-1) \bmod 2. \tag{3.27}$$

Remember that in the case of length independent boundary terms, the value of χ contains the full information about the partition function. Observe now, that it is possible to choose values of κ such that the value of χ in (3.27) becomes independent of L as long as one considers only certain sequences of lattice lengths. This is exactly the case if $\kappa/2$ is rational, i.e. $\kappa/2 = m/n, m \in \mathbb{Z}, n \in \mathbb{N}^+$. In this case χ is independent of L for $L = ln + r, 0 \le r < n, l \in \mathbb{N}$, i.e.

$$\chi = \chi' + \frac{2m(r-1)}{n}. \tag{3.28}$$

The results obtained for the symmetric case can be adopted immediately. This is not possible for irrational values of $\kappa/2$. Note that this kind of commensurability and incommensurability has also been observed for the periodic chain with this type of interaction [68].

3.3.2 $p, q \in \mathbb{R}$

Without loss of generality, we are going to restrict ourselves to $p > q$ which implies $Q < 1$. We have to distinguish two different situations. If $\alpha'_-\beta'_+$ equals zero we can adopt the results for the symmetric case with $F = C = 0$ (see appendix A for details). One has just to exchange $\alpha_\pm$ and $\beta_\pm$ by $\alpha'_\pm$ and $\beta'_\pm$. If otherwise $\alpha'_-\beta'_+ \neq 0$ the situation changes. The energy gaps suggest the partition function for the long chain (2.1) with boundary terms given by (3.24), i.e.

$$\mathcal{Z}_{\text{long}} = \operatorname{tr} z^{\frac{2L}{(Q+1/Q)\pi}(H - e_\infty L - f_\infty)} = \frac{2}{\eta(z)} \sum_{m\in\mathbb{Z}/2} z^{2(m+\frac{\Delta_x}{2})^2 + 2mL\Delta_y} \tag{3.29}$$

where

$$\Delta_x = \frac{\mathrm{i}}{2\pi}\ln\Gamma \qquad \Delta_y = \frac{\mathrm{i}}{\pi}\frac{Q-Q^{-1}}{Q+Q^{-1}} \tag{3.30}$$

and

$$\begin{aligned}\Gamma = &\,(1 - Q^2(1 - 2\alpha_z^2 - 2\alpha'_-\alpha'_+) - 2\alpha_z^2 Q^4)\\ &\times (1 - Q^2(1 - 2\beta_z^2 - 2\beta'_-\beta'_+) - 2\beta_z^2 Q^4)/(\alpha'^2_-\beta'^2_+ Q^4(1+Q^2)^2).\end{aligned} \tag{3.31}$$

Note that the value of Δ_y is purely imaginary. Hence the length dependent term given in the partition function is a phase. Such a term already appeared in the toroidal partition function for the asymmetric model with periodic boundary conditions [71]. Note also that the result (3.29) simplifies to the partition function we obtained in the Neumann-Neumann case for $\mathcal{H}_{\text{long}}$ if one sets $Q = 1$ (see (3.12)).

In [57] the exact ground-state energy on the finite chain for boundaries defined by

$$\alpha_z = \beta_z = 0 \qquad \alpha'_+\alpha'_- = \beta'_+\beta'_- = 1 \tag{3.32}$$

has been computed. If we introduce the parameter χ' via $\beta'_+ = \mathrm{e}^{\mathrm{i}\pi\chi'}\alpha'_+$, then (3.31) simplifies to

$$\Gamma = \left(\mathrm{e}^{\mathrm{i}\pi\chi'} Q^2\right)^{-2}. \tag{3.33}$$

Expanding the exact expression obtained in [57] leads to

$$E_0 \sim -\frac{Q+Q^{-1}}{2\pi}L - \frac{Q+Q^{-1}+(Q-Q^{-1})\frac{1}{2}\ln\Gamma}{2\pi} - \frac{(Q+Q^{-1})\pi}{2L}\left(\frac{1}{24} + \frac{(\ln\Gamma)^2}{8\pi}\right) \tag{3.34}$$

It is only for this case, that we can perform the projection onto the $(+,+)$-sector [1]. We obtain

$$\mathcal{Z} = \frac{1}{\eta(z)}\sum_{m\in\mathbb{Z}} z^{2(m+\chi'/2-\mathrm{i}\ln Q/\pi)^2+2mL\Delta_y} \quad \text{for odd } L \tag{3.35}$$

$$\mathcal{Z} = \frac{1}{\eta(z)}\sum_{m\in\frac{2\mathbb{Z}+1}{2}} z^{2(m+\chi'/2-\mathrm{i}\ln Q/\pi)^2+2mL\Delta_y} \quad \text{for even } L. \tag{3.36}$$

Note that our results for $\mathcal{H}_{\text{long}}$ only apply if (3.31) is different from zero. If the nominator of Γ vanishes we obtain logarithmic terms in the asymptotic behaviour of the energy

[1] The associated long chain with symmetric bulk terms and boundaries given by (3.24) corresponds to case 9 in table 2.1.

gaps similar to the ones obtained for the symmetric chain (see (3.20)). We obtained the fermion energies

$$2\Lambda \sim \frac{Q+Q^{-1}}{2L}\left\{k\pi \pm \frac{1}{2}\left[\arg\Delta - \mathrm{i}\ln L\right]\right\} \pm \mathrm{i}\frac{Q-Q^{-1}}{2} \tag{3.37}$$

where

$$\Delta = \frac{2\alpha_-'^2\beta_+'^2 Q^4(1+Q^2)^2}{2AQ^2+4Q^4(B+E^2)-6Q^6(D+2E^2)+8E^2Q^8}. \tag{3.38}$$

The values of A, B, D, E are given in (2.15). We are not going to consider the case, where the denominator in (3.38) vanishes.

3.4 Conclusions

In this chapter we considered the continuum limit of the spectra of the XX–model with boundary fields given by the Hamiltonian $\mathcal{H}$ in (1.2). In order to obtain our results we also studied the Hamiltonian $\mathcal{H}_{\mathrm{long}}$ defined by (2.1). Furthermore we considered the asymmetric XX–chain (3.23). Here we separated two cases. First we considered the case where the values of p and q in (3.23) are given by $p = \mathrm{e}^{\mathrm{i}\pi\kappa}/2$ and $q = \mathrm{e}^{-\mathrm{i}\pi\kappa}/2$ (this corresponds to Dzyaloshinsky-Moriya interactions). Second we considered the case where p and q are real numbers.

For periodic boundary conditions the partition function for $\mathcal{H}$ is given by the partition function of the free boson with periodic boundary conditions (3.3) [63, 64, 65]. The partition function for $\mathcal{H}_{\mathrm{long}}$ with periodic boundary conditions is just the expression (3.3) multiplied by 4. The spectra of the asymmetric chain with Dzyaloshinsky-Moriya interactions and periodic boundary conditions have been studied in [68], whereas the partition function for real values of p and q and periodic boundary conditions was given in [71].

The results we obtained for $\mathcal{H}$ and $\mathcal{H}_{\mathrm{long}}$ can be encoded in terms of the parameters given in (3.8). Note that as long as we restrict ourselves to hermitian boundary terms we studied the most general case. This is not true for non-hermitian boundaries.

For $\mathcal{H}$ with hermitian boundaries we obtained the partition functions corresponding to one of the three boson partition functions (3.5),(3.6) and (3.7). However, we found these partition functions also for certain non-hermitian boundary terms.

We obtained the Neumann-Neumann partition function (3.6) if all non-diagonal terms are present, where the value of Δ in (3.6) is given by (3.11). The Dirichlet-Neumann partition function (3.7) is obtained for boundary terms which satisfy (3.14). We found the Dirichlet-Dirichlet partition function (3.5) for two types of boundary terms given by (3.16) respectively (3.15). The value of Δ in (3.5) is given by (3.17) in both cases. Furthermore, for the case of non-hermitian boundaries we found a case which is special. For boundary terms given by (3.18) the partition function is the Dirichlet-Dirichlet partition function (3.5) multiplied by 2, where the value of Δ is 0 or 1/2 for odd respectively even values of the lattice length.

The partition functions for $\mathcal{H}_{\text{long}}$ have also been considered. If all non-diagonal terms are present it is given by (3.12). For the other cases it is just the partition function of $\mathcal{H}$ multiplied by 4. We also computed the values of the free surface energies of $\mathcal{H}_{\text{long}}$ and $\mathcal{H}$ for certain boundary terms. They are given in table 3.2. In this table we have also given the values of the lowest highest weights which appear in the spectra of $\mathcal{H}_{\text{long}}$ for these boundary terms.

For the last two cases in table 3.1 we obtained logarithmic corrections to the free surface energy (equation (3.19)). Here we found also logarithmic terms in the asymptotic behaviour of the energy gaps (equation (3.20)).

In the case of Dzyaloshinsky-Moriya interactions, we restricted ourselves to hermitian chains. The value of the phase κ (see (3.25)) has only an effect on the spectra if non-diagonal boundary terms are present at both ends of the chain. In this case we obtain the Neumann-Neumann partition function (3.6) if $\kappa/2$ is a rational number. The value of χ in the definition of Δ in (3.11) has just to be exchanged by the expression in (3.28).

The partition function for the asymmetric chain (3.23) with real values of p and q has only been obtained for one special type of boundaries (see equation (3.32)). It is given by (3.35) for L odd respectively by (3.36) for L even. The asymptotic behaviour of the ground-state energy for this case is given in (3.34).

Chapter 4

The "topological" charge for the finite XX quantum chain

We have seen in chapter 3 that the partition functions for the Hamiltonian $\mathcal{H}$ with hermitian boundary terms are given by the partition functions of the free compactified boson on a cylinder with Neumann-Neumann, Dirichlet-Neumann or Dirichlet-Dirichlet boundary conditions. It is well known [67] that for the case of diagonal boundary terms (corresponding to the Dirichlet-Dirichlet boundary condition) the value of n appearing in the partition function (3.5) is strongly related to the projection of the total spin onto the z-axis. Here we are going to consider the analogous quantity being related to the value of m appearing in the partition function (3.6) for the case of Neumann-Neumann boundary conditions. This chapter is based on [59].

We consider the L sites XX quantum chain with non-diagonal boundary terms given by the Hamiltonian:

$$\mathcal{H} = \frac{1}{4}\sum_{j=1}^{L-1}\left(\sigma_j^x\sigma_{j+1}^x + \sigma_j^y\sigma_{j+1}^y\right) + \lambda\sigma_1^x + \mu\left[\cos(\chi)\sigma_L^x - \sin(\chi)\sigma_L^y\right] \tag{4.1}$$

here λ, μ and χ are parameters [1]. . Obviously the $O(2)$ symmetry on the bulk terms is broken by the boundary terms. The question is if this finite quantum chain has no "hidden" symmetries (hidden symmetries occur normally in the thermodynamic limit only). We will show that it does.

For our purpose one needs to find boundary terms which lead to fermionic energies of a special form (the reason is going to be explained shortly), therefore from our collection of boundary terms where we could find solutions of the secular equation, we will consider only two kinds of boundary conditions:

- $$\lambda = \mu = \frac{1}{\sqrt{8}} \tag{4.2}$$
- $$\lambda = \mu = \frac{1}{4}; \qquad \chi = 0 \tag{4.3}$$

[1] Note that the parameter χ differs from the one introduced in the (3.10) through a factor π.

We have to consider the cases L odd and even separately. The reason is the following one: for L odd and $\chi = 0$ the ground-state of $\mathcal{H}_{\rm long}$ is in the $(+,+)$ sector in which we are interested. For L even the ground-state is in the $(+,-)$ sector. Since we are more interested in the spectra where the ground-state is, we will confine ourselves to the case L odd (as opposed to the case of diagonal boundary terms where the ground-state appears in chains with an even number of sites [74]). One can repeat the whole procedure described below for L even. We now specialize to the boundary condition (4.2). The energy gaps are given [57] by the fermionic energies (the zero mode not included)

$$2\Lambda_n^{\pm} = \sin\left(\frac{2n+1}{L+1}\frac{\pi}{2} \pm \frac{\chi}{L+1}\right) \qquad 0 \leq n \leq (L-1)/2 \tag{4.4}$$

It is convenient to consider the operator

$$T_{\rm long} = \frac{1}{2}\sum_{n=0}^{(L-1)/2}(N_n^+ - N_n^-). \tag{4.5}$$

where $N_n^{\pm}$ are fermionic number operators ($N_n^{\pm} = 0, 1$) corresponding to the energies given by (4.4). The eigenvalues of $T_{\rm long}$ denoted by m are obviously given by integer or half-integer numbers. Obviously this allows a $Z(2)$ grading. It turns out [57] that in the $(+,+)$ sector m takes integer values (even number of fermions) whereas in the $(+,-)$ sector it takes half-integer values (odd number of fermions). We define the partition function corresponding to the eigenvalue m of $T_{\rm long}$, for a chain with L sites

$$Z_m(L) = {\rm tr}\, z^{\frac{2L}{\pi}\left[\sum_{n=0}^{(L-1)/2}\left(\Lambda_n^+ N_n^+ + \Lambda_n^- N_n^-\right)\right]} \tag{4.6}$$

with the constraint

$$\frac{1}{2}\sum_{n=0}^{(L-1)/2}(N_n^+ - N_n^-) = m \tag{4.7}$$

and consider the sectors $(+,+)$ and $(+,-)$ only. In the thermodynamic limit one obtains:

$$Z_m = \lim_{L\to\infty} Z_m(L) = z^{2(m+\chi/(2\pi))^2 - \chi^2/(2\pi^2)}\prod_{n=1}^{\infty}(1-z^n)^{-1} \tag{4.8}$$

which is what one would expect if $T_{\rm long}$ corresponds to the "topological" charge. If we consider the $(+,+)$ sector (which as mentioned corresponds to the original Hamiltonian given by (4.1)) and sum over m integer the partition functions given by (4.8), one gets the known partition function for a compactified bosonic field (with the correct radius) and von Neumann boundary conditions at both ends [58, 66, 62]. Actually the whole algebraic structure of the problem, in the thermodynamic limit, can be read-off from the expressions (4.4):

$$\lim_{L\to\infty}\left(\frac{2L}{\pi}\Lambda_n^{\pm}\right) = n + 1/2 \pm \chi/\pi \tag{4.9}$$

if we keep in mind that the sum of two integer numbers is an integer number. One could pursue this issue further and make contact with the sine-Gordon model with a boundary at the free fermion point where much work was done [75, 76, 77]. In this chapter we are however interested in the properties of the finite chain given by (4.1) and want therefore to get the "topological" charge T for this chain. In order to do so, we have to write T_{long} given by (4.5) in the basis where $\mathcal{H}_{\text{long}}$ is written and project on the $(+,+)$ sector. This is a lengthy calculation where we have used the results of [57]. One obtains

$$
\begin{aligned}
T = \frac{-1}{4L+4} \sum_{\substack{k,j=1 \\ k+j \text{ odd} \\ k<j}}^{L} \Bigg\{ & \\
& \left[f(j-k)\cos(\chi\frac{k-j}{L+1}) - (-1)^k f(k+j)\cos(\chi\frac{k+j}{L+1}) \right] \sigma_k^y \sigma_{k+1}^z \cdots \sigma_{j-1}^z \sigma_j^x \\
& - \left[f(j-k)\cos(\chi\frac{k-j}{L+1}) + (-1)^k f(k+j)\cos(\chi\frac{k+j}{L+1}) \right] \sigma_k^x \sigma_{k+1}^z \cdots \sigma_{j-1}^z \sigma_j^y \\
& + \left[f(j-k)\sin(\chi\frac{k-j}{L+1}) + (-1)^k f(k+j)\sin(\chi\frac{k+j}{L+1}) \right] \sigma_k^y \sigma_{k+1}^z \cdots \sigma_{j-1}^z \sigma_j^y \\
& + \left[f(j-k)\sin(\chi\frac{k-j}{L+1}) - (-1)^k f(k+j)\sin(\chi\frac{k+j}{L+1}) \right] \sigma_k^x \sigma_{k+1}^z \cdots \sigma_{j-1}^z \sigma_j^x \Bigg\} \\
& + \frac{1}{\sqrt{8}(L+1)} \sum_{\substack{j=1 \\ j \text{ odd}}}^{L} \Bigg\{ f(j)\cos(\chi\frac{j}{L+1})\sigma_1^z \cdots \sigma_{j-1}^z \sigma_j^y \\
& + f(j)\sin(\chi\frac{j}{L+1})\sigma_1^z \cdots \sigma_{j-1}^z \sigma_j^x - f(j+L+1)\cos(\chi\frac{j}{L+1})\sigma_j^y \sigma_{j+1}^z \cdots \sigma_L^z \\
& - f(j+L+1)\sin(\chi\frac{j}{L+1})\sigma_j^x \sigma_{j+1}^z \cdots \sigma_L^z \Bigg\}
\end{aligned}
\tag{4.10}
$$

where

$$
f(x) = 1/\sin\left(\frac{x\pi}{2L+2}\right). \tag{4.11}
$$

T is a pseudoscalar for $\chi = 0$ when $\mathcal{H}$ is parity invariant. One can also check that

$$
[T, \mathcal{H}] = 0 \tag{4.12}
$$

only for L odd and not for L even. The expression (4.10) is horrible, what is important is that it exists. Let us stress that we were able to identify T_{long} and therefore T only because the fermionic energies had the form (4.4). We have not found (see table 2.3) any other boundary conditions where we know the spectrum of the finite chain and where the partition functions have the form given by (4.8) with χ different of zero (only in this case we can write T_{long} like in (4.5)). We would have liked to have more examples in order to make sure that the boundary condition (4.2) is not a special case and that only for this case one can find the "topological" charge. There is however one case (given by the boundary condition (4.3)) where although the spectrum of the finite quantum chain $\mathcal{H}$ is twice degenerate (nothing to do with a zero mode but with the fact that in the continuum it gives the partition function (4.8) with $\chi = 0$):

$$
2\Lambda_n^+ = 2\Lambda_n^- = \sin\left(\frac{2n+1}{L+2}\frac{\pi}{2}\right) \qquad 0 \le n \le (L-1)/2 \tag{4.13}
$$

we were able to identify the "topological" charge. We did it using a trick. We took $\lambda = \mu = 1/4$ and a small value for χ, diagonalized $\mathcal{H}_{\text{long}}$ numerically and identified $\Lambda_n^{\pm}$ and the creation and annihilation operators corresponding to these energy levels. This has allowed us to guess T_{long} for $\chi = 0$ where the spectrum of $\mathcal{H}_{\text{long}}$ is known. We found:

$$T_{\text{long}} = \frac{1}{8}\sum_{j=1}^{L-1}\left[\left(1+(-1)^j\right)\sigma_j^x\sigma_{j+1}^y - \left(1-(-1)^j\right)\sigma_j^y\sigma_{j+1}^x\right] + \frac{1}{4}\left(\sigma_0^x\sigma_1^y - \sigma_L^y\sigma_{L+1}^x\right) \quad (4.14)$$

and

$$T = \frac{1}{8}\sum_{j=1}^{L-1}\left[\left(1+(-1)^j\right)\sigma_j^x\sigma_{j+1}^y - \left(1-(-1)^j\right)\sigma_j^y\sigma_{j+1}^x\right] + \frac{1}{4}\left(\sigma_1^y - \sigma_L^y\right). \quad (4.15)$$

Notice that the expressions (4.14) and (4.15) are local ones. One can look at T and consider it as a quantum chain (keep in mind that it commutes with $\mathcal{H}$ only for L odd). This quantum chain has amusing properties. If we disregard the boundary terms, it is trivial to diagonalize it and one obtains

$$\frac{1}{2}\left(\sum_{k=1}^{L-1} N_k\right) - \frac{L-1}{4} \quad (4.16)$$

where N_k are fermionic operators. If one takes into account the boundary terms, in order to diagonalize it, one has to use T_{long} given by (4.14) and project in order to find the spectrum of T (the way we did in order to find the spectrum of $\mathcal{H}$ out of the spectrum of $\mathcal{H}_{\text{long}}$). For L odd the spectrum is the known one (integer values) since T is the "topological" charge. For L even, the spectrum is complicated.

One can ask what we have learned from our exercise. The fact that the quantum chain (4.1) has many conservation laws (the total number of fermions is just one example) should not be a surprise since its spectrum is related to the one of $\mathcal{H}_{\text{long}}$ which is a free system. We think that the fact that we have been able to identify the "topological" charge which is related to the magnetic charge in the Coulomb gas description or to vortices (see [78] for a review on the subject) on a finite lattice is interesting and that this identification can probably be done not only for the XX chain, but for the XXZ chain too. How to do this generalization is by no means clear to us.

Chapter 5

Magnetization profiles and boundary bound states

In this chapter we are going to consider the profiles of the spin operators σ_j^z and σ_j^x. Since we will restrict ourselves to hermitian boundary terms, the values of α_z and β_z are real numbers and α_+ and β_+ are the complex conjugates of α_- respectively β_-.

We have already shown in section 2.2.3 how to compute the one point function of the σ_j^x-operator in terms of pfaffians. The σ_j^z-profiles are easier to compute (see appendix B.1). We will study the ground-state profiles as well as the profiles of certain excited states of $\mathcal{H}$. The excited states of $\mathcal{H}$ we are going to consider correspond to single fermion excitations with respect to the ground-state of $\mathcal{H}_{\text{long}}$, which are characterized by a non-vanishing excitation energy as L goes to infinity and which correspond to boundary bound states.

We are able to obtain exact results for the ground-state profiles only for certain values of the boundary parameters, which are among the factorizable cases given in table 2.1. In the case of the σ_j^z-profiles we will find exact expressions on the finite chain, in the continuum limit $L \gg 1, z = j/L$ fixed and in the limit $L \to \infty, j \gg 1$. Our exact results for the σ_j^x-profiles are restricted to the limit $L \to \infty, j \gg 1$.

A combination of extensive numerical computations (for lattice lengths $L \sim 600$) and of our exact results will lead us to conjectures for the profiles of σ_j^z and σ_j^x in the continuum limit for more general values of the boundary parameters. Note that once we know the σ_j^x-profile for one specific choice of the boundary terms, we know already the profile of σ_j^y for the boundary terms with σ^x and σ^y interchanged in (1.2). Our results for the ground-state profiles will be discussed in the context of conformal field theory. This chapter is based on [60].

5.1 Introduction

The behaviour of one-point functions has been a well studied object in the context of boundary conformal field theory [79]-[87]. According to Burkhardt and Xue [83, 84], in the continuum limit $z = j/L, L \gg 1$ the general form of the profile of any scalar scaling operator ϕ with bulk-scaling dimension x_ϕ is given by

$$\langle \phi(j) \rangle_{ab} = [(L/\pi)\sin(\pi z)]^{-x_\phi} \mathcal{F}_{ab}(z). \tag{5.1}$$

The functional form of $\mathcal{F}_{ab}(z)$ depends on the boundary conditions a and b at the left respectively the right boundary. We have shown in chapter 3 that the XX–model with hermitian boundaries corresponds to the free compactified boson on a cylinder with Neumann-Neumann, Dirichlet-Neumann or Dirichlet-Dirichlet boundary conditions. The bulk-scaling dimensions x_ϕ obtained from the two-point functions for the periodic chain are 1 respectively $\frac{1}{4}$ for σ_j^z respectively σ_j^x [2, 18].

Conformal field theory makes more restrictive predictions for the behaviour of the profiles of scaling operators near the boundary. From (5.1) we obtain that near the boundary the profile is given by

$$\langle \phi(j) \rangle_{ab} = j^{-x_\phi} \psi_{ab}(z) \qquad z \ll 1. \tag{5.2}$$

It was already argued in [88] that if the scaling function $\psi_{ab}(z)$ is different from zero near the boundary, it has the asymptotic form

$$\psi_{ab}(z) = A[1 + \mathcal{B}^\phi_{ab} z^2 + \cdots] \qquad z \ll 1. \tag{5.3}$$

Furthermore it has been shown in [83, 84, 79] that the amplitude $\mathcal{B}^\phi_{ab}$ is related to the Casimir amplitude $\mathcal{A}_{ab}$ via

$$\mathcal{B}^\phi_{ab} / \mathcal{A}_{ab} = -4\pi x_\phi / c \tag{5.4}$$

where c denotes the central charge of the theory. The Casimir amplitude $\mathcal{A}_{ab}$ is defined by the large L behaviour of the ground-state energy E_0, i.e.

$$E_0 = e_\infty L + f_{ab} + \mathcal{A}_{ab} L^{-1} + \cdots \tag{5.5}$$

where by e_∞ and f_{ab} we denote the bulk respectively the surface free energy. The Casimir amplitudes for the boundary terms of the Hamiltonian (1.2) can be read off from the partition functions obtained in chapter 3.

As we are going to show, when dealing with boundaries, it is not a priori clear which combinations of spin operators correspond to the scaling operators of the continuum theory. Our conjectures for the continuum limit of the profiles will yield, that the profiles of σ_j^x and of σ_j^z indeed have the form of (5.1) (see however equation (5.33)).

We will see that if the boundary conditions we are going to consider correspond to Dirichlet-Neumann of the free boson field, the profiles satisfy (5.3) and (5.4). We will also see that for the boundary terms corresponding to Dirichlet-Dirichlet and Neumann-Neumann boundary conditions the profiles show a more complicated behaviour near the boundary. In these cases the equations (5.3) and (5.4) do not hold in general for the profiles of σ_j^x and σ_j^z.

In the case of Dirichlet-Dirichlet boundary conditions we have to build an appropriate linear combination of σ_j^z and σ_{j+1}^z in order to obtain the correct behaviour of a scaling operator. However, in the generic case the linear combination we are going to obtain works only at one boundary at a time. The σ_j^x-profile vanishes exactly in this case.

For the case of Neumann-Neumann boundary conditions we obtain the correct behaviour by considering a linear combination of σ_j^x and σ_j^y. Again this works only at one boundary at a time in the generic case. Here the σ_j^z-profile vanishes if no diagonal boundary terms are present at the boundary (i.e. $\alpha_z = \beta_z = 0$). However, we have also studied a type of boundaries corresponding to the Neumann-Neumann boundary conditions, where diagonal and non-diagonal boundaries are present at a boundary at the same time. In this case the profile of the σ_j^z–operator vanishes only in the leading order and is determined by a secondary field instead by a primary field.

Our results in the limit $L \to \infty, j \gg 1$ are in agreement with the results of Affleck [90]. He has considered the semi-infinite XXZ spin-1/2 chain with a transverse magnetic field applied at the end of the chain (this corresponds to $\alpha_+ = \alpha_- \neq 0$, $\alpha_z = \beta_z = \beta_+ = \beta_- = 0$ and $L \to \infty$ in our notation). Affleck has used the bosonization technique, whereas our results have been obtained on the lattice. Assuming Neumann boundary conditions for the boson field, he obtained the σ_j^x-profile for large values of j. At the free fermion point the result reads

$$\langle \sigma_j^x \rangle = (-1)^j C j^{-\frac{1}{4}} \tag{5.6}$$

where the constant C does not depend on the strength of the field and at the free fermion point its numerical value is given by

$$C = 0.912\,171\,210\,446 \cdots . \tag{5.7}$$

The case of a longitudinal magnetic field at the end of the chain has also been considered in [90] (corresponding to $\alpha_z \neq 0$, $\alpha_+ = \alpha_- = \beta_z = \beta_+ = \beta_- = 0$ and $L \to \infty$). Imposing Dirichlet boundary conditions for the boson field, the large j behaviour of the σ_j^z-profile has been evaluated for small values of α_z, yielding at the free fermion point

$$\langle \sigma_j^z \rangle \approx B \alpha_z (-1)^j j^{-1} \tag{5.8}$$

where the value of B is undetermined. The case of diagonal and non-diagonal boundary terms at the boundary at the same time has not been considered. The boundary conditions where we have been able to compute the profiles exactly in the limit $L \to \infty, j \gg 1$ can always be mapped onto the boundaries treated by Affleck. Our results obtained on the lattice agree with (5.6) and (5.8). For the σ_j^z-profiles we have not restricted ourselves to small values of α_z and we have derived the α_z-dependence of B.

As already mentioned above, we will also consider the magnetization profiles of certain eigenstates of $\mathcal{H}$, which are obtained by the excitation of a massive fermion with respect to the ground-state of $\mathcal{H}_{\text{long}}$. The existence of such fermions has already been mentioned in [57] for special values of the boundary parameters. Before considering the profiles, we are going to study the appearance of such fermions for general, hermitian boundary terms.

We will see that massive fermions appear if the values of certain functions of the boundary parameters become greater than a certain threshold. The respective excitation masses will turn out to depend only on the boundary parameters of one boundary at a time. In the general case (non-diagonal together with diagonal boundary terms) we will find at most one mass per boundary.

In the case of purely diagonal boundary terms the fermion masses correspond exactly to the non-vanishing energy gaps obtained in the Bethe Ansatz by comparing the energy of the reference state with the energy of the one-magnon excitations, which correspond to boundary 1-strings [91].

We will see, that the magnetization profiles for the excited states under study here, show an exponential fall-off into the bulk for diagonal as well as for non-diagonal boundary conditions (the profiles for the non-diagonal boundary terms have been obtained numerically). Hence we are going to refer to these states as to boundary bound states. These profiles appear also for $\mathcal{H}$ since the excited states we are going to study lie in the $(+,+)$-sector of the Hilbert space of $\mathcal{H}_{\text{long}}$ and do therefore correspond directly to eigenstates of $\mathcal{H}$.

This remaining part of this chapter is organized as follows: We start with the exact results in section 5.2. These results are restricted to certain choices of boundary terms. In section 5.3 we will give our conjectures for the profiles in the continuum limit for more general types of boundaries. We are going to discuss these results in the context of conformal field theory in section 5.4. Boundary bound states are the subject of section 5.5. Our conclusions will be given in section 5.6. The details of our calculations will be given in appendix B. Appendix B.1 deals with the exact computations of the σ_j^z-profiles. How we arrived at our exact results for the σ_j^x-profiles is shown in appendix B.2. In appendix B.3 we discuss the numerical verification of our conjectures of the ground-state profiles in the continuum limit.

5.2 Exact results

For technical reasons explained in chapter 2, we have been able to obtain analytical results only for certain choices of boundary terms (see table 5.1 and table 5.2). We will begin with the results for the σ_j^z-profiles on the finite chain, before turning to the respective expressions in the continuum limit. Thereafter we will give our exact results in the limit $L \to \infty, j \gg 1$ for the profiles of σ_j^x and σ_j^z.

5.2.1 Exact results on the finite lattice ($\langle\sigma_j^z\rangle$- profiles)

We have computed the exact profiles of σ_j^z for values of the boundary parameters given in table 5.1 [1]. Note that for technical reasons (see appendix B.1 for details) our result for case e is restricted to the choice $\delta = 0$ in this section. Furthermore, observe that the ground-state is twofold degenerate for case d with L odd and for case e with L

[1] The cases denoted by a,b,c,d,e correspond to the cases $2, 4, 11, 14, 16$ in the notation of chapter 2.

even, due to the existence of additional zero modes (see section 2.1). In these cases, we have obtained the profiles for the two ground-states, which have a well-defined fermion number (see appendix B.1). These profiles are indicated by a $\pm$-sign in the respective expressions.

Table 5.1. The values of the boundary parameters where we have computed the ground-state profiles of σ_j^z exactly on the finite chain and in the continuum limit. By DN (Dirichlet-Neumann) and DD (Dirichlet-Dirichlet) we denote the respective boundary conditions on the free boson (see chapter 3). For case e there appears a free, real parameter δ.

case	α_z	β_z	$\beta_+ = \beta_-$	$\alpha_\pm$	
a	$\frac{1}{\sqrt{2}}$	0	$\frac{1}{\sqrt{2}}$	0	DN
b	$\frac{1}{\sqrt{2}}$	0	1	0	DN
c	$\frac{1}{\sqrt{2}}$	0	0	0	DD
d	$\frac{1}{\sqrt{2}}$	$\frac{-1}{\sqrt{2}}$	0	0	DD
e	$\frac{1}{\sqrt{2}}\tan(\frac{\pi}{4}+\frac{\delta}{2})$	$\frac{1}{\sqrt{2}}\tan(\frac{\pi}{4}-\frac{\delta}{2})$	0	0	DD

- Case a
$$\langle \sigma_j^z \rangle = \frac{1}{2L+2}\left((-1)^L \tan\frac{\pi}{4L+4} + (-1)^j \cot\frac{(2j-1)\pi}{4L+4}\right). \tag{5.9}$$
- Case b
$$\langle \sigma_j^z \rangle = \frac{(-1)^j}{2L+1}\cot\frac{(2j-1)\pi}{4L+2}. \tag{5.10}$$
- Case c
$$\langle \sigma_j^z \rangle = \frac{1}{2L+1}\left((-1)^L + (-1)^j \left(\sin\frac{(2j-1)\pi}{4L+2}\right)^{-1}\right). \tag{5.11}$$
- Case d, L odd: The ground-state is twofold degenerate in this case.
$$\langle \sigma_j^z \rangle_\pm = \frac{1}{L}\left((-1)^j \cot\frac{(2j-1)\pi}{2L} \pm 1\right). \tag{5.12}$$
- Case d, L even
$$\langle \sigma_j^z \rangle = \frac{(-1)^j}{L}\left(\sin\frac{(2j-1)\pi}{2L}\right)^{-1}. \tag{5.13}$$
- Case e, L odd, $\delta = 0$: The same as given for case d, L even.
- Case e, L even, $\delta = 0$: The same as given for case d, L odd. The ground-state is twofold degenerate in this case, too.

5.2.2 Exact results in the continuum limit

The continuum limit defined by $L \gg 1, z = j/L$ fixed of the expressions (5.9)-(5.13) is readily obtained. Furthermore we have been able to compute the profile in the continuum limit for case e for general values of δ (see appendix B.1).

- Case a and case b

$$\langle \sigma_j^z \rangle = (-1)^j \left(L \sin(\pi z)\right)^{-1} \cos^2\left(\frac{\pi z}{2}\right) + \mathrm{Or}(1/L^2). \tag{5.14}$$

- Case c

$$\langle \sigma_j^z \rangle = (-1)^j \left(L \sin(\pi z)\right)^{-1} \cos\left(\frac{\pi z}{2}\right) + (-1)^L/2L + \mathrm{Or}(1/L^2). \tag{5.15}$$

- Case d: The same expression as given for case e with $\delta = 0$ and L even and L odd interchanged.
- Case e, L odd

$$\langle \sigma_j^z \rangle = (-1)^j \cos\delta \left(L \sin(\pi z)\right)^{-1} + \mathrm{Or}(1/L^2). \tag{5.16}$$

- Case e, L even

$$\langle \sigma_j^z \rangle_{\pm} = (-1)^j \cos(\delta \mp \pi z) \left(L \sin(\pi z)\right)^{-1} \pm 1/L + \mathrm{Or}(1/L^2). \tag{5.17}$$

5.2.3 Exact results in the limit $L \to \infty, j \gg 1$

We have obtained exact results for the profiles of σ_j^z in the limit $L \to \infty, j \gg 1$ for the five cases given in table 5.1. For the cases a,b,c,d the result may be read of from the expressions obtained on the finite lattice. This can not be done for case e with arbitrary values of δ, since the respective result on the finite lattice is restricted to $\delta = 0$. However, in the limit $L \to \infty, j \gg 1$ the calculation for case e can be done for arbitrary values of δ (see appendix B.1). Using α_z instead of the parameter δ (see table 5.1 for the relation between δ and α_z) we have obtained

$$\langle \sigma_j^z \rangle = (-1)^j \frac{\sqrt{8}\alpha_z}{(1 + 2\alpha_z^2)\pi} j^{-1} + \cdots. \tag{5.18}$$

The profiles for the cases a,b,c,d are also given by this expression if one replaces α_z by $\frac{1}{\sqrt{2}}$. The result (5.18) has to be compared to (5.8), which yields B as a function of α_z, i.e.

$$B = \frac{\sqrt{8}}{(1 + 2\alpha_z^2)\pi}. \tag{5.19}$$

We have obtained exact results for the profiles of σ_j^x in the limit $L \to \infty$ and $j \gg 1$ for the two cases given in table 5.2[2]. Our computations for case f (see appendix B.2.2) yield

$$\langle \sigma_j^x \rangle = (-1)^j A j^{-\frac{1}{4}} + \cdots \tag{5.20}$$

where A is given by

$$A = \mathrm{e}^{1/4} 2^{7/12} C_G^{-3} \tag{5.21}$$

and C_{G} is Glaishers constant [92], which can be approximately given by

$$C_{\mathrm{G}} = 1.282\,427\,129\,100\,62 \cdots. \tag{5.22}$$

[2] In the notation of chapter 2 these cases correspond to case 2 respectively case 9.

Table 5.2. Boundary parameters for the cases where we found exact expressions for the ground-state profiles of σ_j^x in the limit $L \to \infty, j \gg 1$. The first case corresponds to Dirichlet-Neumann (DN) boundary conditions, whereas the second case corresponds to Neumann-Neumann (NN) boundary conditions on the free boson. The free parameters χ and φ are real constants.

case	α_+	α_-	β_+	β_-	
f	1	1	0	0	DN
g	$\mathrm{e}^{\mathrm{i}\varphi}$	$\mathrm{e}^{-\mathrm{i}\varphi}$	$\mathrm{e}^{\mathrm{i}(\chi+\varphi)}$	$\mathrm{e}^{-\mathrm{i}(\chi+\varphi)}$	NN

For case g we have obtained (see appendix B.2.1)

$$\langle \sigma_j^x \rangle = (-1)^j A \cos\varphi j^{-\frac{1}{4}} + \cdots . \tag{5.23}$$

Comparing the value of C in (5.7) and the value of A in (5.21) using (5.22) shows that our results (5.20) and (5.23) for $\varphi = 0$ are in agreement with (5.6).

At this point we want to draw the readers attention to an interesting by-product we have obtained during our computations for case g. It is of major interest for our conjecture of the continuum limit of the σ_j^x profiles in the case of Neumann-Neumann boundary conditions presented in the next section. We have obtained that the ground-state profile of σ_j^x for arbitrary values of φ and χ (see table 5.2) is given by

$$\langle \sigma_j^x \rangle = \cos\left(\varphi + \frac{\chi + 2m\pi}{L+1} j\right) f(j, L) \tag{5.24}$$

where $f(j, L)$ does not depend on φ, χ and may be computed numerically (see appendix B.2.1). The value of m depends on the value of χ and on the lattice length L. For odd L we have $m = 0$ for $-\pi < \chi < \pi$. If $\chi = \pi$ the ground-state of $\mathcal{H}$ is twofold degenerate. The value of m is either $m = 0$ or $m = -1$. For even L the value of m is $\frac{1}{2}$ for $0 > \chi > -\pi$ and $-\frac{1}{2}$ for $0 < \chi \leq \pi$. Here the ground-state is twofold degenerate for $\chi = 0$ the value of m being either $\frac{1}{2}$ or $-\frac{1}{2}$.

5.3 Conjectures

Our results given so far allow to conjecture the ground-state profiles in the continuum limit for more general values of the boundary parameters. We have checked our results by computing the profiles on the finite chain numerically for lattice lengths up to $L = 700$. Thereafter we have used the finite size data to extrapolate the profiles for $L \to \infty$ and fixed values of $z = j/L$. We have performed these extrapolations for 150 different values of the boundary parameters each with 19 (L even) respectively 20 (L odd) values of z.

The accuracy of our extrapolations varies with the choice of the boundary parameters. In most of the cases the relative deviation from our conjectures presented in the following has been of the order of $10^{-12} - 10^{-7}$ (see appendix B.3 for details).

We have considered the following types of boundary terms:

- Dirichlet-Dirichlet:

$$\alpha_\pm = \beta_\pm = 0 \qquad \alpha_z = \frac{1}{\sqrt{2}} \tan\left(\frac{\omega+\delta}{2}\right) \qquad \beta_z = \frac{1}{\sqrt{2}} \tan\left(\frac{\omega-\delta}{2}\right) \tag{5.25}$$

  Note that for $\omega = \frac{\pi}{2}$ we recover the boundary terms of case e in table 5.1.
- Dirichlet-Neumann: Here we have considered only a special type of boundary terms, i.e.

$$\beta_+ = \beta_- \neq 0 \qquad \beta_z = \alpha_\pm = 0 \qquad \alpha_z \text{ free} \tag{5.26}$$

- Neumann-Neumann: We have studied two types of boundary terms, i.e.

$$\alpha_z = \beta_z = 0 \qquad \alpha_\pm = R_\alpha \mathrm{e}^{\pm \mathrm{i}\varphi} \qquad \beta_\pm = R_\beta \mathrm{e}^{\pm \mathrm{i}(\chi+\varphi)} \tag{5.27}$$

  respectively

$$\alpha_z = -\beta_z \qquad \alpha_+ = \alpha_- = \beta_+ = \beta_- \neq 0. \tag{5.28}$$

Note that the boundary terms (5.27) are identical to the boundaries of case g in table 5.2 if one sets $R_\alpha = R_\beta = 1$, whereas no case in table 5.1 and table 5.2 corresponds to boundary terms which satisfy (5.28). In this case our result is based on purely numerical computations. Observe also, that this is the only type of boundary terms with diagonal and non-diagonal terms at one end of the chain, which is studied in this chapter.

5.3.1 Dirichlet-Dirichlet boundary conditions

For this type of boundary conditions the ground-state profile of σ_j^x vanishes if the ground-state is non-degenerate, since the Hamiltonian commutes with $\sigma_1^z \sigma_2^z \cdots \sigma_L^z$. Therefore we have restricted ourselves to the ground-state profiles of σ_j^z. Our results for the cases c,d,e from table 5.1 and our numerical investigations suggest the σ_j^z-profiles for general values of α_z and β_z, i.e.

$$\langle \sigma_j^z \rangle = (-1)^j \frac{\sin(\omega + \delta - 2(\omega + Q\pi)z)}{L \sin(\pi z)} + \frac{2(\omega + Q\pi)}{\pi L}. \tag{5.29}$$

This equation is valid for L even and L odd. The value of Q depends on the values of ω and the lattice length L. This dependence is given in table 5.3. The discontinuities are due to level crossings in the spectrum at the respective values of ω. At these points ($\omega = 0$ for L odd and $\omega = \pm\pi/2$ for L even) the ground-state is twofold degenerate.

Table 5.3. Dependence of Q on ω and L.

	$-\pi < \omega < -\frac{\pi}{2}$	$-\frac{\pi}{2} < \omega < 0$	$0 < \omega < \frac{\pi}{2}$	$\frac{\pi}{2} < \omega < \pi$
L even	$Q = 1$	$Q = 0$	$Q = 0$	$Q = -1$
L odd	$Q = \frac{1}{2}$	$Q = \frac{1}{2}$	$Q = -\frac{1}{2}$	$Q = -\frac{1}{2}$

5.3.2 Dirichlet-Neumann boundary conditions

Our numerical computations suggest the following profile of the σ_j^x-operator:

$$\langle \sigma_j^x \rangle = \pi^{1/4} A (-1)^{L+1-j} \left[\sin\left(\frac{\pi z}{2}\right)\right]^{\frac{1}{2}} (L \sin(\pi z))^{-\frac{1}{4}} \tag{5.30}$$

where A is given by (5.21).

For two cases corresponding to this type of boundaries we have already considered the exact σ_j^z-profiles, namely for case a and b from table 5.1. The given expression (5.14) suggests universal behaviour with respect to the variation of the value of $\beta_\pm$. Our numerical calculations for various values of $\beta_\pm$ confirmed our guess. Furthermore they yield the dependence of the profile on the second parameter α_z. We have obtained

$$\langle \sigma_j^z \rangle = (-1)^j \frac{\sqrt{8}\alpha_z}{1 + 2\alpha_z^2} \cos^2\left(\frac{\pi z}{2}\right) (L \sin(\pi z))^{-1}. \tag{5.31}$$

Note that the form of the profile does not depend on the value of α_z. However, observe also that the amplitude does. For $\alpha_z = 0$ the profile vanishes, since then the Hamiltonian H commutes with $\sigma_1^x \sigma_2^x \cdots \sigma_L^x$ (the ground-state of $\mathcal{H}$ is non-degenerate (see section 2.1).

5.3.3 Neumann-Neumann boundary conditions

Our exact result for case g from table 5.2, in particular equation (5.24), in combination with numerical computations yields the σ_j^x-profile for the first type of boundaries in question (see (5.27)):

$$\langle \sigma_j^x \rangle = \pi^{1/4} A (-1)^j \cos\left(\varphi + (\chi + 2m\pi) z\right) (L \sin(\pi z))^{-\frac{1}{4}} \tag{5.32}$$

where the value of m depends on the values of χ and the lattice length L as already discussed at the end of section 5.2.3. The σ_j^z profiles vanish, as long as the ground-state is non-degenerate (see appendix B.1 for details). We did not consider the σ_j^z profiles where the ground-state is degenerate.

For the second type of boundary terms (5.28) the σ_j^z profile does not vanish. For odd values of L our numerical investigations suggest

$$\langle \sigma_j^z \rangle = (-1)^j \pi \sqrt{2} \frac{\alpha_z}{\alpha_+^2} \cos(\pi z) (L \sin(\pi z))^{-2}. \tag{5.33}$$

We have not been able to find an analytic expression for the profile for even values of L. For $\alpha_+ = 0$ the prefactor in (5.33) diverges. However, in this case the profile is already given by (5.29). For $\alpha_z = 0$ the profile vanishes as in the case of the Dirichlet-Neumann boundary condition (5.26), since in this case the Hamiltonian $\mathcal{H}$ has a higher symmetry. It commutes with $\sigma_1^x \sigma_2^x \cdots \sigma_L^x$ (the ground-state of $\mathcal{H}$ is also non-degenerate here (see section 2.1).

Comparing (5.33) with (5.1) yields that the leading term of the σ_j^z-profile is zero as for the boundary terms (5.27), since according to the long range behaviour of the two-point function the bulk-scaling dimension x_ϕ associated to the σ_j^z operator is 1. Since there exists no spinless primary field with bulk-scaling dimension 2 [93] we conclude that the profile (5.33) is determined by a secondary field (the profile of a primary field with spin vanishes [84]).

We have checked the σ_j^x-profile only for odd L. It is not affected by the presence of the diagonal terms in (5.28) and is already given by (5.32) using $\varphi = \chi = m = 0$.

5.4 Comparison with the predictions of Conformal Field Theory

In this section we are going to consider the behaviour of the profiles we have conjectured near the boundaries, i.e. we consider the limit $z \ll 1$ (respectively $(1-z) \ll 1$) , in order to check for the validity of the equations (5.3) and (5.4).

5.4.1 Dirichlet-Dirichlet boundary conditions

The behaviour of (5.29) near the left boundary is readily obtained:

$$\langle \sigma_j^z \rangle = (-1)^j \frac{\sin(\omega+\delta)}{j\pi} \left(1 - \cot(\omega+\delta) 2\omega' z + \left(\frac{1}{6} - \frac{2\omega'^2}{\pi^2} \right) (\pi z)^2 + \cdots \right) + \frac{2\omega'}{\pi L}. \quad (5.34)$$

where $\omega' = \omega + Q\pi$. The behaviour of the profile near the right boundary may be obtained by exchanging δ by $-\delta$ and performing the transformation $j \mapsto L+1-j$. This can be seen from (5.25). Note that (5.34) does not agree with equation (5.3), since in (5.3) there appears no term which is linear in z. This problem is avoided by considering the profile of the following linear combination of σ_j^z and σ_{j+1}^z for odd values of j:

$$\left\langle \tan\left(\frac{\omega+\delta}{2}\right) \sigma_j^z - \cot\left(\frac{\omega+\delta}{2}\right) \sigma_{j+1}^z \right\rangle = -\frac{2}{j\pi} \left(1 + \left(\frac{1}{6} - \frac{2\omega'^2}{\pi^2} \right) (\pi z)^2 + \cdots \right). \quad (5.35)$$

The value of the Casimir amplitude $\mathcal{A}_{ab}$ can be obtained from our results in chapter 3. It is given by $\mathcal{A}_{ab} = -\frac{\pi}{24} + \frac{\omega'^2}{2\pi^2}$. Hence (5.35) is in agreement with (5.4). Note that this operator does not yield the correct scaling behaviour near the right boundary, since the given linear combination of σ_j^z and σ_{j+1}^z depends on the value of δ, which enters the left boundary term in a different way than the right boundary term (see (5.25)). Another linear combination can be chosen to obtain the correct behaviour near the right boundary.

5.4.2 Dirichlet-Neumann boundary conditions

The Casimir amplitude for this type of boundary conditions is independent from the explicit values of the boundary parameters. Its value is given by $\mathcal{A}_{ab} = \frac{\pi}{48}$. The profiles (5.30) and (5.31) vanish near the left respectively near the right boundary and therefore the predictions (5.3) and (5.4) are not valid. Near the right boundary we obtain from (5.30)

$$\langle \sigma^x_{L+1-j} \rangle = (-1)^j A j^{-\frac{1}{4}} \left(1 - \frac{(\pi z)^2}{48} + \cdots \right) \tag{5.36}$$

whereas (5.31) yields near the left boundary

$$\langle \sigma^z_j \rangle = (-1)^j \frac{\sqrt{8}\alpha_z}{1+2\alpha_z^2} (j\pi)^{-1} \left(1 - \frac{(\pi z)^2}{12} + \cdots \right). \tag{5.37}$$

Both expressions are in agreement with the predictions (5.3) and (5.4).

5.4.3 Neumann-Neumann boundary conditions

From (5.32) we obtain the profiles of σ^x_j near the left boundary, i.e.

$$\begin{aligned} \langle \sigma^x_j \rangle &= (-1)^j A j^{-\frac{1}{4}} \cos\varphi \\ &\times \left(1 - \tan(\varphi)(\chi + 2m\pi) z + \left(\frac{\pi^2}{24} - \frac{(\chi+2m\pi)^2}{2} \right) z^2 + \cdots \right). \end{aligned} \tag{5.38}$$

The Casimir amplitude has been shown in chapter 3 to be $\mathcal{A}_{ab} = -\frac{\pi}{24} + 2\pi \left(m + \frac{\chi}{2\pi} \right)^2$ (observe, that the parameter χ used in chapter 3 differs from the one introduced here through a factor π). Note that the profile is in disagreement with the predicted behaviour for a true scaling operator given in (5.3). In order to obtain the correct behaviour near the boundary, we have to consider an appropriate linear combination of σ^x_j and σ^y_j. At the left boundary we obtain

$$\langle \cos\varphi \sigma^x_j - \sin\varphi \sigma^y_j \rangle = (-1)^j A j^{-\frac{1}{4}} \left(1 + \left(\frac{\pi^2}{24} - \frac{(\chi+2m\pi)^2}{2} \right) z^2 + \cdots \right) \tag{5.39}$$

which is in agreement with (5.3) and (5.4). Note that building the given linear combination is equivalent to performing a rotation around the z-axis such that $\varphi = 0$ in (5.27). However, similar to the case of the σ^z_j profile for the Dirichlet-Dirichlet boundary condition, this linear combination does not lead to the correct behaviour near the right boundary. To obtain the correct behaviour near the right boundary one has to perform a different rotation as long as $\chi \neq 0$.

It is interesting to consider the respective profile of the orthogonal linear combination of σ^x_j and σ^y_j, which yields

$$\langle \sin\varphi \sigma^x_j + \cos\varphi \sigma^y_j \rangle = -(-1)^j A j^{-\frac{1}{4}} \left((\chi + 2m\pi) z + \cdots \right). \tag{5.40}$$

Note that this profile vanishes near the left boundary and therefore the predictions (5.3) and (5.4) do not apply.

5.5 Boundary bound states

As already mentioned in the introduction, we have also studied the profiles of certain excited states of $\mathcal{H}$. These states are obtained by the excitation of a massive fermion with respect to the ground-state of $\mathcal{H}_{\text{long}}$. We refer to these excitations as to boundary excitations, since we are going to see, that they give rise to a contribution to the profile which decays exponentially into the bulk.

First, we are going to look for massive excitations for general, hermitian boundary terms in section 5.1 by studying the secular equation $p(x^2) = 0$ which determines the fermion energies and which has been given in (2.14). In section 5.2 we will study the magnetization profiles near the boundaries of the states, where one massive fermion is excited, for two special types of boundary terms.

In the case of diagonal boundary terms the energy gaps defined with respect to the ground-state energy are in one to one correspondence to the boundary 1-strings found as solutions of the Bethe Ansatz equations. The 1-strings define the energy gaps between the energy of the reference state and the eigenstates in the one magnon sector. At the free fermion point a boundary 1-string appears if $2\alpha_z^2 > 1$ or $2\beta_z^2 > 1$ [91]. The energy gaps corresponding to the boundary 1-strings in the limit $L \to \infty$ are given by

$$E_\alpha = \frac{1}{2}\left(\frac{1}{\sqrt{2}\alpha_z} + \sqrt{2}\alpha_z\right) \qquad E_\beta = \frac{1}{2}\left(\frac{1}{\sqrt{2}\beta_z} + \sqrt{2}\beta_z\right) \tag{5.41}$$

where by E_α and E_β we denote the energy gaps corresponding to the boundary 1-string which appears for $2\alpha_z^2 > 1$ respectively $2\beta_z^2 > 1$.

5.5.1 Massive excitations

The fermion energies are obtained by

$$2\Lambda = \frac{1}{2}(x + 1/x) \tag{5.42}$$

where the values of x are given by the roots of the polynomial $p(x^2)$ (see (2.14)). Since the energies have to be real numbers, the roots of the polynomial lie either on the unit circle or on the real axis. We will focus on the roots which lie on the real axis for $L \to \infty$. Due to (5.42) these roots yield fermions with a finite energy in this limit. We have not been able to determine whether there exist massive fermions corresponding to roots lying on the unit circle.

We are going to restrict ourselves to the search for zeros satisfying $|x| < 1$, since if x is a zero of $p(x^2)$ so is $1/x$. In the limit $L \to \infty$, the secular equation $p(x^2) = 0$ reduces to

$$\left(1 + (1 - 2\alpha_z^2 - 2\alpha_-\alpha_+)x^2 - 2\alpha_z^2 x^4\right)\left(1 + (1 - 2\beta_z^2 - 2\beta_-\beta_+)x^2 - 2\beta_z^2 x^4\right) = 0. \tag{5.43}$$

Solving for x^2 yields two solutions with $|x^2| < 1$, i.e.

$$x^2 = \frac{1}{4\alpha_z^2}\left[1 - 2\alpha_-\alpha_+ - 2\alpha_z^2 + \sqrt{8\alpha_z^2 + (2\alpha_z^2 + 2\alpha_-\alpha_+ - 1)^2}\right] \tag{5.44}$$

and

$$x^2 = \frac{1}{4\beta_z^2}\left[1 - 2\beta_-\beta_+ - 2\beta_z^2 + \sqrt{8\beta_z^2 + (2\beta_z^2 + 2\beta_-\beta_+ - 1)^2}\right]. \tag{5.45}$$

Note that these solutions depend only on the parameters of one boundary at a time. The fermion energies are obtained by taking the positive square root of (5.44) respectively (5.45) and using (5.42). Hence we conclude that the maximum number of massive excitations obtained by our ansatz is two (one per boundary). This result is interesting since it confirms an analogous result obtained by Ameduri et al [94] in their study of the boundary sine-Gordon theory at the free fermion point.

If the value of α_z or β_z equals zero, the expression (5.44) respectively (5.45) has to be replaced by

$$x^2 = 1/(2\alpha_-\alpha_+ - 1) \quad \text{respectively} \quad x^2 = 1/(2\beta_-\beta_+ - 1). \tag{5.46}$$

If $\alpha_- = 0$ or $\alpha_+ = 0$ respectively $\beta_- = 0$ or $\beta_+ = 0$ the result simplifies to

$$x^2 = 1/(2\alpha_z^2) \quad \text{respectively} \quad x^2 = 1/(2\beta_z^2). \tag{5.47}$$

All solutions of (5.43) are only asymptotic solutions of the original polynomial if they satisfy the assumption $|x| < 1$. In the case of diagonal boundary terms this condition coincides with the condition for the existence of boundary 1-strings in the Bethe Ansatz. The energies of the one-magnon excitations corresponding to the boundary 1-strings given in (5.41) correspond exactly to the fermion energies (5.42) obtained by the roots in (5.47).

5.5.2 Magnetization profiles near the boundary

We have studied the magnetization profiles for certain states, which differ from the ground-state of $\mathcal{H}_{\text{long}}$ by a boundary excitation, for two types of boundaries. Note that the ground-state of $\mathcal{H}_{\text{long}}$ is at least twofold degenerate. We have chosen it such that the excited state in question lies in the $(+,+)$-sector. Therefore these states correspond also to eigenstates of $\mathcal{H}$. First we have considered diagonal boundary terms

$$\alpha_z = 1/(2\beta_z) = \mathrm{e}^{\xi}/\sqrt{2} \qquad \alpha_\pm = \beta_\pm = 0 \tag{5.48}$$

for even and odd values of L. Without loss of generality we have restricted ourselves to $\xi > 0$. In this case $2\alpha_z^2$ becomes larger than 1 and according to (5.47) and (5.42) there exists one boundary excitation with energy $2\Lambda = \cosh\xi$. We are able to compute the σ_j^z-profile analytically in the limit $L \to \infty, j \gg 1$ (see appendix B.1), i.e.

$$\langle \xi \mid \sigma_j^z \mid \xi \rangle \approx \frac{(-1)^j}{\pi}\frac{1}{\cosh\xi} j^{-1} + 2(\mathrm{e}^{2\xi} - 1)\mathrm{e}^{-2j\xi} \tag{5.49}$$

where $|\xi\rangle$ denotes the state obtained by the excitation of the massive fermion. Observe that the correlation length $1/(2\xi)$ is related to the excitation mass $2\Lambda = \cosh\xi$. The profile near the right boundary is

$$\langle \xi \mid \sigma_{L+1-j}^z \mid \xi \rangle \approx \frac{(-1)^j}{\pi}\frac{1}{\cosh\xi} j^{-1} \tag{5.50}$$

as expected. The $U(1)$ charge, which is given by the projection of the total spin onto the z-axis, of the state $\mid \xi\rangle$ is 0 for L even and $\frac{1}{2}$ for L odd.

Notice that the exponential part in (5.49) is not present if one considers the respective ground-state profile (see (5.18)). We conclude, that adding a massive excitation to the ground-state yields an additive contribution to the profile which decays exponentially into the bulk.

The second type of boundaries we have considered are non-diagonal and given by

$$\alpha_\pm = \sqrt{\cosh \xi_\alpha \exp \xi_\alpha} \qquad \beta_\pm = \sqrt{\cosh \xi_\beta \exp \xi_\beta} \qquad \alpha_z = \beta_z = 0. \tag{5.51}$$

We restricted ourselves to even values of L, since in this case for odd values of L the excitation of a fermion with respect to the ground-state of $\mathcal{H}_{\text{long}}$ does not lead to a state which lies in the $(+,+)$-sector and hence does not correspond to an eigenstate of $\mathcal{H}$ (see appendix B.2.3 for details). Since the σ_j^z-profile vanishes exactly for the boundaries (5.51), we have studied the σ_j^x-profile in this case. In contrast to the σ_j^z-profiles given in (5.49) and (5.50) our results for the σ_j^x-profiles we are going to present are based on numerical computations for $L = \infty$ in the special case $\xi_\beta = -\xi_\alpha$ and for $L = 800$ in the general case.

In section 2.2.3 we have shown that the σ_j^x-profiles for the boundaries given in (5.51) may be computed in terms of determinants of $j \times j$ matrices. In the case $\xi_\beta = -\xi_\alpha$ it is possible to compute these matrices analytically in the limit $L \to \infty$ (see appendix B.2.3). Thus the numerical study of the profile near the boundaries is easier than in the general case. Here one boundary excitation appears with energy $2\Lambda = \cosh \xi_\alpha$ (see (5.46) and (5.42)). For $\xi_\alpha > 0$ we have obtained by numerical extrapolation from data for $j = 1 \ldots 100$

$$\langle \xi_\alpha \mid \sigma_j^x \mid \xi_\alpha \rangle \approx (-1)^{j+1} A j^{-\frac{1}{4}} \left(1 - 2\mathrm{e}^{(-1)^j \xi_\alpha} \mathrm{e}^{-2j\xi_\alpha}\right) \tag{5.52}$$

and

$$\langle \xi_\alpha \mid \sigma_{L+1-j}^x \mid \xi_\alpha \rangle \approx (-1)^j A j^{-\frac{1}{4}} \tag{5.53}$$

where A is given by (5.21) and $\mid \xi_\alpha\rangle$ denotes the state obtained by the excitation of the fermion with energy $2\Lambda = \cosh \xi_\alpha$. Again the exponential term is absent in the respective expressions for the ground-state profile. Note again the relation between the correlation length and the excitation mass.

Inspired by this result we have also studied the case $\xi_\alpha \neq -\xi_\beta$. If $\xi_\alpha, \xi_\beta > 0$ there exist two boundary excitations with energies $2\Lambda_\alpha = \cosh \xi_\alpha$ and $2\Lambda_\beta = \cosh \xi_\beta$ in the limit $L \to \infty$. We have considered the respective magnetization profiles on the finite chain numerically ($L = 800$). Exemplarily the figures 1 and 2 show the profiles we have obtained numerically for the state $\mid \xi_\alpha\rangle$ near the left and the right boundary, where we have chosen $\xi_\alpha = 0.075, \xi_\beta = 0.05$.

Our results suggest that as long as $\xi_\alpha \neq \xi_\beta$ the profile for the state $\mid \xi_\alpha\rangle$ is still given by (5.52) and (5.53) (the deviation from the expression in (5.52) for large j in figure 1 is expected due to the presence of the right boundary). The profile for the state

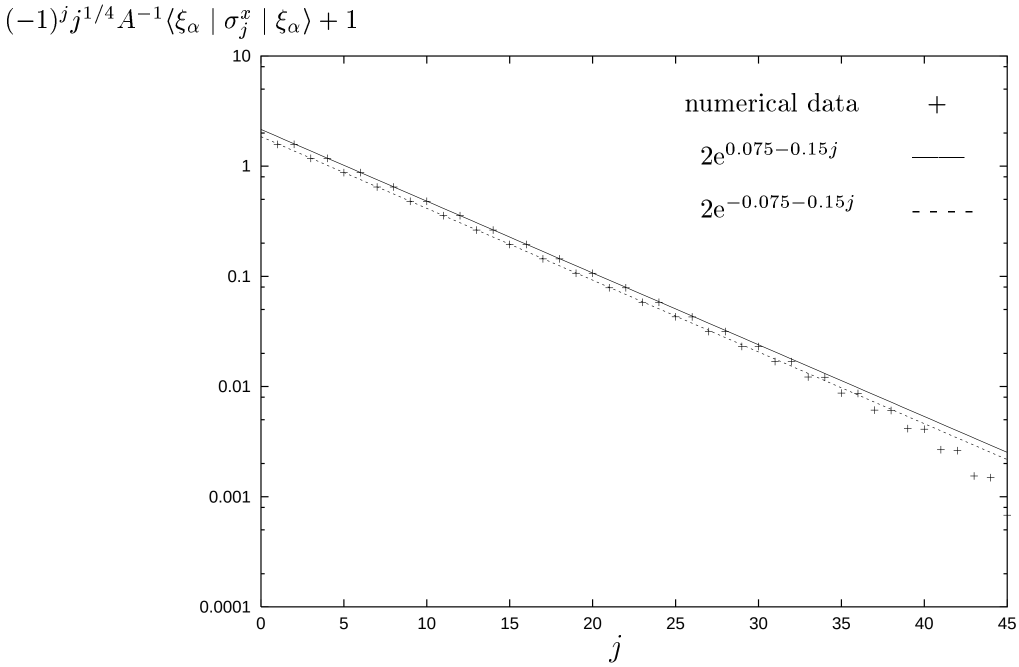

Figure 5.1. The exponential part of the σ_j^x–profile of the state $\mid \xi_\alpha \rangle$ near the left boundary for the choice $\xi_\alpha = 0.075, \xi_\beta = 0.05$ in (5.51). The numerical data (+) have been obtained for $L = 800$. The two lines show the behaviour according to (5.52) for even respectively odd values of j. The deviation of the numerical data from the straight lines for large values of j is an effect of the finite lattice.

$\mid \xi_\beta \rangle$ (obtained by the excitation of the fermion with energy $2\Lambda_\beta = \cosh \xi_\beta$) near the left boundary is just

$$\langle \xi_\beta \mid \sigma_j^x \mid \xi_\beta \rangle \approx (-1)^j A j^{-\frac{1}{4}} \tag{5.54}$$

whereas at the right boundary we have

$$\langle \xi_\beta \mid \sigma_{L+j-1}^x \mid \xi_\beta \rangle \approx (-1)^{j+1} A j^{-\frac{1}{4}} \left(1 - 2e^{(-1)^j \xi_\beta} e^{-2j\xi_\beta} \right) . \tag{5.55}$$

However, if $\xi_\alpha = \xi_\beta = \xi$ our computations suggest a different behaviour, i.e.

$$\langle \xi_\alpha \mid \sigma_j^x \mid \xi_\alpha \rangle = \langle \xi_\beta \mid \sigma_j^x \mid \xi_\beta \rangle \approx (-1)^j A j^{-\frac{1}{4}} e^{(-1)^j \xi} e^{-2j\xi} \tag{5.56}$$

near the left boundary and

$$\langle \xi_\alpha \mid \sigma_{L+1-j}^x \mid \xi_\alpha \rangle = \langle \xi_\beta \mid \sigma_{L+1-j}^x \mid \xi_\beta \rangle \approx (-1)^j A j^{-\frac{1}{4}} e^{(-1)^j \xi} e^{-2j\xi} \tag{5.57}$$

near the right boundary. In contrast to the profiles we have obtained so far, these profiles are left-right symmetric. Furthermore the leading term proportional to $j^{-\frac{1}{4}}$ does not appear, unlike in equations (5.52) and (5.55).

Note that the Hamiltonian with boundary conditions (5.51) conserves parity if $\xi_\alpha = \xi_\beta$. Our numerical computations yield that the energies $2\Lambda_\alpha$ and $2\Lambda_\beta$ are non-degenerate on the finite chain. Only in the limit $L \to \infty$ the degeneracy appears.

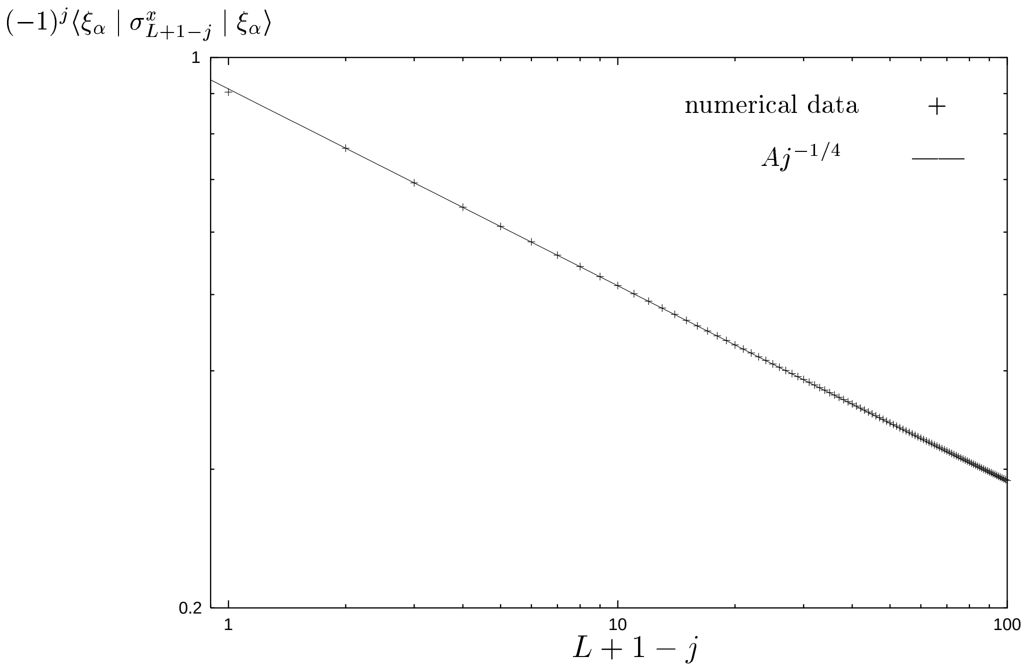

Figure 5.2. The σ^x_j–profile of the state $\mid \xi_\alpha\rangle$ near the right boundary for the choice $\xi_\alpha = 0.075, \xi_\beta = 0.05$ in (5.51). The numerical data (+) have been obtained for $L = 800$. The straight line shows the behaviour according to (5.53).

Hence the parity of the states $\mid \xi_\alpha\rangle$ and $\mid \xi_\beta\rangle$ is well-defined. This explains why the profiles reflect the symmetry of the Hamiltonian.

5.6 Conclusions

In this chapter we have studied the one point functions of the σ^z_j and σ^x_j operator for the XX-chain with hermitian boundaries, which in the continuum limit corresponds to a free boson field on a cylinder with Dirichlet-Dirichlet, Dirichlet-Neumann or Neumann-Neumann boundary conditions (see chapter 3).

No results for the magnetization profiles in the ground-state have previously been obtained on the lattice. The only known results have been found by means of the bosonization technique [90] and were restricted to the limit $L \to \infty$ and $j \gg 1$ (see (5.6) and (5.8)). The expression (5.8) is valid only for small values of the longitudinal boundary field, i.e. for small values of α_z in our notation.

We have obtained the exact ground-state profiles of the σ^z_j-operator on the finite chain for the boundary terms given in table 5.1. The respective profiles are given in (5.9)-(5.13). The continuum limit of the profiles is given in (5.14)-(5.17).

The σ^z_j-profiles for the cases from table 5.1 in the limit $L \to \infty, j \gg 1$ are given in (5.18). Exact results for the σ^x_j-profiles in this limit have been found for the cases in table 5.2 and are given in (5.20) respectively (5.23). Our results obtained on the lattice agree to the expressions (5.6) and (5.8) which have been found using the bosonization technique [90]. Note that in contrast to (5.8) our result (5.18) is not restricted to small values of the boundary field.

Supported by numerical computations, these exact results have led us to conjectures for the profiles in the continuum limit for more general values of the boundary parameters (see (5.25)-(5.28)). For the Dirichlet-Dirichlet case we have studied the most general boundary terms (5.25). The σ_j^z-profile for these boundary terms is given in (5.29) (the σ_j^x profile vanishes exactly, if the ground-state is non-degenerate).

We also considered a type of boundary terms, which correspond to the Dirichlet-Neumann boundary condition (see (5.26)). The σ_j^x profile we conjectured is given in (5.30). The profile of the σ_j^z operator is given in (5.31).

The boundary terms given by (5.27) and (5.28) correspond to Neumann-Neumann boundary conditions on the boson field. The σ_j^x-profile for the first type of boundaries (5.27) is given in (5.32). Here the σ_j^z-profile vanishes exactly, if the ground-state is non-degenerate. For the second type of boundary terms (5.28) the profile of the σ_j^z operator is given in (5.33). As in the case of the Dirichlet-Neumann boundary condition the σ_j^x profile is not affected by the presence of the diagonal boundary terms.

The expressions we have obtained for the profiles in the case of the Dirichlet-Dirichlet respectively the Neumann-Neumann boundary conditions do not coincide with the predictions (5.3) and (5.4) conformal field theory makes for the profiles of scaling operators near a boundary. Here one has to consider certain linear combinations of spin-operators to obtain the correct behaviour. These combinations and the respective behaviour near the boundary are given in (5.35) and (5.38).

In this chapter we have also discussed the appearance of massive excitations, i.e. of fermions with a non-vanishing energy as L goes to infinity. Such a fermion appears if the reciprocal value of one of the expressions (5.44) or (5.45) becomes larger than 1. These expressions reduce to (5.46) respectively (5.47) in the case of purely non-diagonal respectively diagonal boundary terms.

We have computed the profiles near the boundaries in the limit $L \to \infty, j \gg 1$ for certain states with differ from the ground-state of $\mathcal{H}_{\text{long}}$ by a massive excitation for boundary parameters satisfying (5.48) or (5.51). For the first type of boundary terms there exists one massive excitation, whereas for the second type there might appear two of them. The profiles near the boundaries are given by (5.49),(5.50) respectively by (5.52)-(5.55). If the value of ξ_α equals ξ_β (see (5.51)) the profiles are given by (5.56) and (5.57).

Chapter 6

Summary and Outlook

In this thesis, the XX spin 1/2 quantum chain (1.2) with arbitrary boundary terms has been investigated. Although this model is one of the most studied in the literature, there is still a lack of results for the model in the presence of non-diagonal boundary terms. It was the aim of thesis to fill this gap.

In chapter 2 we have shown how to obtain the spectra and the wavefunctions of the Hamiltonian (1.2) by introducing an auxiliary Hamiltonian, which is obtained from the original chain by appending an additional lattice site at each end of the chain (see (2.1)) and which may be diagonalized in terms of free fermions [1, 56]. The whole information on how to obtain the spectra of the original chain from the spectra of the prolonged chain has been shown to be encoded in a single parameter η. The value of η may be $+1$ or -1. If $\eta = +1$ one has to pick up the sector with an even number of excited fermions. Otherwise the spectrum of $\mathcal{H}$ is given by an odd number of fermion excitations, where in both cases one has to disregard the spurious zero mode which is always present in the excitation spectrum of the long chain.

Applying these results we have considered the finite size scaling spectra of the model in section 3. It has been known for a long time that for periodic boundary conditions the partition function is given by the partition function of the free compactified boson field on a torus [62, 63, 64], whereas diagonal boundary terms lead to the partition function of the boson on a cylinder with the Dirichlet-Dirichlet boundary condition [62, 67]. However, there are two further conformally invariant boundary conditions for the free boson, i.e. the Dirichlet-Neumann and the Neumann-Neumann. In the hermitian case we have been able to show that the Neumann-Neumann partition function is obtained if non-diagonal boundary terms are present at both ends of the chain. The diagonal boundary terms become totally irrelevant. If there is a non-diagonal term only at one end of the chain, the partition function corresponds to the Dirichlet-Neumann boundary condition. Again the diagonal boundary terms are irrelevant.

However, for non-hermitian boundaries the picture changes. Here the Dirichlet-Dirichlet partition function might also be realized in the presence of diagonal and non-diagonal boundary terms. Furthermore, for certain types of non-hermitian boundary terms we have obtained logarithmic corrections to the free surface energy and to the energy gaps. In the case of periodic boundary conditions logarithmic corrections to the finite-size scaling behaviour of the energies are predicted by conformal field theory in the presence of a marginally irrelevant operator [97]. Whether the occurrence of logarithmic corrections in our case can be explained in a similar way has to be clarified.

We have also studied the chain with Dzyaloshinsky-Moriya interactions. The Dzyaloshinsky-Moriya interaction affects the partition function only if non-diagonal boundary terms are present at both ends of the chain and for rational values of a certain parameter the partition function obtained on the lattice corresponds to the partition function of the free boson with Neumann-Neumann boundary conditions.

However, it is most interesting that we have been able to identify the "topological" charge on the finite chain for at least two types of non-diagonal boundary terms (chapter 4). The resulting operator commutes with the Hamiltonian and represents the analogue of the $U(1)$ charge in the case of diagonal boundary terms, i.e. the projection of the total spin onto the z-axis. If the Hamiltonian conserves parity the "topological" charge is a pseudoscalar.

In chapter 5 we studied the magnetization profiles of the σ_j^x and σ_j^z operator for hermitian boundary conditions. For certain cases, we have obtained exact results on the finite chain, in the limit $L \to \infty, j \gg 1$ and in the continuum limit $L \to \infty, z = j/L$ fixed. These results have led us to conjectures for the profiles in the continuum limit for more general values of the boundary parameters. We have checked these conjectures by extensive numerical computations. The predictions conformal field theory makes for the continuum limit of the profiles of scaling operators near the boundaries are very restrictive. If not vanishing, it is expected that the profiles diverge algebraically near the boundary where the exponent is given by the bulk scaling dimension of the respective scaling operator [88]. Furthermore the coefficient of the next to leading order is fully determined by the bulk scaling dimension, the central charge of the model and the Casimir amplitude [83, 84, 79]. The latter one can be obtained from our results for the partition functions presented in chapter 3 immediately.

However, it is not a priori clear which spin operators correspond to the scaling operators of the continuum theory. We have shown that in the case of Dirichlet-Dirichlet and in the case of Neumann-Neumann boundary conditions the profiles of σ_j^z respectively σ_j^x do not satisfy the predictions, but we have been able to identify the proper linear combinations of spin operators which do. In the case of the Dirichlet-Dirichlet boundary condition one has to choose a linear combination of σ_j^z and σ_{j+1}^z, whereas in the case of the Neumann-Neumann boundary condition one has to built a linear combination of σ_j^x and σ_j^y to obtain the predicted behaviour. However, in both cases the linear combinations we have obtained work only at one boundary at a time. In the case of the Dirichlet-Neumann boundary condition no complications arise.

Our exact results for the σ_j^x profiles obtained in the limit $L \to \infty, j \gg 1$ coincide with former results of [90] for the XXZ chain which have been obtained by means of the bosonization technique. However, our result for the σ_j^z profile in the presence of a diagonal boundary term generalizes the result of [90] (which is only valid for small values of the boundary field) to arbitrary values of the boundary field.

We have also studied the appearance of boundary bound states in chapter 5. If certain functions of the boundary parameters exceed a well defined threshold, special solutions of the secular equation defining the fermion energies appear. The associated energies lie on top of the fermion spectra and do not vanish as the system size L goes to infinity (in contrast to the low lying energy gaps which vanish as $1/L$). The maximum number of such massive fermions is two (one per boundary). This result is interesting since it confirms an analogous result obtained by Ameduri *et al* [94] in their study of the boundary sine-Gordon theory at the free fermion point. In the case of diagonal boundary terms the energy gaps obtained by the excitation of the massive fermions are in one to one correspondence to the boundary 1-strings appearing in Bethe-Ansatz calculations [91]. We have shown that the excitation of a massive fermion leads to an exponentially into the bulk decaying contribution to the magnetization profiles for diagonal (σ_j^z-profile) as well as for non-diagonal boundaries (σ_j^x-profile). This justifies referring to them as to boundary bound states.

Much room is left for further investigations. There are two main directions one can choose. First, it would be interesting to generalize our results to the more general problem of the XXZ quantum chain with boundaries. From the known results for periodic boundary conditions we expect that the radius of compactification of the associated boson field becomes a function of the anisotropy of the chain. This should affect the partition functions as well as the magnetization profiles and might be checked using numerical methods such as exact diagonalization or the DMRG. However, it would be most interesting to find the generalization of the "topological" charge for the finite XXZ chain. The understanding of this symmetry on the finite chain might open a new way to an analytic solution of the problem.

The second direction in which one could go, would be to make the connection to the continuum limit of the model, i.e. to the free boson respectively the boundary sine-Gordon model. Here one might start using the method of abelian bosonization following Affleck [90]. The identification of the partition functions is just a first step in this direction. A better understanding of the relation of the operators appearing in the continuum limit and the spin operators on the chain would surely be welcome.

Acknowledgements

At this point I want to take the opportunity to thank everybody who has supported me and my work during the past years.

First, I would like to thank Vladimir Rittenberg for many discussions and useful suggestions. I would also like to thank Birgit Wehefritz for the fruitful collaboration.

It is a pleasure to acknowledge my former colleagues Peter Arndt, Thomas Heinzel, Klaus Krebs and Horatiu Simon with whom I used to spend my time for lunch and for countless cups of coffee, respectively, tea. Beyond this, I am grateful to Klaus Krebs for carefully reading my manuscripts and to Peter Arndt and Thomas Heinzel for introducing me to the secrets of the BST-algorithm.

Furthermore, I would like to thank Dagmar Fassbender and Patricia Zündorf for their help in various situations. I am also grateful to the rest of the theory group and to all my friends.

I am thankful to the "Graduiertenförderung the Landes Nordrhein-Westfalen" for financial support.

Last but not least, I am most grateful to my parents for their patience and everlasting support.

References

[1] Jordan P and Wigner E 1928 *Z. Phys.* **47** 631
[2] Lieb E, Schultz T and Mattis D 1961 *Ann. Phys.* **16** 407
[3] Krebs K, Pfannmüller M P, Wehefritz B and Hinrichsen H 1995 J. Stat. Phys **78** 1429
[4] den Nijs N in *Phase Transitions and Critical Phenomena*, Eds. Domb C and Lebowitz J L, vol 12, Academic Press 1988
[5] Siggia E D 1977 *Phys. Rev.* B **16** 2319
[6] Manabe Y, Tokihiro T and Hanamura E 1993 *Phys. Rev.* B **48** 2773
[7] Suzuura H, Tokihiro T and Yasuhiro O 1994 *Phys. Rev.* B **49** 4344
[8] Heisenberg W 1928 *Z. Phys.* **49** 619
[9] Belavin A A, Polyakov A M and Zamolodchikov A B 1984 *Nucl. Phys.* B **241** 333
[10] D'Iorio M, Armstrong R L and Taylor D R 1983 *Phys. Rev.* B **27** 1664
[11] Taylor D R and Zaremba E 1981 *Phys. Rev.* B **23** 3384
[12] Bevis M, Sievers A J, Harrison J P, Taylor D R and Thouless D J 1978 *Phys. Rev. Lett.* **41** 987
[13] Folinsbee J T, Harrison J P, McColl D B and Taylor D R 1977 *J. Phys. C: Solid State Phys.* **10** 743
[14] Harrison J P, Hessler J P and Taylor D R 1976 *Phys. Rev.* B **14** 1979
[15] Duxburry P M, Oitmaa J, Barber M N, van der Bilt A, Joung K O and Carlin R L 1981 *Phys. Rev.* B **24** 5149
[16] Groen J P, Capel H W, Perk J H H, Klaassen T O and Poulis N J 1979 *Physica* B **97** 126
[17] Katsura S 1962 *Phys. Rev.* **127** 1508
[18] McCoy B M 1968 *Phys. Rev.* **173** 531
[19] Barouch E and McCoy B M 1971 *Phys. Rev.* A **3** 786
[20] Niemejer T 1967 *Physica* **36** 377
[21] Katsura S, Horiguchi T and Suzuki M 1976 *Physica* **46** 67
[22] McCoy B M, Barouch E and Abraham D B 1971 *Phys. Rev.* A **4** 2331
[23] Vaidya H G and Tracy C A 1978 *Physica* A **92** 1
[24] Johnson J D and McCoy B M 1971 *Phys. Rev.* A **4** 2314
[25] Sur A, Jasnow D and Lowe I J 1975 *Phys. Rev.* B **12** 3845
[26] Capel H W and Perk J H H 1977 *Physica* A **87** 211
[27] Brandt U and Jacoby K 1977 *Z. Phys.* B **26** 245
[28] Cruz H B and Gonçalves L L 1981 *J. Phys. C: Solid State Phys.* **14** 2785
[29] Colomo F, Izergin A G and Korepin V E 1992 *Phys. Lett.* A **169** 243
[30] Itz A R, Izergin A G, Korepin V E and Slavnov N A 1993 *Phys. Rev. Lett.* **70** 1704
[31] Mazur P 1969 *Physica* **43** 533
[32] Suzuki M 1970 *Prog. Theor. Phys.***43** 882
[33] Girardeau M D 1969 *Phys. Lett.* **30** 442
[34] Barouch E, McCoy B M and Dresden M 1970 *Phys. Rev.* A **2** 1075

[35] Barouch E and Dresden M 1969 *Phys. Rev. Lett.* **114** 114

[36] Barouch E and McCoy B M 1971 *Phys. Rev.* A **3** 2137

[37] Hoeger C, von Gehlen G and Rittenberg V 1985 *J. Phys. A: Math. Gen.* **18** 1813

[38] Jullien R and Pfeuty P 1979 *Phys. Rev.* B **19** 4646

[39] Siskens Th J, Capel H W and Gaemers K J F 1975 *Physica* A **79** 259

[40] Siskens Th J and Capel H W 1975 *Physica* A **79** 296

[41] Zvyagin A A 1995 *Low. Temp. Phys.* **21** 636

[42] Stolze J and Vogel M 2000 *Phys. Rev.* B **61** 4026

[43] Tjon J A 1970 *Phys. Rev.* B **2** 2411

[44] Zvyagin A A 1991 *Sov. J. Low. Temp. Phys.* **17** 68

[45] Smith E R 1970 *J. Phys. C: Solid State Phys.* **3** 1419

[46] Derzhko O and Richter J 1996 *Phys. Lett.* A **222** 338

[47] Barouch E and Oppenheim I 1974 *Physica* A **76** 410

[48] Nishimori H 1984 *Phys. Lett.* A **100** 239

[49] Luck J M and Nieuwenhuizen Th M 1986 *Europhys. Lett.***2** 257

[50] Hinrichsen H and Rittenberg V 1992 *Phys. Lett.* B **275** 350

[51] Hinrichsen H and Rittenberg V 1993 *Phys. Lett.* B **304** 115

[52] Hinrichsen H 1994 *J. Phys. A: Math. Gen.* **27** 1121

[53] Guinea F 1985 *Phys. Rev.* B **32** 7518
Guinea F, Hakim V and Muramatsu A 1985 *Phys. Rev. Lett* **54** 263

[54] de Vega H J and Gonzales-Ruiz A 1994 *J. Phys. A: Math. Gen.* **27** 6129

[55] Inami T and Konno H 1994 *J. Phys. A: Math. Gen.* **27** L913

[56] Kaufmann B 1999 *PhD Thesis* Bonn IR 9904

[57] Bilstein U, Wehefritz B 1999 *J. Phys. A: Math. Gen.* **32** 191

[58] Bilstein U 2000 *The XX–model with boundaries. Part II: Finite size scaling and partition functions* cond-mat/0002162, to appear in *J. Phys. A: Math. Gen.*

[59] Bilstein U and Rittenberg V 2000 *The "topological" charge for the finite XX quantum chain* cond-mat/0004241

[60] Bilstein U 2000 *The XX–model with boundaries. Part III: Magnetization profiles and boundary bound states* cond-mat/0004484

[61] Affleck I in *Fields, Strings and Critical Phenomena* Les Houches 1988 (North-Holland: Amsterdam)

[62] Saleur H 1998 *Lectures on Non Perturbative Field Theory and Quantum Impurity Problems* cond-mat/9812110

[63] Alcaraz F C, Baake M, Grimm U and Rittenberg V 1988 *J. Phys. A: Math. Gen.* **21** L117

[64] Alcaraz F C, Barber M N and Batchelor M T 1987 *Phys. Rev. Lett.* **58** 771

[65] Alcaraz F C, Barber M N and Batchelor M T 1988 *Ann. Phys., NY* **182** 280

[66] Oshikawa M and Affleck I 1997 *Nucl. Phys.* B **495** 533

[67] Alcaraz F C, Baake M, Grimm U and Rittenberg V 1989 *J. Phys. A: Math. Gen.* **22** L5

[68] Alcaraz F C and Wreszinski W F 1990 *J. Stat. Phys.* **58** 45

[69] Bilstein U and Wehefritz B 1997 *J. Phys. A: Math. Gen.* **30** 4925

[70] Cardy J L 1986 *Nucl. Phys.* B **275** 200

[71] Noh J D and Kim D 1996 *Phys. Rev.* E **53** 3225

[72] Bugrij A I and Shadura V N 1990 *Phys. Lett.* **150** 171

[73] Corless R M, Gonnet G H, Hare D E G, Jeffrey D J and Knuth D E *On the Lambert W Function* Maple Share Library

[74] Alcaraz F C, Barber M N, Batchelor M T, Baxter R J and Quispel G R W 1987 *J. Phys. A: Math. Gen.* **20** 6397

[75] Goshal S and Zamolodchikov A B 1994 *Int.J.Mod.Phys.* A **9** 3841,4353
[76] Ameduri M, Konik R and LeClair A 1995 *Phys. Lett.* B **354** 376
[77] Mezincescu L and Nepomechie R I 1998 *Int.J.Mod.Phys.* A **13** 2747
[78] Nienhuis B in *Phase Transitions and Critical Phenomena*, Eds. Domb C and Lebowitz J L, vol 11, Academic Press 1987, p.1.
[79] Cardy J L 1990 *Phys. Rev. Lett.* **65** 1443
[80] Burkhardt T W and Eisenriegler E 1985 *J. Phys. A: Math. Gen.* **18** L83
[81] Reš I, Straley J P 1999 *Order parameter for two-dimensional critical systems with boundaries* cond-mat/9910467
[82] Burkhardt T W, Guim I 1987 *Phys. Rev.* B **36** 2080
[83] Burkhardt T W and Xue T 1991 *Phys. Rev. Lett.* **66** 895
[84] Burkhardt T W and Xue T 1991 *Nucl. Phys.* B **354** 653
[85] Burkhardt T W and Eisenriegler E 1994 *Nucl. Phys.* B **424** 487
[86] Igloi F and Rieger H 1997 *Phys. Rev. Lett.* **78** 2473
[87] Carlon E and Igloi F 1998 *Phys. Rev.* B **57** 7877
[88] Fisher M E and de Gennes P G 1978 *C. R. Acad. Sci. Ser. B* **287** 207
[89] Alcaraz F C, Baake M, Grimm U and Rittenberg V 1989 *J. Phys. A: Math. Gen.* **22** L5
[90] Affleck I 1998 *J. Phys. A: Math. Gen.* **31** 2761
[91] Skorik S and Saleur H 1995 *J. Phys. A: Math. Gen.* **28** 6605
[92] Glaisher J W L 1894 *Messenger of Math.* **24** 1
[93] Alcaraz F C, Baake M, Grimm U and Rittenberg V 1988 *J. Phys. A: Math. Gen.* **21** L117
[94] Ameduri M, Konik R and LeClair A 1995 *Phys. Lett.* B **354** 376
[95] Luke Y L 1969 *The Special Functions and Their Approximations* (New York and London: Academic Press)
Watson G N 1918 *Trans. Cambridge Philos. Soc.* **22** 277
[96] McCoy B M and Wu T T 1973 *The Two Dimensional Ising Model* (Cambridge, Massachusetts: Harvard University Press) pp 261-264
[97] Cardy J L 1986 *J. Phys. A: Math. Gen.* **19** L1093
[98] Ginsparg P in *Fields, Strings and Critical phenomena* Les Houches 1988 (North-Holland: Amsterdam)

Appendix A

Asymptotic behaviour of the energy gaps

In this appendix we are going to explain how to obtain the asymptotic behaviour of the fermion energies for $L \gg 1$ in the general case, i.e. without making use of the factorization properties of the polynomial (2.14). Using the Jacobi triple product identity [98] this leads to our results for the partition functions presented in chapter 3 immediately.

Since we have been interested into the large L behaviour of the low lying energy levels, we looked for the asymptotics of the zeros of $p(x^2)$ (see (2.14)) in the vicinity of the point $x = \pm \mathrm{i}$ using the ansatz $x = \mathrm{e}^{\mathrm{i}\frac{\pi}{2} - \mathrm{i}\frac{\phi}{L}}$, where we assumed ϕ to be a constant in leading order. For the first four cases given in table 3.1 we obtained the following equations:

- $F \neq 0$

$$\cos(2\phi) + \frac{2C}{F} = 0 \tag{A.1}$$

- $F = C = 0, G \neq 0$

$$\phi \sin(2\phi) = 0 \tag{A.2}$$

- $F = C = G = 0, K \neq 0$

$$\phi^2 \left[\cos(2\phi) + (-1)^{L+1} \frac{J}{K} \right] = 0 \tag{A.3}$$

- $F = C = G = K = J = 0$

$$\phi^4 \exp(2\mathrm{i}\phi) = (-1)^L \tag{A.4}$$

Solving these equations for ϕ yields the energy gaps (cf. (2.13)) in leading order. We obtained the following expressions:

- $F \neq 0$

$$2\Lambda \sim \frac{1}{L} \left[\frac{2n-1}{2}\pi \pm \frac{1}{2} \arccos\left(\frac{2C}{F} \right) \right] \qquad 1 \leq n \tag{A.5}$$

- $F = C = 0, G \neq 0$

$$2\Lambda \sim \frac{1}{L}\frac{n}{2}\pi \qquad 0 \leq n \tag{A.6}$$

- $F = C = G = 0, K \neq 0$

$$2\Lambda \sim \frac{1}{L} \left[\frac{2n-1}{2}\pi \pm \frac{1}{2} \arccos\left((-1)^{L+1} \frac{J}{K} \right) \right] \qquad 1 \leq n \tag{A.7}$$

In addition to these modes there appears an additional zero mode.

- $F = C = G = K = J = 0$

$$2\Lambda \sim \frac{1}{L}n\pi \qquad 1 \leq n \qquad \text{for } L \text{ even} \tag{A.8}$$

$$2\Lambda \sim \frac{1}{L}\frac{2n-1}{2}\pi \qquad 1 \leq n \qquad \text{for } L \text{ odd} \tag{A.9}$$

Furthermore we found 3 additional zero modes for L even and 2 additional zero modes for L odd.

For the last two cases in table 3.1 the asymptotic zeros of the polynomial can only be found using the ansatz $x = \mathrm{e}^{\mathrm{i}\frac{\pi}{2} - \mathrm{i}\frac{\phi}{L}}$ if we assume the imaginary part of ϕ to diverge as L goes to infinity. Hence we generalize our ansatz to $x = \mathrm{e}^{\mathrm{i}\frac{\pi}{2} - \mathrm{i}\frac{\phi(L)}{L}}$, where $\phi(L)$ is a complex function. Furthermore we assume $\lim_{L\to\infty} \frac{\phi(L)}{L} = 0$ and $\lim_{L\to\infty} \mathrm{e}^{-\mathrm{i}\phi(L)} = 0$. The second assumption will be explained shortly. In both cases our ansatz leads to the solution of an equation of the form

$$a\mathrm{e}^{-2\mathrm{i}\phi(L)}\left[1 + \mathrm{Or}\left(\frac{\phi(L)}{L}\right)\right] + \frac{2\mathrm{i}\phi(L)}{L}\left[b + \mathrm{Or}\left(\frac{\phi(L)}{L}\right)\right] = 0. \tag{A.10}$$

From this expression one can see that our second assumption is indeed necessary to solve this equation, since otherwise the first term would be finite for all values of L, whereas the second term vanishes as L goes to infinity. Neglecting the terms of order $\phi(L)/L$ this equation is solved in terms of the so called Lambert W function $\mathcal{L}$ which is defined by the property $\mathcal{L}(x)\mathrm{e}^{\mathcal{L}(x)} = x$. We obtain

$$\phi(L) = -\mathrm{i}\mathcal{L}(\Delta L)/2 \quad \text{where} \quad \Delta = -\frac{a}{b}. \tag{A.11}$$

The asymptotic behaviour of $\mathcal{L}$ is well known [73], i.e.

$$\mathcal{L}(L) \sim 2\mathrm{i}k\pi + \ln L - \ln(\ln L + 2\mathrm{i}\pi k) + ... \tag{A.12}$$

Note that this expression is in accordance with our assumptions we made concerning the asymptotic behaviour of $\phi(L)$. We have not considered the case $b = 0$.

In this section 3.3 we also considered the asymmetric chain, which is similar to the symmetric chain with length dependent boundary parameters (cf. (3.24)). This length dependence enters the polynomial (2.14) only via the coefficient C, which becomes

$$C = \alpha'^2_- \beta'^2_+ Q^{2-2L} + \alpha'^2_+ \beta'^2_- Q^{2L-2}. \tag{A.13}$$

For $Q < 1$ (the case considered in section 3.2) the first term on the RHS of (A.13) diverges exponentially whereas the second term vanishes exponentially as a function of the lattice length L. Hence we have to distinguish two different situations. If $\alpha'_-\beta'_+$ equals zero we may find the asymptotic zeros of the polynomial as for the symmetric case with $F = C = 0$. If otherwise $\alpha'_-\beta'_+ \neq 0$ then C diverges as L is increased. This has to be compensated by modifying our ansatz to $x = \mathrm{e}^{\mathrm{i}\frac{\pi}{2} - \mathrm{i}\frac{\phi}{L} + \ln Q}$. This works as long as the nominator of Γ in (3.31) is different from zero. Otherwise we have to modify our ansatz another time to $x = \mathrm{e}^{\mathrm{i}\frac{\pi}{2} - \mathrm{i}\frac{\phi(L)}{L} + \ln Q}$, where $\lim_{L\to\infty} \frac{\phi(L)}{L} = 0$ and $\lim_{L\to\infty} \mathrm{e}^{-\mathrm{i}\phi(L)} = 0$. This leads again to an equation of the form (A.10) which can be solved as described above.

Appendix B

Calculation of the magnetization profiles

B.1 Calculation of the σ_j^z profiles

In this appendix we are going to show how to compute the σ_j^z-profiles and how we have derived the ground-state profiles for the boundary terms in table 5.1, i.e. equations (5.9)-(5.18). We will also derive the profiles (5.49) and (5.50) associated to the excitation of the massive fermion appearing for the boundaries (5.48). Note that these boundaries coincide with the boundary terms of case e in table 5.1 if one identifies e^{ξ} with $\tan(\frac{\pi}{4}+\frac{\delta}{2})$.

Using (2.48), (2.20) and (2.17) one can show that the σ_j^z profile for $1 \leq j \leq L$ and for any excited state $\mid \psi_r^{\pm}\rangle = \prod_{n=1}^{r} b_{k_n} \mid v^{\pm}\rangle$ with $k_n \neq 0$ is given by

$$\langle \psi_r^{\pm} \mid \sigma_j^z \mid \psi_r^{\pm}\rangle = \langle vac \mid \sigma_j^z \mid vac\rangle + \mathrm{i}\sum_{n=1}^{r} \left[(\phi_{k_n}^-)_j^+(\phi_{k_n}^+)_j^- - (\phi_{k_n}^+)_j^+(\phi_{k_n}^-)_j^-\right] \tag{B.1}$$

where

$$\langle vac \mid \sigma_j^z \mid vac\rangle = -\mathrm{i}\langle vac \mid \tau_j^+\tau_j^- \mid vac\rangle = -\mathrm{i}\sum_{k=0}^{L+1}(\phi_k^-)_j^+(\phi_k^+)_j^- . \tag{B.2}$$

Before turning to the profiles for the boundaries in table 5.1, consider the case $\alpha_z = \beta_z = 0$. According to section 2.2.2 it is always possible to chose the eigenvectors $(\phi_k^{\pm})$ such that the RHS of (B.1) and (B.2) vanishes for $0 < j < L+1$ (see the equations (2.40) and (2.42)). In this case the profiles for all the states $\mid \psi_r^{\pm}\rangle$ vanish identically. Thus the profile for the ground-state of $\mathcal{H}$ vanishes also if it is non-degenerate. The partition functions obtained in chapter 3 show that for $L \gg 1$ this is the generic case. Therefore we considered only cases with at least one diagonal boundary term. If the ground-state of $\mathcal{H}$ is degenerate one has also to consider linear combinations of the states $\mid \psi_r^{\pm}\rangle$ which correspond to ground-states $\mathcal{H}$.

For the cases given in table 5.1 the polynomial $p(x^2)$ factorizes into cyclotomic polynomials (see table 2.1). This enables us to compute the eigenvectors $(\phi_k^{\pm})$ exactly on the finite chain, as explained in [56]. The explicit computations are cumbersome but straight forward and will therefore not be given.

For all cases in table 5.1 there appears an additional zero mode on top of the spurious mode which does not give a contribution to the RHS of (B.1). Hence the profiles for the two states $|v^+\rangle$ and $b_z|v^-\rangle$, where b_z denotes the creation operator corresponding to the additional zero mode, are identical. One of these states is element of the $(+,+)$ sector and corresponds to the ground-state of $\mathcal{H}$. However we do not have to know which one, since we are only interested into the profile (note that (2.22) is not applicable, due to the zero mode). Hence in the following we may assume the state $|v^+\rangle$ to be in the $(+,+)$-sector.

For the cases a,b,c and d with L even no complications arise. The ground-state of $\mathcal{H}$ is non-degenerate and using the expressions for the $(\phi_k^\pm)$ in (B.2) leads to a geometric series for each case. Performing the computations yields (5.9)-(5.11) and (5.13).

For case d with L odd the ground-state is two-fold degenerate, since here two zero modes appear on top of the spurious zero mode. The non-vanishing components of the respective eigenvectors are given by

$$(\phi_{z_1}^\pm)_0^- = 1 \qquad (\phi_{z_1}^\pm)_{L+1}^+ = \pm\mathrm{i} \tag{B.3}$$

respectively

$$(\phi_{z_2}^+)_j^- = -\mathrm{i}(\phi_{z_2}^+)_j^+ = \frac{(-\mathrm{i})^j}{\sqrt{L}} \begin{cases} \mathrm{i} & \text{for } j \text{ even} \\ 1 & \text{for } j \text{ odd} \end{cases} \tag{B.4}$$

where $0 < j \leq L$ and $(\phi_k^-)_j^\pm = \pm(\phi_k^+)_j^\pm$. In this case we computed the profiles for the two states $|v^+\rangle$ and $b_{z_2}b_{z_1}|v^+\rangle$. This leads to (5.12) where one has to choose the $-$ sign for the profile of $|v^+\rangle$ respectively the $+$ sign for the profile of $b_{z_2}b_{z_1}|v^+\rangle$.

However, the computations for case e respectively the boundary terms (5.48) are more involved. It is convenient to use the parameter $s = \mathrm{e}^{-2\xi}$ where ξ has been introduced in (5.48) instead of δ being used in table 5.1. For odd values of L we have obtained

$$\langle\sigma_j^z\rangle = \frac{\varsigma_j}{\sqrt{s}L} - \frac{1-s}{1-s^L}s^{j-1}. \tag{B.5}$$

where

$$\varsigma_j = \sum_{k=1}^{N} \frac{x_k^{2j-3} + x_k^{-2j+3} - x_k^{2j-1} - x_k^{-2j+1} + s\left(x_k^{2j+1} + x_k^{-2j-1} - x_k^{2j-1} - x_k^{-2j+1}\right)}{1/s + s - x_k^2 - 1/x_k^2} \tag{B.6}$$

with $x_k = \mathrm{e}^{\mathrm{i}\frac{k\pi}{L}}$ and $N = (L-1)/2$. This expression simplifies to a geometric series for $s = 1$. Straight forward computation yields (5.13) as for case d with L even. We have not been able to compute this expression for $s \neq 1$.

As for case d with L odd, there appear two zero-modes on top of the spurious zero mode if we take L even. The non-vanishing components of the corresponding eigenvectors for the first zero mode are again given by (B.3) whereas for the second zero mode they read

$$(\phi_{z_2}^+)_j^- = -\mathrm{i}(\phi_{z_2}^+)_j^+ = \mathrm{i}^j\left(\frac{2}{L(1+s)}\right)^{1/2} \begin{cases} \mathrm{i} & \text{for } j \text{ even} \\ -\sqrt{s} & \text{for } j \text{ odd} \end{cases} \tag{B.7}$$

where $0 < j \leq L$ and $(\phi_k^-)_j^\pm = \pm(\phi_k^+)_j^\pm$. Again we computed the profiles for the two states $|v^+\rangle$ and $b_{z_2}b_{z_1}|v^+\rangle$. Labelling the profile for the state $|v^+\rangle$ by a $-$ sign and the profile for the state $b_{z_2}b_{z_1}|v^+\rangle$ by a + sign, we have obtained

$$\langle\sigma_j^z\rangle_\pm = \frac{\varsigma_j}{\sqrt{s}L} - \frac{1-s}{1-s^L}s^{j-1} \pm \frac{2}{L(1+s)}\begin{cases} 1 & \text{for } j \text{ even} \\ s & \text{for } j \text{ odd} \end{cases} \tag{B.8}$$

where ς is again given by (B.6) as for L odd, but with $N = L/2-1$. Choosing $s=1$ allows for the computation of the sum in (B.6) and yields (5.12) as for case d with L odd.

Although our results on the finite chain are restricted to $s=1$, one can show that in the continuum limit ($z = j/L$ fixed, $L\to\infty$) ς_j is given by

$$\varsigma_j = \frac{(-1)^j}{1/s+1}\frac{1}{\sin(\pi z)} \tag{B.9}$$

for L odd respectively by

$$\varsigma_j = \frac{(-1)^j}{1/s+1}\cot(\pi z) \tag{B.10}$$

for L even. Plugging this into (B.8) and (B.5) respectively results in the equations (5.16) and (5.17). Note that the exponential contributions in (B.5) and (B.8) vanish in the continuum limit.

The profile in the limit $L\to\infty, j$ fixed, leading to (5.18), may also be computed. In this limit the quantity ς_j/L appearing in (B.5) and (B.8) can be represented as an integral, i.e.

$$\varsigma_j^\infty = \lim_{L\to\infty}\frac{\varsigma_j}{L} = \frac{2}{\pi}\int_0^{\frac{\pi}{2}} \frac{\cos((2j-3)t) - (s+1)\cos((2j-1)t) + s\cos((2j+1)t)}{1/s+s-2\cos(2t)}\mathrm{d}t. \tag{B.11}$$

This integral can be calculated exactly in terms of hypergeometric functions. We obtained

$$\begin{aligned}\varsigma_j^\infty &= \frac{2}{\pi}\left[\frac{(-1)^j}{2j-1} - (-1)^j(\frac{1}{s}-1)\frac{F(1,1/2+j;3/2+j;-1/s)}{2j+1}\right] \quad \text{for } s>1 && \text{(B.12)}\\ &\sim \frac{2}{\pi}\left[\frac{(-1)^j}{j}\frac{s}{1+s}\right] + \mathrm{Or}(j^{-2}) && \text{(B.13)}\end{aligned}$$

and

$$\begin{aligned}\varsigma_j^\infty &= \frac{2}{\pi}\left[\frac{(-1)^j}{2j-1} - (-1)^j(1-s)\frac{F(1,1/2-j;3/2-j;-s)}{2j-1}\right] \quad \text{for } 0<s<1 && \text{(B.14)}\\ &\sim \frac{2}{\pi}\left[\frac{(-1)^j}{j}\frac{s}{1+s} + \frac{\pi(1-s)}{2}s^{j-1/2}\right] + \mathrm{Or}(j^{-2}). && \text{(B.15)}\end{aligned}$$

For the asymptotic expansions of the hypergeometric functions see [95]. Using these results in (B.8) and (B.5) gives for even and odd values of L

$$\langle\sigma_j^z\rangle = \frac{(-1)^j}{\pi\cosh\xi}j^{-1} + \cdots \tag{B.16}$$

Using $\mathrm{e}^{\xi} = \sqrt{2}\alpha_z$ yields (5.18). Note that the exponential contributions in (B.8) and (B.5) (which, in the limit in question, are present only for $0 < s < 1$) are cancelled by the exponential part in (B.15).

We have also considered the profile for a state where the massive fermion is excited, i.e. $\mid \xi\rangle = b_\xi b_z \mid v^+\rangle$ for L odd respectively $\mid \xi\rangle = b_\xi b_{z_1} \mid v^+\rangle$ for L even (there are two zero modes for L even, where the one labelled by z_1 gives no contribution to the profile (B.1)). Using (B.1),(B.16) and the explicit expressions of the eigenvectors $(\phi_\xi^\pm)$ corresponding to the massive fermion, i.e.

$$(\phi_\xi^+)_j^- = -\mathrm{i}(\phi_\xi^+)_j^+ = \mathrm{i}(-1)^j \left(\frac{1-\mathrm{e}^{-2\xi}}{1-\mathrm{e}^{-2\xi L}}\right)^{1/2} \mathrm{e}^{-2\xi(j-1)}. \tag{B.17}$$

where $0 < j < L+1$ and $(\phi_\xi^-)_j^\pm = \pm(\phi_\xi^+)_j^\pm$, yields (5.49) for $\xi > 0$ ($s < 1$).

Note that for $\xi < 0$ ($s > 1$) and j fixed the vector components (B.17) vanish as L goes to infinity and the profile for the excited state $\mid \xi\rangle$ equals the ground-state profile given in (B.16). By symmetry (see (5.48)) this yields the profile near the right boundary for the case $\xi > 0$ ($s < 1$), i.e. equation (5.50).

The $U(1)$ charge, i.e. the projection of the total spin onto the z-axis, of the state $\mid \xi\rangle$ can be computed using the explicit expressions of the $(\phi_k^\pm)$ and summing over j in (B.1) and (B.2) before summing over k (in this way the computation can be done exactly on the finite chain, independently of the value of s). This yields 0 for L even respectively $\frac{1}{2}$ for L odd as stated in section 5.5.2.

B.2 Calculation of the σ_j^x-profiles

In this appendix we are going to derive our exact results for the σ_j^x profiles for the two cases from table 5.2, i.e. equations (5.20),(5.23) and (5.24). Furthermore we are going to explain how we have obtained the profiles (5.52) and (5.53) corresponding to the boundary excitation for the boundary terms in (5.51) with $\xi_\beta = -\xi_\alpha$.

We have shown in section 2.2.3 how to compute the expectation values of the σ_j^x-operator in terms of pfaffians. Here we will only consider cases where diagonal boundary terms are absent (see table 5.2 and (5.51)). This enables us to represent $\langle\sigma_j^x\rangle$ in terms of the determinant of a $j \times j$ matrix (see section 2.2.3), i.e.

$$\langle v^+ \mid \sigma_j^x \mid v^+\rangle = f_{0j} \begin{vmatrix} \langle\tau_0^-\tau_1^+\rangle & \langle\tau_0^-\tau_1^-\rangle & \langle\tau_0^-\tau_3^+\rangle & \cdots \\ \langle\tau_2^+\tau_1^+\rangle & \langle\tau_2^+\tau_1^-\rangle & \langle\tau_2^+\tau_3^+\rangle & \cdots \\ \langle\tau_2^-\tau_1^+\rangle & \langle\tau_2^-\tau_1^-\rangle & \langle\tau_2^-\tau_3^+\rangle & \cdots \\ \vdots & \vdots & \vdots & \ddots \end{vmatrix} \tag{B.18}$$

where $f_{0j} = -\mathrm{i}$ for odd values of j and $f_{0j} = 1$ for even values of j. The expectation values of the basic contractions of pairs $\langle\tau_i^\mu\tau_j^\nu\rangle$ are given by (2.53). The profiles for the excited states

$$\mid r\rangle = \prod_{j=1}^{r} b_{k_j} \mid v^{(-1)^r}\rangle \tag{B.19}$$

are also given by the RHS of (B.18) if one exchanges the $\langle\tau_i^\mu\tau_j^\nu\rangle$ in (B.18) by

$$\langle\tau_i^\mu\tau_j^\nu\rangle_r = \langle\tau_i^\mu\tau_j^\nu\rangle + \sum_{l=1}^{r}\left[(\phi_{k_l}^+)_i^\mu(\phi_{k_l}^-)_j^\nu - (\phi_{k_l}^-)_i^\mu(\phi_{k_l}^+)_j^\nu\right]. \tag{B.20}$$

We will start with our computations for case g from table 5.2 and will then turn to case f from table 5.2. Afterwards we will consider the boundary terms (5.51). Again it is possible to solve the eigenvalue equation (2.6) exactly, since the boundary terms correspond to one of the factorizable cases listed in table 2.1. As for the case of the σ_j^z-profiles we will not give the explicit expressions for the eigenvectors $(\phi_k^\pm)$. They have been obtained as explained in [57] [1].

B.2.1 Case g

We will first show, how to derive equation (5.24). Afterwards we will compute the function $f(j,L)$ in (5.24) in the limit $L\to\infty, j\gg 1$. Using (5.24) this yields (5.23).

It turns out, that for our purpose it is convenient to consider the Hamiltonian $\mathcal{H}_{\text{long}}$ in a different basis, i.e. we consider the Hamiltonian

$$\mathcal{H}'_{\text{long}} = U_n \mathcal{H}_{\text{long}} U_n^{-1} \tag{B.21}$$

where U_n is given by

$$U_n = \begin{pmatrix} 1 & 0 \\ 0 & 1 \end{pmatrix} \otimes \bigotimes_{j=1}^{L} \begin{pmatrix} 1 & 0 \\ 0 & \mathrm{e}^{\mathrm{i}\varphi}\Gamma^j \end{pmatrix} \otimes \begin{pmatrix} 1 & 0 \\ 0 & (-1)^n \end{pmatrix} \tag{B.22}$$

and

$$\Gamma = \exp\left(\mathrm{i}\frac{\chi + n\pi}{L+1}\right). \tag{B.23}$$

The σ_j^x profile for any state $\mid g\rangle$ in the original basis is related to the magnetization profiles for the state $\mid g'\rangle = U \mid g\rangle$ via

$$\langle g \mid \sigma_j^x \mid g\rangle = \cos\left(\varphi + \frac{\chi+n\pi}{L+1}j\right)\langle g' \mid \sigma_j^x \mid g'\rangle + \sin\left(\varphi + \frac{\chi+n\pi}{L+1}j\right)\langle g' \mid \sigma_j^y \mid g'\rangle. \tag{B.24}$$

The Hamiltonian in the new basis can still be written in terms of free fermions. Of course the fermion energies are not affected by the transformation. The $L+1$ non-zero fermion energies are given by

$$2\Lambda_k = \sin\left(\frac{2k+1}{L+1}\frac{\pi}{2} - \frac{\chi}{L+1}\right) \tag{B.25}$$

where $1 \le k \le L+1$. Computing the eigenvectors $(\phi_k^\pm)'(\chi,\varphi)$ in the new basis yields that they are independent from the values of χ and φ and can be given in terms of the

[1] The boundary terms (5.51) correspond to case 10 in the notation of chapter 2.

vectors $(\phi_k^{\pm})(0,0)$ in the original basis, i.e. for $n \geq 0$ we have found

$$(\phi_k^{\pm})'(\chi,\varphi) = (\phi_{k+n}^{\pm})(0,0) \qquad \text{for } 1 \leq k \leq L+1-n \tag{B.26}$$
$$(\phi_k^{\pm})'(\chi,\varphi) = (\phi_{k+n-(L+1)}^{\mp})(0,0) \qquad \text{for } L+1-n < k \leq L+1 \tag{B.27}$$

whereas for $n < 0$

$$(\phi_k^{\pm})'(\chi,\varphi) = (\phi_{k-|n|}^{\pm})(0,0) \qquad \text{for } |n|+1 \leq k \leq L+1 \tag{B.28}$$
$$(\phi_k^{\pm})'(\chi,\varphi) = (\phi_{L+1+j-|n|}^{\mp})(0,0) \qquad \text{for } 1 \leq k < |n|+1. \tag{B.29}$$

Now define for n fixed the state

$$\mid n\rangle = b_{L+2-n}\dots b_{L+1} \mid v^{(-1)^n}\rangle \qquad \text{for } n > 0 \tag{B.30}$$

respectively

$$\mid n\rangle = b_1\dots b_{|n|} \mid v^{(-1)^n}\rangle \qquad \text{for } n < 0. \tag{B.31}$$

For $n = 0$ define $\mid 0\rangle = \mid v^+\rangle$. The expectation values in the new basis may be computed in the same way than in the original basis by exchanging the $(\phi_k^{\pm})$ in (B.20) and (2.53) by the $(\phi_k^{\pm})'$. Using (B.26)-(B.29) yields that the σ_j^x-profiles for the states $\mid n\rangle$ in the new basis are given by

$$\langle n' \mid \sigma_j^x \mid n'\rangle = \langle v^+ \mid \sigma_j^x \mid v^+\rangle. \tag{B.32}$$

where the RHS has to be evaluated in the old basis and for the choice $\chi = \varphi = 0$. In the same way one can show that

$$\langle n' \mid \sigma_j^y \mid n'\rangle = \langle v^+ \mid \sigma_j^y \mid v^+\rangle \tag{B.33}$$

where again the RHS has to be computed in the original basis for the choice $\chi = \varphi = 0$. Since for $\chi = \varphi = 0$ the Hamiltonian $\mathcal{H}_{\text{long}}$ commutes not only with σ_0^x and σ_{L+1}^x, but also with $\sigma_0^x\sigma_1^x\cdots\sigma_{L+1}^x$, the σ_j^y profile in (B.33) vanishes.

However, we have been interested in the ground-state profiles. Computing the value of η using (2.73) with (B.25) yields $\eta = (-1)^{L+1}$ and hence the state $\mid n\rangle$ is element of the $(+,(-1)^{L+1+n})$-sector (the excitation of a fermion changes the sector from $(\pm,\epsilon)$ to $(\mp,\epsilon)$ (see section 2.2.1)). Which of states $\mid n\rangle$ corresponds to the ground-state of $\mathcal{H}$ may be determined by computing the associated energies using (B.25).

For L odd the ground-state of $\mathcal{H}$ corresponds to the state $\mid 0\rangle = \mid v^+\rangle$ if $\chi \neq \pi$. For $\chi = \pi$ the ground-state of $\mathcal{H}$ is twofold degenerate. We obtain two linear independent ground-states by choosing the states $\mid 0\rangle$ and $\mid -2\rangle$.

For L even and $\chi > 0$ the ground-state of $\mathcal{H}$ corresponds to $\mid -1\rangle$ whereas for $\chi < 0$ the ground-state corresponds to $\mid 1\rangle$. For $\chi = 0$ the ground-state is twofold degenerate and we obtain two linear independent ground-states choosing the states $\mid \pm 1\rangle$. Finally, using (B.24) and (B.32) with $f(j,L) = \langle v^+ \mid \sigma_j^x \mid v^+\rangle$ (for the choice $\chi = \varphi = 0$) and $m = n/2$ yields (5.24) and the values of m as explained in the text.

In order to compute $f(j,L)$ we have calculated the expectation values of the basic contractions of pairs (2.53) using the vectors $(\phi_k^{\pm})(0,0)$. For $i,j < L+1$ this results in

$$\langle \tau_i^{\pm}\tau_j^{\pm}\rangle = 0 \qquad \langle \tau_0^{-}\tau_j^{+}\rangle = \sqrt{2}g(j) \tag{B.34}$$

$$\langle \tau_i^{+}\tau_j^{-}\rangle = g(i+j) - g(i-j) \qquad \langle \tau_i^{-}\tau_j^{+}\rangle = g(i+j) + g(i-j) \tag{B.35}$$

where the values of i are always even and the values of j are always odd. Furthermore we have defined

$$g(r) = \frac{-\mathrm{i}}{L+1}\frac{\sin(r\pi/2)}{\sin(r\pi/(2L+2))}. \tag{B.36}$$

Using elementary operations on determinants in (B.18) one can show that

$$f(j,L) = (-1)^j \left(\frac{2}{\pi}\right)^j \sqrt{2}\det \mathsf{Q}_j, \tag{B.37}$$

where the matrix elements of the $j \times j$-matrix Q_j are given by

$$(\mathsf{Q}_j)_{kl} = \left(\frac{\pi}{2L+2}\right)^j \left(\sin\frac{(2k-2l+1)\pi}{2L+2}\right)^{-1}. \tag{B.38}$$

The boundary behaviour of the profile (i.e. (5.23)) is obtained taking the limit $L \to \infty$ of Q_j, which yields

$$\lim_{L\to\infty} \mathsf{Q}_j = \begin{pmatrix} 1 & -1 & -\frac{1}{3} & \cdots & \frac{1}{3-2j} \\ \frac{1}{3} & 1 & -1 & \cdots & \frac{1}{5-2j} \\ \frac{1}{5} & \frac{1}{3} & 1 & \cdots & \frac{1}{7-2j} \\ \vdots & \vdots & \vdots & \ddots & \vdots \\ \frac{1}{2j-1} & \frac{1}{2j-3} & \frac{1}{2j-5} & \cdots & 1 \end{pmatrix}. \tag{B.39}$$

The large j behaviour of the determinant of this matrix is already known [96]. With (B.37) we obtain for $j \gg 1$

$$f(j,\infty) = (-1)^j A j^{-\frac{1}{4}} + \cdots \tag{B.40}$$

where A is defined by (5.21). Using (5.24) this yields (5.23). The function $f(j,L)$ may also be calculated on the finite chain using (B.38) in (B.37) and computing the determinant numerically.

B.2.2 Case f

For this case there exists an additional zero mode in the spectrum. Hence the ground-state of $\mathcal{H}$ corresponds to $\mid v^+\rangle$ or to $b_z \mid v^-\rangle$, but we can not decide which one, since (2.22) can not be applied. However, the eigenvectors $(\phi_z^{\pm})$ corresponding to the additional zero mode give no contribution to (B.20) as long as $i,j < L+1$. Hence the profiles for states $\mid v^+\rangle$ and $b_z \mid v^-\rangle$ are identical for $j < L+1$. Defining

$$f(r) = \cos\left(\frac{r}{2L+2}\pi\right) g(r) \tag{B.41}$$

where $g(r)$ is already given in (B.36), we have obtained for L odd:

$$\langle \tau_i^{\pm} \tau_j^{\pm} \rangle = 0 \qquad \langle \tau_0^{-} \tau_j^{+} \rangle = \sqrt{2} g(j) \tag{B.42}$$

$$\langle \tau_i^{+} \tau_j^{-} \rangle = f(i+j) - f(i-j) \qquad \langle \tau_i^{-} \tau_j^{+} \rangle = g(i+j) + g(i-j) \tag{B.43}$$

where i is always even and j is always odd. For L even we obtain

$$\langle \tau_i^{\pm} \tau_j^{\pm} \rangle = 0 \qquad \langle \tau_0^{-} \tau_j^{+} \rangle = \sqrt{2} f(j) \tag{B.44}$$

$$\langle \tau_i^{+} \tau_j^{-} \rangle = g(i+j) - g(i-j) \qquad \langle \tau_i^{-} \tau_j^{+} \rangle = f(i+j) + f(i-j). \tag{B.45}$$

The expressions (B.42)-(B.45) have the same large L limit as the respective expressions for case g in (B.34) and (B.35). Thus the behaviour of the ground-state profile near the left boundary is also given by the RHS of equation (B.40) which yields (5.20).

B.2.3

Here we consider the σ_j^x-profile for the boundaries in (5.51) with $\xi_\beta = -\xi_\alpha$. In this case there appears a massive fermion with energy $2\Lambda = 2\cosh \xi_\alpha$ (see section 5). Here we are interested into the effect of the excitation of this fermion onto the magnetization profile. For simplicity we use $\xi \equiv \xi_\alpha$ in the following.

We have restricted ourselves to even values of L. Since $\eta = (-1)^{L+1}$ the state $|\xi\rangle = b_\xi \mid v^-\rangle$ (where by b_ξ we denote the creation operator associated to the massive fermion) lies in the $(+,+)$-sector of the Hilbert-space of $\mathcal{H}_{\text{long}}$ and hence corresponds to an eigenstate of $\mathcal{H}$. For odd values of L the $(+,+)$-sector is given by the excitations of an even number of fermions with respect to the ground-state $|v^+\rangle$ and hence the state $|\xi\rangle$ does not correspond to an eigenstate of $\mathcal{H}$ for L odd.

A lengthy computation yields the expectation values of the basic contractions of pairs (2.53), i.e.

$$\langle \tau_i^{+} \tau_j^{-} \rangle = g(i+j) - g(i-j) \tag{B.46}$$

$$\langle \tau_i^{-} \tau_j^{+} \rangle = \mathrm{i}\frac{\Xi(i+j)+1}{L+1} + g(i-j) + \frac{2\mathrm{i}\sinh(2\xi)\mathrm{e}^{-(i+j)\xi}}{\mathrm{e}^{-2(L+1)\xi}-1} \tag{B.47}$$

$$\langle \tau_0^{-} \tau_j^{+} \rangle = \frac{\sqrt{2}\alpha_+}{\mathrm{e}^{2\xi}+1}\left(\mathrm{i}\frac{\Xi(j)+1}{L+1} + g(j) + \frac{2\mathrm{i}\sinh(2\xi)\mathrm{e}^{-j\xi}}{\mathrm{e}^{-2(L+1)\xi}-1}\right) \tag{B.48}$$

where $g(r)$ has been defined in (B.36) and

$$\Xi(q) = \sum_{n=1}^{\frac{L}{2}} \left[\mathrm{e}^{2\xi}\cos\left(\frac{q-2}{L+1}n\pi\right) + \mathrm{e}^{-2\xi}\cos\left(\frac{q+2}{L+1}n\pi\right) - 2\cos\left(\frac{q}{L+1}n\pi\right)\right] \tag{B.49}$$

$$\times \left[\cosh(2\xi) - \cos\left(\frac{2n}{L+1}\pi\right)\right]^{-1}. \tag{B.50}$$

For $L \to \infty$ we can rewrite $\frac{\Xi(q)}{L+1}$ in terms of an integral which can be calculated using standard methods. In this limit we may write

$$\langle \tau_i^{+} \tau_j^{-} \rangle = -\frac{2\mathrm{i}}{\pi}\left(\frac{\sin((i+j)\pi/2)}{i+j} - \frac{\sin((i-j)\pi/2)}{i-j}\right) \tag{B.51}$$

$$\langle \tau_i^- \tau_j^+ \rangle = -\frac{2\mathrm{i}}{\pi}\Bigg[\frac{\sin((i-j)\pi/2)}{i-j} + \frac{\sin((i+j)\pi/2)}{i+j}\mathrm{e}^{2\xi} - 2\sinh(2\xi)\mathrm{e}^{-(i+j)\xi}\Bigg(\sum_{m=0}^{\frac{i+j-1}{2}} \frac{(-1)^m \mathrm{e}^{(2m+1)\xi}}{2m+1} - \arctan(\mathrm{e}^{\xi})\Bigg)\Bigg] \qquad \text{(B.52)}$$

$$\langle \tau_0^- \tau_j^+ \rangle = -\frac{2\sqrt{2}\alpha_+ \mathrm{i}}{\mathrm{e}^{2\xi}+1}\Bigg[\frac{\sin(j\pi/2)}{j}(1+\mathrm{e}^{2\xi}) - 2\sinh(2\xi)\mathrm{e}^{-j\xi}\Bigg(\sum_{m=0}^{\frac{j-1}{2}} \frac{(-1)^m \mathrm{e}^{(2m+1)\xi}}{2m+1} - \arctan(\mathrm{e}^{\xi})\Bigg)\Bigg]. \qquad \text{(B.53)}$$

We used these expressions for the numerical calculation of the determinant in (B.18) for $j = 1, 2 \ldots 100$. We have chosen 48 different values of ξ in the range between -4.0 and 4.0. Numerical extrapolation yields

$$\langle v^+ \mid \sigma_j^x \mid v^+ \rangle \sim (-1)^j A j^{-1/4} \qquad \text{(B.54)}$$

where the numerical value of A is given by the RHS of (5.7) with an accuracy of the order of 10^{-13}.

As already mentioned above here we are interested into the profile of the state where the massive fermion is excited with respect to $|v^-\rangle$. The eigenvectors $(\phi_\xi^\pm)$ associated to the massive fermion are given by

$$(\phi_\xi^+)_0^- = \frac{-\alpha_+}{\cosh\xi}/\rho \quad (\phi_\xi^+)_0^+ = 0 \qquad \text{(B.55)}$$

$$(\phi_\xi^+)_j^- = \begin{cases} -\sqrt{2}\exp((1-j)\xi)/\rho & \text{for } j \text{ even} \\ 0 & \text{for } j \text{ odd} \end{cases} \qquad \text{(B.56)}$$

$$(\phi_\xi^+)_j^+ = \begin{cases} 0 & \text{for } j \text{ even} \\ \mathrm{i}\sqrt{2}\exp((1-j)\xi)/\rho & \text{for } j \text{ odd} \end{cases} \qquad \text{(B.57)}$$

$$(\phi_\xi^+)_{L+1}^- = 0, \quad (\phi_\xi^+)_{L+1}^+ = \frac{\mathrm{i}\beta_+}{\cosh\xi}\exp((1-L)\xi)/\rho \qquad \text{(B.58)}$$

where

$$\rho = \sqrt{\frac{\mathrm{e}^{-2L\xi} - \mathrm{e}^{2\xi}}{\sinh(2\xi)}} \qquad \text{(B.59)}$$

and $(\phi_k^-)_j^\mu = (-1)^j(\phi_k^+)_j^\mu$. In the case $\xi < 0$ this mode does not contribute to (B.20) in the limit $L \to \infty$, since (B.59) diverges, i.e.

$$\langle \xi \mid \sigma_j^x \mid \xi \rangle \sim (-1)^j A j^{-1/4} \quad \text{for } \xi < 0. \qquad \text{(B.60)}$$

This changes for $\xi > 0$. We assumed the following behaviour of the profile:

$$\langle \xi \mid \sigma_j^x \mid \xi \rangle \sim (-1)^{j+1} A(1 - c\mathrm{e}^{-j\eta}) j^{-1/4}. \qquad \text{(B.61)}$$

Using (B.51)-(B.53) and (B.55)-(B.59) in (B.20) we computed the profile for $j = 1, 2 ... 100$ for 24 different values of ξ in the range between 0 and 4. The values of c and η have been computed using numerical extrapolation by considering the quantity

$$\ln\left(1 + \frac{\langle \xi \mid \sigma_j^x \mid \xi \rangle}{\langle v^+ \mid \sigma_j^x \mid v^+ \rangle}\right) \sim \ln c - j\eta \tag{B.62}$$

Our results have confirmed our assumption (B.61) and the numerical estimates from our extrapolations suggest

$$c = 2\mathrm{e}^{(-1)^j \eta} \quad \eta = 2\xi \tag{B.63}$$

which yields (5.52). The largest deviation of the extrapolated values for c and η from (B.63) has been of the order of 10^{-11}. We omit any tables on this. Computing the profile for $\xi > 0$ near the right boundary is equivalent to the computation of the profile near the left boundary for $\xi < 0$ (see (5.51)) which is given by (B.60). This yields (5.53).

B.3 Numerical verification of the conjectures in section 5.3

We have verified our conjectures (5.29)-(5.33) for the continuum limit of the magnetization profiles for the boundary terms (5.25)-(5.28). In order to do so, we have used numerical diagonalization to obtain the vectors $(\phi_k^{\pm})$ (see (2.6)) numerically and used (B.1) and (B.18) to obtain the profiles of σ_j^z respectively σ_j^x on the finite chain. Notice that (B.18) is only valid if $\alpha_z = \beta_z = 0$ and can not be applied to compute the σ_j^x profile for the boundary terms (5.28). In this case we made use of the determinant representation (2.59) of the pfaffian which determines the profiles.

We computed the profiles on finite lattices with $L = 20, 60, 100, \ldots$ respectively $L = 21, 63, 105, \ldots$, where the maximum value of L has been chosen in the range of $500 - 700$. For each type of boundaries in (5.25)-(5.28) we have used $30 - 50$ different values of the respective free parameters.

The values obtained on the finite lattice have been extrapolated to $L = \infty$ for $z = j/L$ fixed using the BST algorithm, where $z = \frac{n}{20}$ for L even respectively $z = \frac{n}{21}$ for L odd with $n \in \mathbb{N}$.

As already mentioned in the text, the relative deviation of our numerical results from the conjectures is typically of the order of $10^{-12} - 10^{-7}$. In general the accuracy of our computations depends on the choice of the parameters in (5.25)-(5.28) and we have searched for regions in the parameter space where the accuracy of our computations breaks down. We found that this is the case for small values of $\alpha_{\pm}$ and $\beta_{\pm}$ in (5.26) respectively in (5.27) and (5.28). As an example figure B.1 shows the relative deviation of the extrapolated σ_j^x-profile for the Dirichlet-Neumann boundary condition (5.26) with $\alpha_z = 0$ from the exact expression (5.30) for $\beta_{\pm} = \sqrt{8}, \beta_{\pm} = \sqrt{8}/20$, $\beta_{\pm} = \sqrt{8}/100$ and for even values of L, where we have used finite size data from $L = 20$ up to $L = 700$. The deviations are always in the range of the accuracy of the extrapolations. Hence we avoid any error bars.

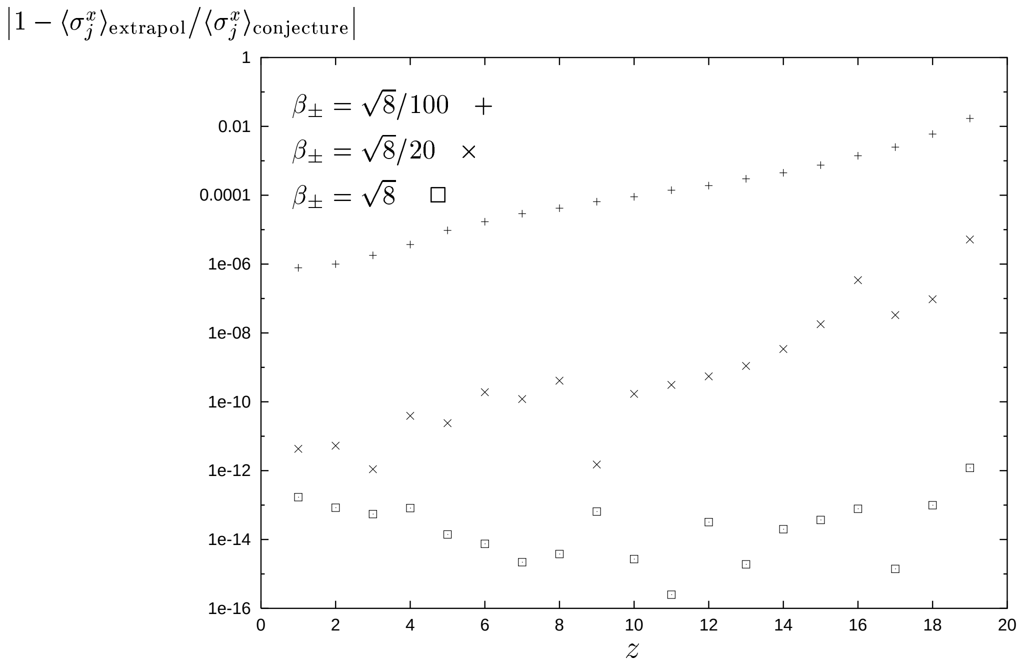

Figure B.1. The absolute value of the relative deviation of the extrapolated profile $\langle\sigma_j^x\rangle_{\text{extrapol}}$ from our conjecture (5.30) for the boundaries (5.26). The extrapolated profiles have been obtained from finite size data for lattice lengths $L = 20, 60, \ldots, 700$.

The behaviour illustrated in figure B.1 is not unexpected, since the vanishing of a non-diagonal boundary term implies a sudden change of the respective boundary condition on the free boson from Neumann to Dirichlet. For the boundaries in question this change implies that the σ_j^x profile vanishes exactly even on the finite chain (the Hamiltonian $\mathcal{H}$ commutes with $\sigma_1^z\sigma_2^z\cdots\sigma_L^z$ for $\beta_\pm = 0$ and the ground-state of $\mathcal{H}$ is non-degenerate). Since the profiles on the finite chain are smooth functions of all parameters appearing in the Hamiltonian, the deviation of the finite size data from the profile (5.30) we conjectured for the case $\beta_\pm \neq 0$ in the continuum limit (which does not depend on the value of $\beta_\pm$) increases as $\beta_\pm$ goes to zero. Assuming that our conjecture is correct, it is not surprising that the accuracy of our extrapolations decreases simultaneously.